ERDC/GSL TR-22-16

US Army Corps
of Engineers®
Engineer Research and
Development Center

ERDC
ENGINEER RESEARCH & DEVELOPMENT CENTER

Validation of the Automatic Dynamic Cone Penetrometer

Ernest S. Berney IV, Jami Lynn Daugherty, and Lulu Edwards

July 2022

Geotechnical and Structures Laboratory

Approved for public release; distribution is unlimited.

The U.S. Army Engineer Research and Development Center (ERDC) solves the nation's toughest engineering and environmental challenges. ERDC develops innovative solutions in civil and military engineering, geospatial sciences, water resources, and environmental sciences for the Army, the Department of Defense, civilian agencies, and our nation's public good. Find out more at www.erdc.usace.army.mil.

To search for other technical reports published by ERDC, visit the ERDC online library at https://erdclibrary.on.worldcat.org/discovery.

ERDC/GSL TR-22-16
July 2022

Validation of the Automatic Dynamic Cone Penetrometer

Ernest S. Berney, Jami Lynn Daugherty, and Lulu Edwards

Geotechnical and Structures Laboratory
U.S. Army Engineer Research and Development Center
3909 Halls Ferry Road
Vicksburg, MS 39180-6199

Final report

Approved for public release; distribution is unlimited.

Prepared for U.S. Army Research Laboratory
Adelphi, MD 20783-1197

Under MIPR 011460210, "Validation of the Automatic Dynamic Cone Penetrometer"

Abstract

The U.S. military requires a rapid means of measuring subsurface soil strength for construction and repair of expeditionary pavement surfaces. Traditionally, a dynamic cone penetrometer (DCP) has served this purpose, providing strength with depth profiles in natural and prepared pavement surfaces. To improve upon this device, the Engineer Research and Development Center (ERDC) validated a new battery-powered automatic dynamic cone penetrometer (A-DCP) apparatus that automates the driving process by using a motor-driven hammering cap placed on top of a traditional DCP rod. The device improves upon a traditional DCP by applying three to four blows per second while digitally recording depth, blow count, and California Bearing Ratio (CBR). An integrated Global Positioning Sensor (GPS) and Bluetooth® connection allow for real-time data capture and stationing. Similarities were illustrated between the DCP and the A-DCP by generation of a new A-DCP calibration curve. This curve relates penetration rate to field CBR that nearly follows the DCP calibration with the exception of a slight offset. Field testing of the A-DCP showed less variability and more consistent strength measurement with depth at a speed five times greater than that of the DCP with minimal physical exertion by the operator.

DISCLAIMER: The contents of this report are not to be used for advertising, publication, or promotional purposes. Citation of trade names does not constitute an official endorsement or approval of the use of such commercial products. All product names and trademarks cited are the property of their respective owners. The findings of this report are not to be construed as an official Department of the Army position unless so designated by other authorized documents.

DESTROY THIS REPORT WHEN NO LONGER NEEDED. DO NOT RETURN IT TO THE ORIGINATOR.

Contents

Abstract ii

Figures and Tables v

Preface viii

1 Introduction 1

1.1 Background 2

1.1.1 Description of the DCP 2

1.1.2 Automation of the driving mechanism 3

1.1.3 Automation of the driver 5

1.2 Objective 6

1.3 Approach 7

1.4 Scope 7

2 Validation of First Generation A-DCP Prototype 9

2.1 A-DCP apparatus 9

2.2 Test section design 10

2.3 Data collection plan 15

2.4 Uncorrected cumulative blow-count comparison 16

2.5 Corrected blow-count correlation 21

2.6 Comparison of penetration rate to CBR response 24

2.7 Single blow versus automatic mode 27

3 Validation of Second Generation A-DCP prototype 31

3.1 Soil selection and test section construction 31

3.1.1 Heavy clay - CH 32

3.1.2 Silt - ML 33

3.1.3 Sand - SP 34

3.1.4 Limestone – GP-GM 35

3.1.5 Silty sand - SM 36

3.1.6 Clayey sand - SC 37

3.1.7 Lean clay - CL 38

3.2 Test section construction 39

3.2.1 Layout 39

3.2.2 Equipment 40

3.3 Testing devices 46

3.3.1 Nuclear density gauge 46

3.3.2 Automatic dynamic cone penetrometer 47

3.3.3 Dual-mass dynamic cone penetrometer 48

3.3.4 Instrumented dynamic cone penetrometer 49

3.3.5 In situ California Bearing Ratio 50

3.3.6 Clegg hammer 51

3.4 Data collection layout 52

3.5 Initial performance of the A-DCP 54

4 Data Analysis for Second Generation A-DCP Prototype 56

4.1 Data organization 56
4.2 Data distribution 57
4.3 Selection of valid data points 58
4.4 Regression analysis 59

5 Energy Analysis 66

5.1 Field blow-count analysis 68
5.2 Force analysis 70
5.3 Impulse analysis 71
5.4 Summary of energy study 74

6 Conclusions and Recommendations 76

6.1 Conclusions 76
6.1.1 Feasibility study (2018) 76
6.1.2 Validation study (2020) 76
6.2 Recommendations 79

References 80

Appendix A: Soil Properties 81

Appendix B: Second Generation A-DCP Field Data 113

Appendix C: Selected Data from Second Generation A-DCP Testing 123

Appendix D: Second Generation A-DCP Correlation Data 126

Appendix E: Second Generation A-DCP Correlation Results 128

Unit Conversion Factors 140

Report Documentation Page

Figures and Tables

Figures

Figure 1. Automatic DCP (A-DCP) in operation. 1
Figure 2. Schematic of a dynamic cone penetrometer. 3
Figure 3. RaVEn vehicle with DCP attachment. 5
Figure 4. A-DCP, run in automatic mode (left) and manual mode (right). 9
Figure 5. Pit 1 – Clay gravel over sand layering. 11
Figure 6. Pit 2 – Crushed rock over silt layering. 11
Figure 7. Pit 3 – Silt over clay gravel over limestone base. 11
Figure 8. Pit 4 – Limestone over clay gravel over heavy clay. 12
Figure 9. Pit 5 – Heavy clay. 12
Figure 10. Pit 6 – Natural test site. 13
Figure 11. Pit 7 – Limestone base. 14
Figure 12. Pit 8 – Natural test site. 15
Figure 13. Locations for the comparison testing: in situ CBR was taken at location A. 16
Figure 14. Cumulative correlation for Happy, no correction factor. 19
Figure 15. Cumulative correlation for Sneezy, no correction factor. 20
Figure 16. Cumulative correlation for Happy with correction factor of 1.6. 22
Figure 17. Cumulative correlation for Sneezy with correction factor of 1.6. 23
Figure 18. Example of the penetration rate, or index, plotted by depth. 24
Figure 19. Summary of penetration rate for the A-DCP units and the dual-mass DCP. 25
Figure 20. Penetration rate for the historical DCP data and the current DCP data. 26
Figure 21. Penetration rate for the historical DCP data and the current A-DCP data. 26
Figure 22. Setup of A-DCP on load cell for calibration of single-blow energy. 29
Figure 23. Load cell measurements. 29
Figure 24. Cumulative blow count plotted by depth for Pit 8, comparing the single blow count and the automatic method for Happy A-DCP. 30
Figure 25. Cumulative blow count plotted by depth for Pit 8, comparing the single blow count and the automatic method for the Sneezy A-DCP. 30
Figure 26. Heavy clay (CH) during processing. 33
Figure 27. Silt (ML). 34
Figure 28. Sand (SP). 35
Figure 29. Limestone (GP-GM). 36
Figure 30. Silty sand (SM). 37
Figure 31. Clayey sand (SC). 38
Figure 32. Lean clay (CL). 39
Figure 33. Test section design. 39
Figure 34. CAT 277. 40
Figure 35. Front-end loader. 41

Figure 36. Smooth-wheel roller compactor. 42
Figure 37. Pneumatic roller compactor. 43
Figure 38. Plate compactor. 44
Figure 39. Sheepsfoot roller. 45
Figure 40. Mini-excavator. 46
Figure 41. Troxler nuclear density gauge. 47
Figure 42. Automatic Dynamic Cone Penetrometer. 48
Figure 43. Conventional dual-mass DCP testing. 49
Figure 44. Instrumented Dynamic Cone Penetrometer. 50
Figure 45. Truck-mounted in situ CBR testing. 51
Figure 46. CBR test trench. 51
Figure 47. Clegg hammer. 52
Figure 48. Test section marking. 53
Figure 49. Test section labeling. 53
Figure 50. Forklift used to retrieve mired rod from CH material after testing. 55
Figure 51. Broken nut on A-DCP. 55
Figure 52. Layout of truck-mounted in situ CBR tests. 57
Figure 53. Percentage of unique in situ CBR/A-DCP Index pairs. 58
Figure 54. Total number of unique in situ CBR-A-DCP PI pairs. 58
Figure 55. Legacy in situ CBR versus Penetration Rate correlation. 60
Figure 56. A-DCP SN1 correlation between in situ CBR and penetration rate. 62
Figure 57. A-DCP SN5 correlation between in situ CBR and penetration rate. 62
Figure 58. Standard curve for all A-DCP data and ERDC manual DCP data. 63
Figure 59. Absolute value of average differential in predicted CBR for each A-DCP unit tested. 65
Figure 60. Force-Impulse experimental setup. 66
Figure 61. Total blows per meter differential between A-DCP and DCP devices by average soil strength tested. 70
Figure 62. Illustration of ideal impulse force-time plot and typical force-time plot from A-DCP experiment. 71
Figure 63. Typical impact and rebound response of manual DCP test. 72
Figure 64. Calculation of impulse for each hit on a manual DCP test using triangular force distributions. 73
Figure 65. Correlation between PR-CBR equation and impulse of each device. 78

Tables

Table 1. Estimated soil properties for first generation A-DCP experiment. 10
Table 2. Comparison of final cumulative blow-count values for the A-DCPs and dual-mass DCP. 17
Table 3. Penetration rates for the three devices tested, for each location, A, B, and C. 27
Table 4. Soil properties. 32

Table 5. Heavy clay test section properties. 33
Table 6. Silt test sections properties. 34
Table 7. Sand test section properties. 35
Table 8. Limestone test section properties. 36
Table 9. Silty sand test section properties. 37
Table 10. Clayey sand test section properties. 38
Table 11. Lean clay test section properties. 38
Table 12. Caterpillar 277 multi-terrain loader specifications. 40
Table 13. Komat'su WA 150 front-end loader specifications. 41
Table 14. Dynapac CA25 smooth-wheel roller specifications. 42
Table 15. Ingram 10,000 pneumatic roller specifications. 43
Table 16. Northern Industrial JPC-80 plate compactor specifications. 44
Table 17. CAT CS-433E sheepsfoot compactor specifications. 45
Table 18. Bobcat E45 mini-excavator specifications. 46
Table 19. Coefficient matrix for A-DCP and DCP regression correlations. 60
Table 20. Series of hammer blow experiments performed with each test device. 68
Table 21. Average total blows per meter to penetrate each soil test section by device and associated differential. 69
Table 22. Maximum force produced per hammer blow from each A-DCP unit. 71
Table 23. Impulse recorded for each single blow experiment for A-DCP and manual DCP devices. 73

Preface

This study was conducted for the Army Research Laboratory under MIPR 011460210, "Validation of the Automatic Dynamic Cone Penetrometer." The technical monitor was Dr. Greg Fischer.

The work was performed by the Airfields and Pavements Branch (GMA) of the Engineer Systems and Materials Division (GM), Geotechnical and Structures Laboratory, U.S. Army Engineer Research and Development Center (ERDC-GSL). At the time of publication, Ms. Anna M. Jordan was Chief, GMA; Mr. Justin S. Strickler was Chief, GM; and Mr. R. Nicholas Boone, GVT, was the Technical Director for Force Projection and Maneuver Support. Mr. Charles W. Ertle II was Deputy Director of ERDC-GSL, and the Director was Mr. Bartley P. Durst.

COL Teresa A. Schlosser was the Commander of ERDC, and Dr. David Pittman was the Director.

1 Introduction

The Air Force Special Operations Command (AFSOC) requires an expedited means of measuring subsurface soil strength for contingency airfield landing sites. Its goal is to achieve a device capable of obtaining data identical to data from a standard Dynamic Cone Penetrometer (DCP) test but conducted by a single airman in approximately 1 min. AFSOC, in cooperation with the Army Research Laboratory (ARL) and Honeybee Robotics, developed a prototype automatic dynamic cone penetrometer (A-DCP) apparatus (Figure 1) that uses a motorized, spring-loaded mass to hammer a DCP rod into the ground while measuring the penetration depth. In the automated driving process, the A-DCP hammers the DCP rod into the soil at a rate of three to four blows per second and is operated by a single individual, who provides the reaction mass to the driving force.

Figure 1. Automatic DCP (A-DCP) in operation.

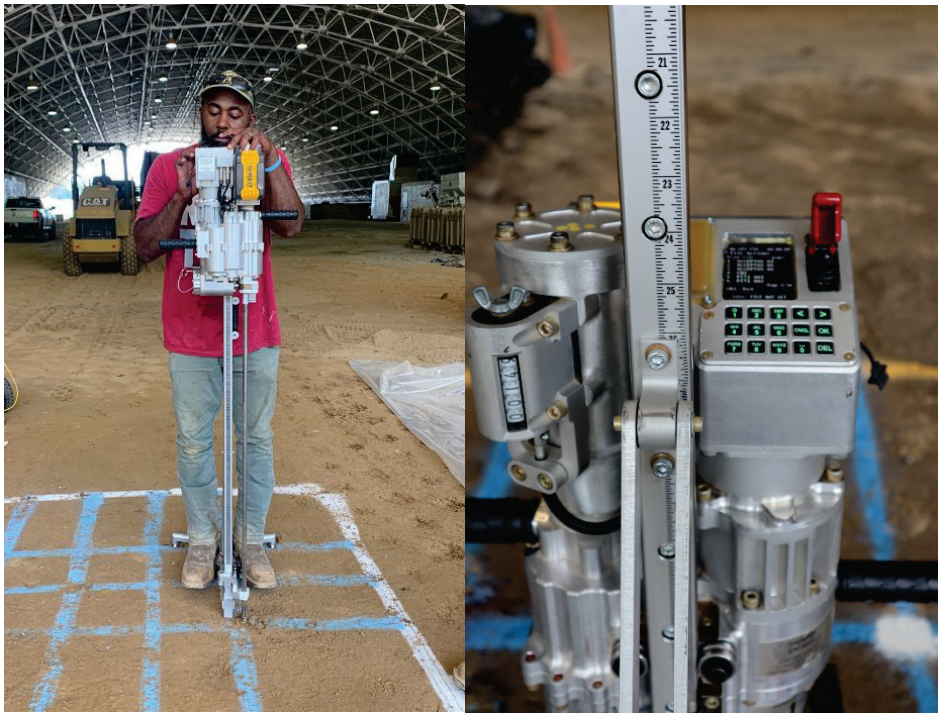

The U. S. Army Engineer Research and Development Center (ERDC) was tasked to validate the operational capability of A-DCP devices by comparing their performances to both the manual dual-mass DCP methodology and the in situ California Bearing Ratio (CBR). The in situ CBR was measured with

depth by using a traditional truck-mounted CBR apparatus. Two generations of the A-DCP are evaluated and discussed in this report, which concludes with a final calibration curve for the A-DCP unit for field operations.

1.1 Background

1.1.1 Description of the DCP

The DCP (Figure 2) is an in situ geotechnical assessment device used to evaluate the strength of soil by measuring the penetration rate of a cone from a known force. The DCP was created to characterize the shearing resistance of a soil, which is correlated to a soil's ability to withstand a load. The DCP was first developed in 1956 in South Africa for use in evaluating pavement layer strength (Scala 1956). A DCP is a simple tool, consisting of a steel rod tipped with a steel cone, which is hammered into the ground using a sliding hammer weight. The DCP has a cone angle of 30 deg with a rod diameter of 0.79 in. (20 mm) and a drop mass of 17.6 lb (8.0 kg) from a drop height of 22.6 in. (575 mm). When the drop weight is raised to the appropriate drop height, the weight strikes the anvil and generates a known force. The tip penetrates the soil with each drop, and the corresponding number of blows for a given penetration distance is recorded. This measurement is described as the penetration rate (PR) and sometimes referred to as the penetration index (DPI). The penetration rate of the DCP can be used to estimate the CBR of the soil. The DCP offers a quick, reliable, and inexpensive form of testing. The U. S. Army Corps of Engineers (USACE) developed a dual-mass modification of the DCP (Webster et al. 1992). The dual-mass DCP offers a 10.1-lb (4.6-kg) hammer weight and a 17.6-lb (8-kg) hammer weight. The 10.1-lb hammer is desirable for testing in soft materials, whereas the heavier hammer is favored for testing in stronger materials.

Figure 2. Schematic of a dynamic cone penetrometer.

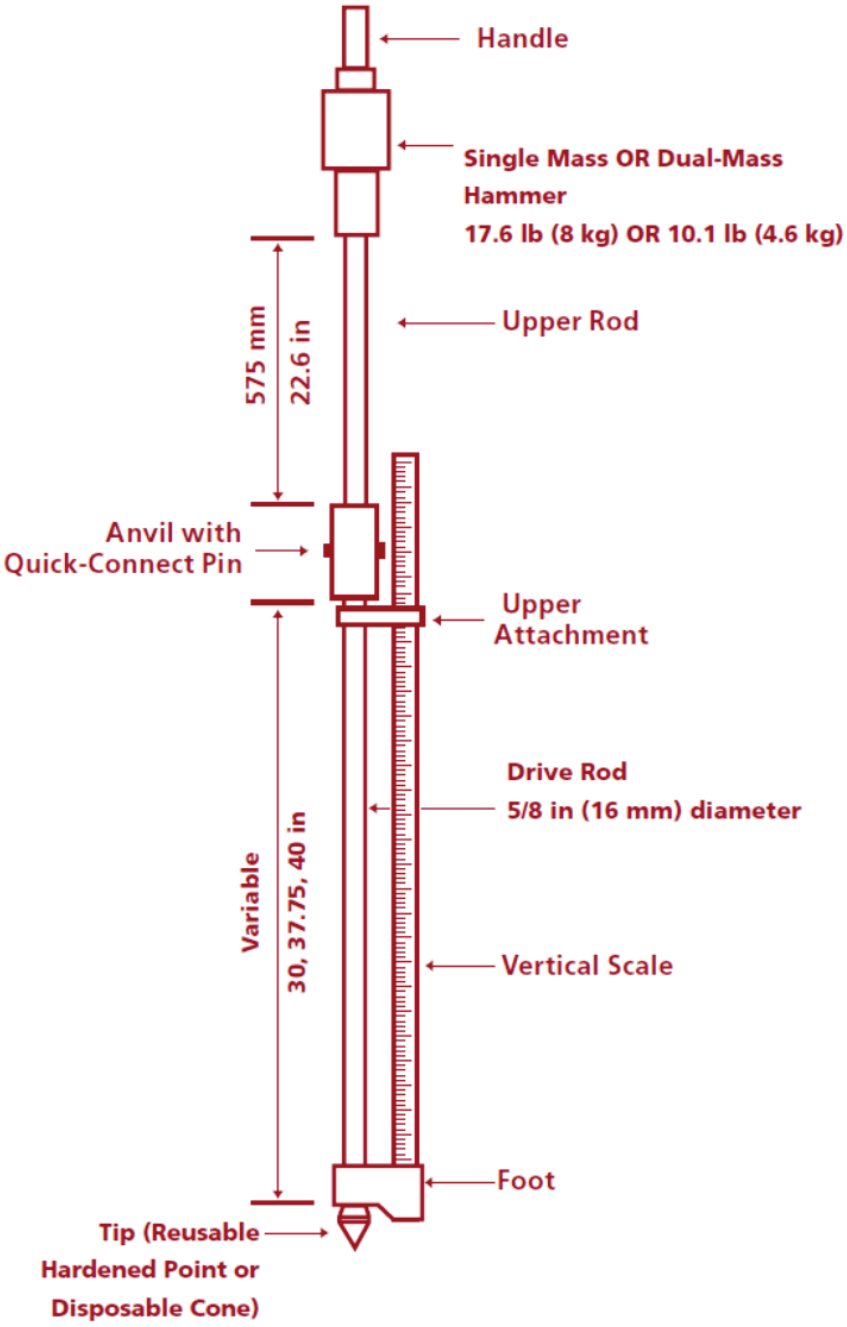

1.1.2 Automation of the driving mechanism

While the DCP and its simplistic operation make it a very desirable field tool for identifying subsurface soil layering and strength, it requires a minimum of two or three personnel to properly conduct a test. The ability to automate the original design of the DCP would alleviate user fatigue when conducting multiple tests, especially in harder soils; provide consistent results between

tests; and reduce operator bias. Many researchers have attempted to automate drop sequence of the DCP. To date, most research in automating the DCP has focused on automating the dropping process of the hammer, while still maintaining a full upper-rod assembly.

1. An automated DCP was fabricated in Israel at the Israeli Institute of Technology (Parker et al. 1998). The Israeli automated DCP consists of a pneumatic system to raise the weight to the appropriate drop height. The weight is then released and allowed to free fall down the rod to generate the force.
2. Norway later developed another form of the automated DCP. The Norwegian DCP consisted of two pneumatic cylinders to raise the DCP hammer. This model measures the penetration of the rod into the soil by using a rotary encoder. The DCP is connected to a computer to determine penetration rates. The DCP's motor can work in the reverse direction to easily remove the rod from the soil (Parker et al. 1998).
3. The Minnesota Department of Transportation in 1992 furthered the research efforts on the automated DCPs by fabricating a trailer-mounted apparatus to automatically lift the hammer. The hammer is released from the drop height and falls freely, striking the anvil and producing a force. The penetration is then recorded by a laptop computer (Parker et al. 1998).
4. In 2004, ERDC developed the Rapid Vehicle Engineer (RaVEn) (Figure 3) for use in expeditious evaluations of remote airfield. An automated and autonomous DCP system was manufactured as an attachment for a Bobcat enabled vehicle (Anderton et al. 2021). The automated DCP allows a soil strength test to be conducted from inside the cab without human interaction. The test results are displayed and stored on a computer located inside the vehicle. The DCP attachment consists of a standard DCP inside a device that mechanically lifts and drops the hammer by using the auxiliary hydraulics on the front of the machine. Sensors on the side of the device accurately measure the penetration of the cone, as well as the location of the hammer, after each blow. This process is automatically controlled by software on the laptop in the cab of the vehicle, eliminating the need for post-processing data as with current methods. The device provides an efficient way to conduct DCP tests by reducing the personnel requirement to one soldier, eliminating the physically demanding aspects of the manual method, and providing instantaneous results in a safe environment.

Figure 3. RaVEn vehicle with DCP attachment.

In all cases, the automation of the driving mechanism of the DCP eliminated user fatigue and increased consistency of the tip force; however, it did not improve the logistics of the system. Automating the hammer drop required extensive hardware, chain systems, hydraulics, and mounting systems that were not portable to a user. For expeditionary military purposes, a portable automated solution was sought.

1.1.3 Automation of the driver

In 2011, the Air Force Research Laboratory developed an automated DCP known as the Mosquito. The Mosquito was an automated DCP mounted on the back of a small dirt bike. The Mosquito utilized a smaller diameter rod and a battery-powered actuator that provided a consistent force to drive the rod into the soil. The Mosquito used a similar penetration rate assessment and provided results in terms of CBR. However, the Mosquito was deemed not practical because it was mounted on a dirt bike, limiting its maneuver and transport. Because it was smaller than a conventional DCP, the Mosquito experienced difficulty penetrating stronger soils. Most importantly, the Mosquito did not produce the same tip pressure as a DCP, owing to its smaller diameter rod. Extensive calibration would be required to build confidence in its ability to replicate field CBR comparable to that of a DCP.

Because modifications to the driving force and the rod/tip configurations have not produced the exact force as the dual hammer DCP, extensive testing and correlation between the different DCP models is necessary.

Before adoption of a new test device, the user community needs confidence in the correlation between the DCP models and the CBR. Although many attempts have been made to automate the DCP, many have failed due to the difficulty of calibrating the system to the manual DCP. Also, many of the automated alternatives have not provided the benefits of the manual DCP such as ease of transportation, storage, and use.

1.2 Objective

Airmen within AFSOC are required to evaluate contingency runway locations throughout the world. This is accomplished through the use of a DCP to measure the thickness and strength of underlying soil layers beneath the natural ground or pavement surface to estimate the size and number of potential aircraft sorties that can be conducted. Their mission often requires insertion into contested locales where operational logistics must be kept to a minimum. The current DCP requires two to three personnel to operate. The first operator lifts and drops the hammer, the second records the number of blows and records the depth of the hammer rod, and the third potentially records the information onto a paper document, tablet, or laptop. Sacrificing three men to conduct one test can put the team at risk of attack with so many eyes focused on the DCP and not on the surrounding environment. Further, a typical DCP test can take several minutes to conduct, limiting the number of tests that can be run in a compressed time window. This can increase the risk of damage to the aircraft due to missed data that may identify potential weak spots within the landing zone. Finally, decision-making based on the paper-recorded data is tedious and introduces the potential for transcription error by requiring manual input of the data stream after the test is completed, thereby further delaying an answer as to the suitability of the landing zone.

The goal of the AFSOC is fourfold in this research.

1. Reduce the number of required personnel to one to operate a test, freeing up two men to provide security.
2. Reduce the time required to conduct the test to 1 min to ensure that a sufficient number of tests can successfully be completed in a compressed time frame.
3. Expedite the data collection and processing capability to enable faster decision making in the field.
4. Provide a defining calibration equation that correlates the A-DCP PR value to the CBR of the soil.

The A-DCP represents the first generation of new tools that aims to address these limitations and provide AFSOC with a faster, easier solution to accessing landing zone suitability.

1.3 Approach

To determine the differences and thereby quantify the improved efficiency of the A-DCP versus the manual DCP, a series of experiments was conducted at the ERDC in Vicksburg, MS. These experiments were conducted over a 6-month period in the summer and winter of 2020. The experimental plan consisted of the following.

1. Large-scale test beds of uniform soil material were constructed that enabled side-by-side data collection between two unique A-DCP units, a manual DCP and an instrumented manual DCP. The test beds were of sufficient size to allow multiple test instances of each device.
2. A wide range of soil types was used within the test sections to ensure that the devices were validated against the broad scope of soil types and moisture conditions likely to be encountered during survey operations.
3. A specific impulse study was made to ascertain calibration differences occurring between the manual DCP and the A-DCP and between unique A-DCP devices.

This report presents data collected from two independent studies conducted by ERDC on the A-DCP. The first was an initial cursory study of the A-DCP in 2018 to evaluate its fundamental characteristics to ensure the device functioned as promised. The second was conducted in 2020 to validate the A-DCP's performance and produce a calibration equation correlating the A-DCP PI to CBR, allowing its deployment to the field. Data were reduced using Microsoft Excel, which was also used to develop the required correlation curves for each A-DCP device.

1.4 Scope

This research validates a new piece of test equipment designed to provide soil layer thicknesses and CBR strength in a manner similar to that of the manual DCP. As described earlier, a number of research efforts have been attempted to automate or simplify the DCP, but no solution has yet been adopted, owing to the lack of a strong correlation to the manual DCP. It was found during the cursory 2018 ERDC study documented in Chapter 2 that

the A-DCP's PR correlation to CBR, while similar to the DCP, suffered a lateral offset, owing to an energy differential between the two devices. This required the more rigorous testing program conducted in 2020 and documented in Chapters 3-5 to create a sufficient amount of well-controlled field data to generate a strong correlation plot between the A-DCP PR and CBR. This was necessary to provide confidence to the user community that the A-DCP could be used as a replacement to the manual DCP.

The experiments conducted during this study were intended to provide a direct comparison between differing A-DCP devices and the manual DCP. Test sections consisted of soil types and conditions typically found during airfield reconnaissance. Soils were prepared to evaluate the A-DCP's ability to handle soft clay soil, hard compacted gravel, and a variety of intermediate soil types at or near the optimum moisture content for strength. Test sections were constructed to a minimum 36-in. depth to validate the ability of the A-DCP to penetrate the full rod depth and still respond appropriately. A truck-mounted CBR test device was used to collect CBR strength data with depth for validation with the A-DCP PR. The environmental effect of the A-DCP operation in wet or severe climatic extremes was not evaluated. The initial study in 2018 evaluated the ability to use the internal Bluetooth® system to transmit data to a customized application for real-time processing, but this was not replicated in the 2020 study.

2 Validation of First Generation A-DCP Prototype

In 2018, a series of experiments was conducted by ERDC on the first generation A-DCP apparatus developed by AFSOC in cooperation with the Army Research Laboratory and Honeybee Robotics. This initial study was designed to evaluate whether the A-DCP had the capability of capturing CBR strength with depth in a manner similar to that of the manual dual-mass DCP apparatus. Due to the success of this initial study, a more formal study was conducted to develop the required calibration criteria to enable accurate CBR values from the A-DCP apparatus.

2.1 A-DCP apparatus

The A-DCP automates the driving process by using a motor-driven hammering cap placed on top of a traditional DCP rod (Figure 4, left). The motor-driven hammering mechanism can drive the A-DCP rod at three to four blows per second. This reduces the operational time frame of collecting data by up to 80%, based on a maximum one blow per second operation for a manual DCP. A manual crank mode of operation (Figure 4, right) was also available in this early prototype in the event the automatic mode failed in a remote environment. Two rotations of the side-mounted manual crank provided enough energy to fire one blow of the A-DCP.

Figure 4. A-DCP, run in automatic mode (left) and manual mode (right).

2.2 Test section design

Field evaluation of the A-DCP was accomplished by using a series of test pits constructed to evaluate both routine and extreme conditions imposed upon the DCP equipment. Each test pit was constructed to a depth 48 in. below the surrounding surface to ensure that the 36-in.-long DCP rod always penetrated a prepared layer. The plan dimensions of each test pit were 6 ft x 6 ft to ensure sufficient area was available for multiple DCP tests. Each test pit consisted of varying soil types compacted in 6-in. lifts to represent soft, medium, and hard layering in various configurations. The representative soil properties of each soil type are given in Table 1.

Table 1. Estimated soil properties for first generation A-DCP experiment.

Material	USCS[a]	Estimated Optimum Moisture (%)	Estimated Maximum Dry Density (pcf)	Liquid Limit	Plasticity Index
Clay	CH	22.8	102.4	84	55
Silt	ML	14.5	115.0	31	6
Sand	SP	1.9	111.5	NV	NP
Limestone	GW	6.4	120.2	NV	NP
Clay Gravel	GP	5.5	137.5	34	21
Crushed Rock*	GP	N/A	N/A	N/A	N/A

*Data were unavailable

[a] Unified Soil Classification System (ASTM 2017)

Eight test pits were used for evaluating the A-DCP, with five constructed from the soils listed in Table 1 and three from naturally occurring ground sites or ongoing test areas of uniform soil. The following illustrations note the soil condition for each test pit with depth.

Test Pit 1 (Figure 5). A confined sand layer to assess increasing strength with depth due to confinement on a clean frictional material and to determine whether there is any softening of the sand layer due to vibrations occurring from the blow frequency of the A-DCP device.

Figure 5. Pit 1 – Clay gravel over sand layering.

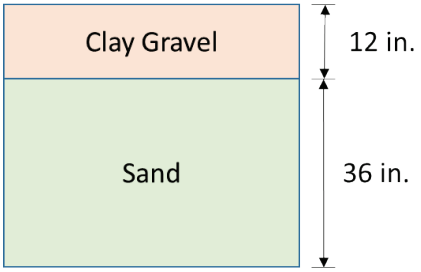

Test Pit 2 (Figure 6). A clean gravel surface that uses washed gravel to evaluate the influence A-DCP blow-count frequency may have on the strength of a coarser fraction of soil.

Figure 6. Pit 2 – Crushed rock over silt layering.

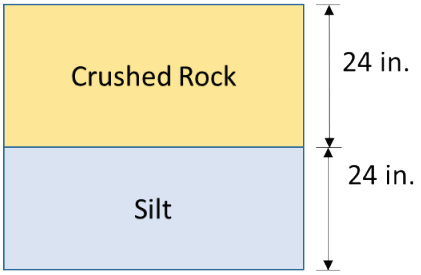

Test Pit 3 (Figure 7). A soft-to-hard layering system to simulate an undisturbed ground condition typical during contingency airfield surveys.

Figure 7. Pit 3 – Silt over clay gravel over limestone base.

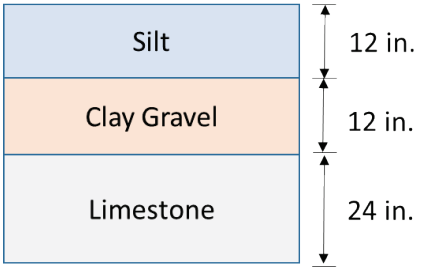

Test Pit 4 (Figure 8). A hard surface layer that is representative of a typical airfield with limestone base course, a compacted subbase, and a soft subgrade.

Figure 8. Pit 4 – Limestone over clay gravel over heavy clay.

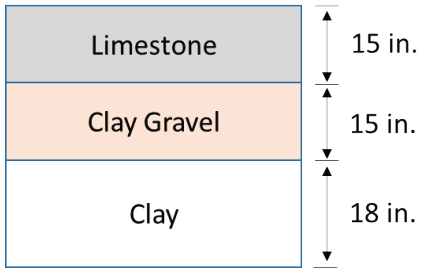

Test Pit 5 (Figure 9). A heavy clay section that has high plasticity whereby the DCP rod can penetrate easily, but extraction of an embedded rod 3 in. deep may prove difficult.

Figure 9. Pit 5 – Heavy clay.

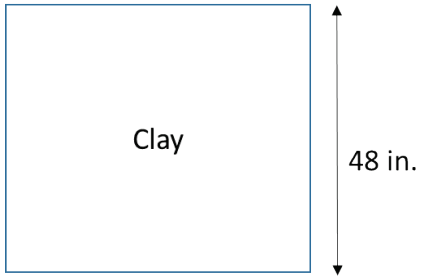

Test Pit 6 (Figure 10). A natural test site to evaluate an unknown cross section to test the system blindly and to provide variable CBR values with depth.

Figure 10. Pit 6 – Natural test site.

Test Pit 7 (Figure 11). A test section having 12 in. of compacted limestone overlying a natural subgrade consisting of a lean silty clay.

Figure 11. Pit 7 – Limestone base.

Test Pit 8 (Figure 12). A natural test site used to evaluate the potential difference between single blows and the continuous automatic mode.

Figure 12. Pit 8 – Natural test site.

2.3 Data collection plan

The experimental plan involved conducting a manual DCP (dual-mass DCP, using the large 17.6-lb hammer) alongside the A-DCP in both its manual and automatic modes across each test pit described in the previous section. Two identical A-DCP units were tested: Happy (serial number 4) and Sneezy (serial number 5). Each test pit had three test locations, labeled A, B, and C, as shown in Figure 13. Three tests were conducted using each method and device. Triplicates of a truck-mounted CBR test (in situ CBR) were conducted close to location A. The in situ CBRs were collected at the top/interface of each layer and the middle of each layer. The A-DCP's and manual DCP's penetration rates were compared directly

to assess similarity among the different devices and methods. The cumulative blows versus depth of penetration were also used to quickly assess the difference using the different methods and devices.

Figure 13. Locations for the comparison testing: in situ CBR was taken at location A.

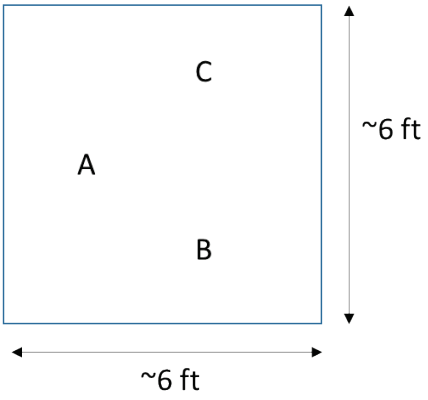

2.4 Uncorrected cumulative blow-count comparison

Comparisons between the two A-DCP units and the manual dual-mass DCP were based on an evaluation of the cumulative blow count occurring in each test pit. Traditionally, DCP data have been visualized as a plot using the ASTM conversion of penetration rate to CBR and comparing that CBR to depth of the penetration. However, cumulative blow count with depth of penetration removes any bias associated with the DCP-CBR correlation. Further, if the energy per blow is the same between the A-DCP and the manual DCP, then they should accumulate blow counts with depth at the same rate, quickly allowing for identification of any deviations in response.

For each A-DCP unit, Happy and Sneezy, a plot of the depth of penetration versus the cumulative blow count was created for each of the eight test sections. Initially, Happy was chosen as the device to run an additional set of tests in its manual hand-crank mode; but during testing of Test Pit 2, the manual mode failed; therefore, Sneezy was used to continue testing the manual mode. After testing the manual mode for the first six pits, it was noted that the manual mode data were not producing blow-count results with depth similar to those of the automatic data. Additionally, the manual mode was difficult to use in that it required two people to operate (i.e., one to turn the crank and one to stand on the device to ensure it was in the proper position). Occasionally, the two people operating the device would have to switch roles because of operator fatigue from turning the hand crank. After completion of the initial six pits, the manual mode

testing was discontinued due to its difficulty and inconsistent results when compared to automatic mode. Figure 14 and Figure 15 illustrate the uncorrected response of the A-DCP operating in automatic mode.

The cumulative blow count for each device for each test pit was analyzed as a way to determine the variability. The final cumulative blow-count value used for each test within each pit was determined by recording the cumulative blow count at the greatest depth for all three tests, generally from 34 to 36 in. Because the exact final depth varied, care was taken so that the final blow count was recorded for the three tests within 1 in. of each other. These three values were averaged, and the standard deviation and coefficient of variation (COV) were computed, as shown in Table 2. For both Happy and Sneezy, the COV values for all the test pits were compared to the dual-mass DCP COV. The average COV between the A-DCP and the Dual-Mass DCP units are all within 5% of each other, indicating a comparable blow-count response with depth.

Table 2. Comparison of final cumulative blow-count values for the A-DCPs and dual-mass DCP.

Test	Pit #	Final Cumulative Blow-Count Values for A-DCP				Final Cumulative Blow-Count Values for Dual-Mass DCP			
		Avg[a]	Stdev[b]	COV[c]	Avg COV[d]	Avg[a]	Stdev[b]	COV[c]	Avg COV[d]
Happy (SN4)	1	64.0	22.9	35.7	16.6	46.0	12.5	27.2	15.9
	2	78.0	7.0	9.0		53.0	6.2	11.8	
	3	166.0	25.7	15.5		98.3	2.1	2.1	
	4	68.7	4.9	7.2		39.0	2.6	6.8	
	5	108.3	8.5	7.9		43.7	9.0	20.7	
	6	85.3	10.4	12.2		53.0	12.1	22.9	
	7	233.0	35.8	15.3		127.0	20.8	16.4	
	8	120.3	35.8	29.8		89.7	17.8	19.8	
Sneezy (SN5)	1	71.3	10.0	14.0	14.2	46.7	12.9	27.6	16.0
	2	74.7	13.6	18.2		53.0	6.2	11.8	
	3	157.0	14.8	9.4		98.3	2.1	2.1	
	4	60.0	15.6	26.0		39.0	2.6	6.8	
	5	82.0	3.0	3.7		43.7	9.0	20.7	
	6	80.7	10.7	13.3		54.0	12.8	23.6	
	8	117.3	17.4	14.8		90.7	17.8	19.6	

[a]Average

[b]Standard deviation

[c]Coefficient of variation

[d]Average coefficient of variation for all the test pits

Several patterns can be observed in the data.

1. Table 2 indicates the error associated with A-DCP blow-count accumulation with depth was similar between devices, independent of soil type.
2. The A-DCP captured layer breaks between dissimilar soil types at the same location as the manual dual-mass DCP (i.e., Test Pit 3 in Figure 14), suggesting similar sensitivities to soil strength.
3. The A-DCP accumulated a greater number of blows with depth than the manual dual-mass DCP, as evidenced on the plots by the drift of the curves to the right of those of the dual-mass DCP.
4. When operating in single-blow mode, the A-DCP produced a very similar cumulative blow count to the automatic mode.

It is pertinent to note that similar conclusions were achieved for patterns 1 through 3 during the formal validation study presented later in this report.

Figure 14. Cumulative correlation for Happy, no correction factor.

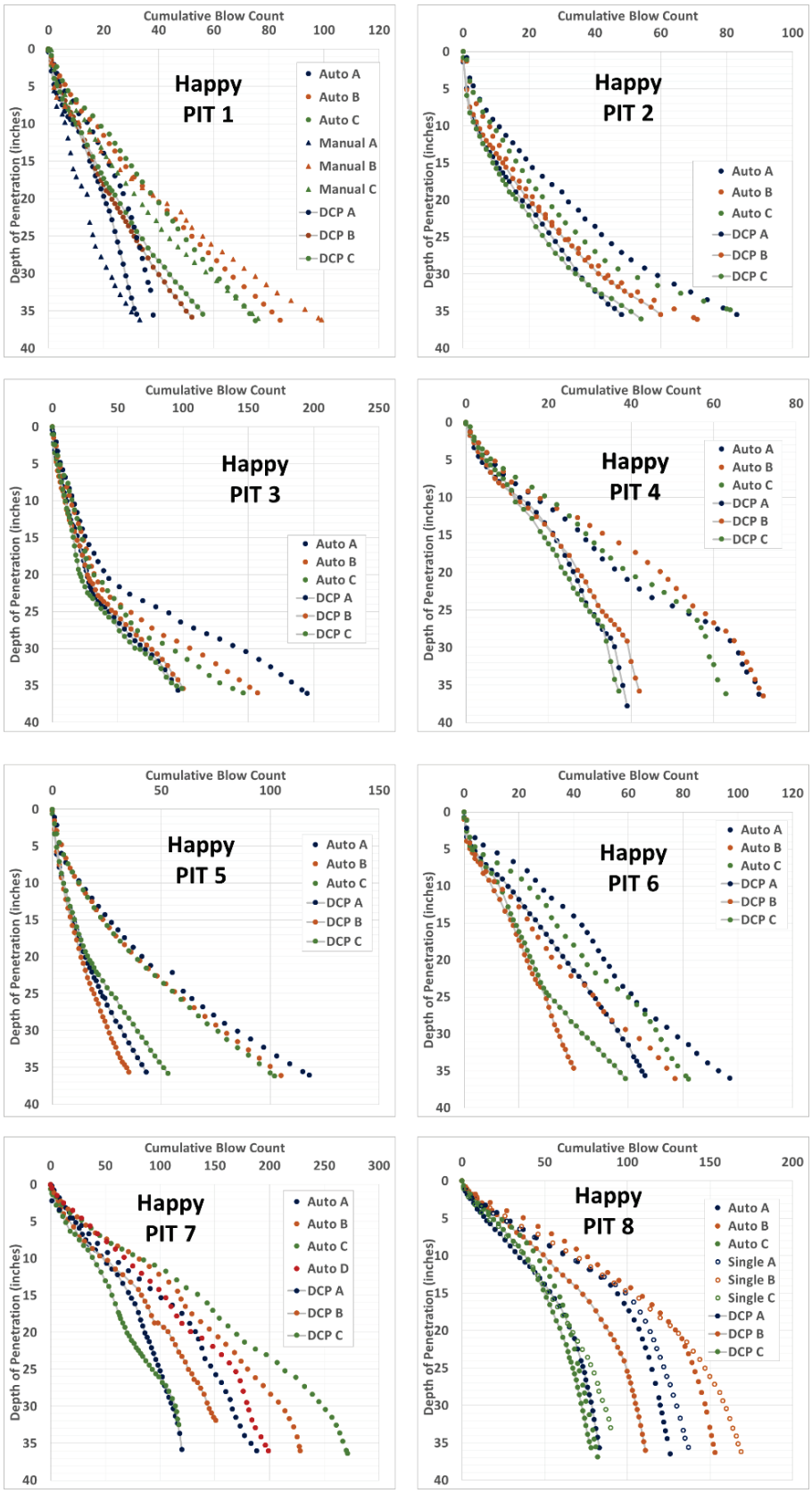

Figure 15. Cumulative correlation for Sneezy, no correction factor.

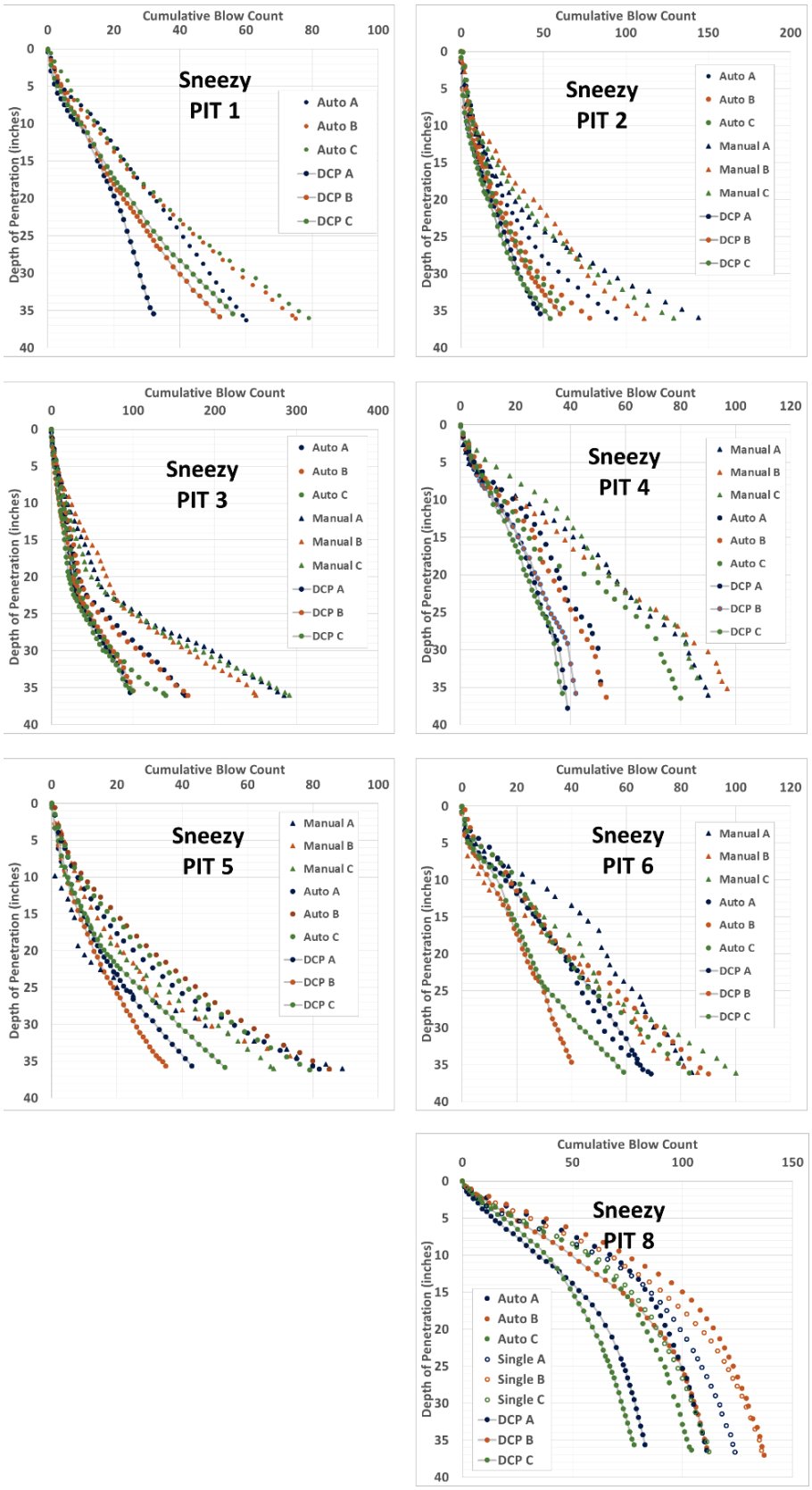

2.5 Corrected blow-count correlation

Two of the most concerning issues with the data were the higher accumulated blow count and the behavior of the A-DCP in single-blow mode. Through trial and error, a shift that is assumed to be associated with an energy differential was noted between the A-DCP and the manual DCP blow count. A correction factor, applied by dividing the cumulative blow count of the A-DCP by a factor of 1.6, appeared to improve the comparison between the A-DCP cumulative blow curves and the DCP curves (Figure 16 and Figure 17, respectively). The observation that a factor must be incorporated to get the two devices to match responses suggests that the penetration rate to CBR correlation is not the same for the A-DCP as for the dual-mass DCP. Thus, the same general equation (i.e., CBR = 292/(penetration rate)$^{1.12}$) cannot be used to correlate the A-DCP data to CBR. This critical finding highlighted the need to perform a formal validation study in which a new correlation is developed to produce accurate CBR values from the A-DCP devices.

Figure 16. Cumulative correlation for Happy with correction factor of 1.6.

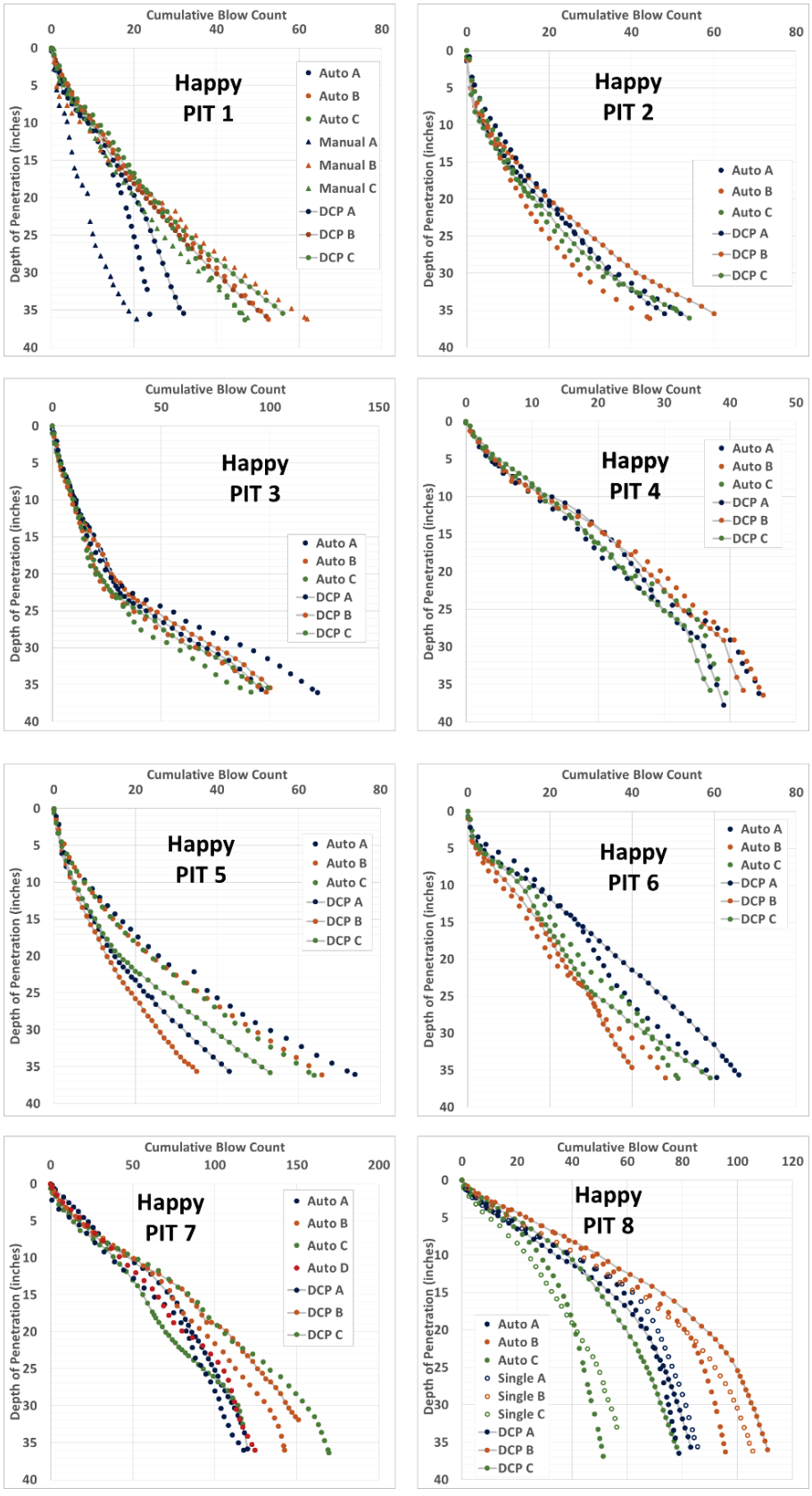

Figure 17. Cumulative correlation for Sneezy with correction factor of 1.6.

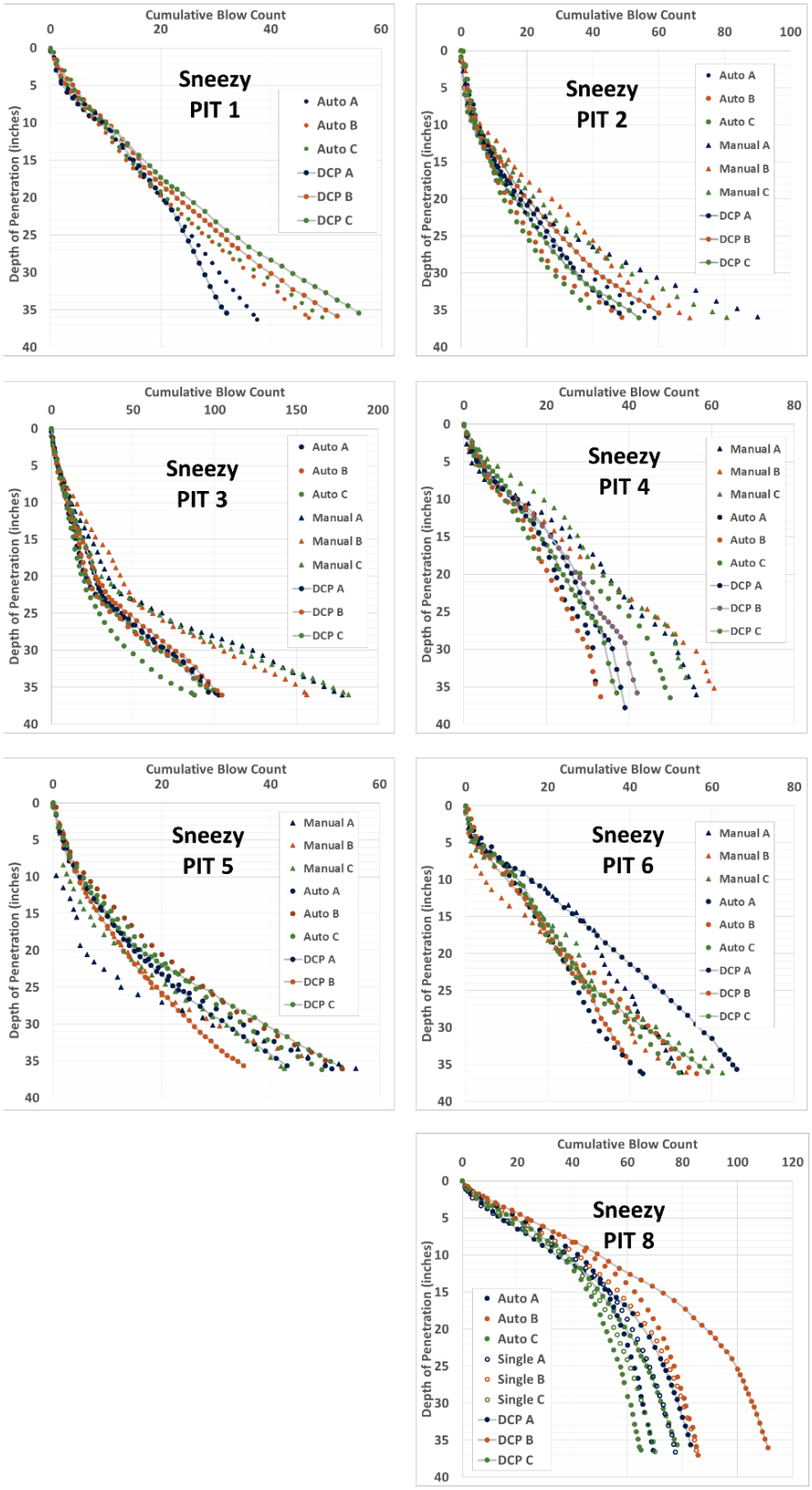

2.6 Comparison of penetration rate to CBR response

The DCP index, or penetration rate, is the measurement of penetration in mm's divided by the number of blows. Penetration rate is the basis for the development of the DCP Index-CBR curve correlation previously mentioned. To show the influence of varying blow-count accumulation, the penetration rate was plotted versus depth to highlight the trend as the manual dual-mass DCP or A-DCP progressed into the ground. Figure 18 shows a graphical example of this, using data obtained from Test Pit 1, Location C. For each test pit, the penetration rate for each device was recorded at the same depth at which an in situ CBR was measured. A summary of the data used for the analysis can be found in Table 3.

Figure 18. Example of the penetration rate, or index, plotted by depth.

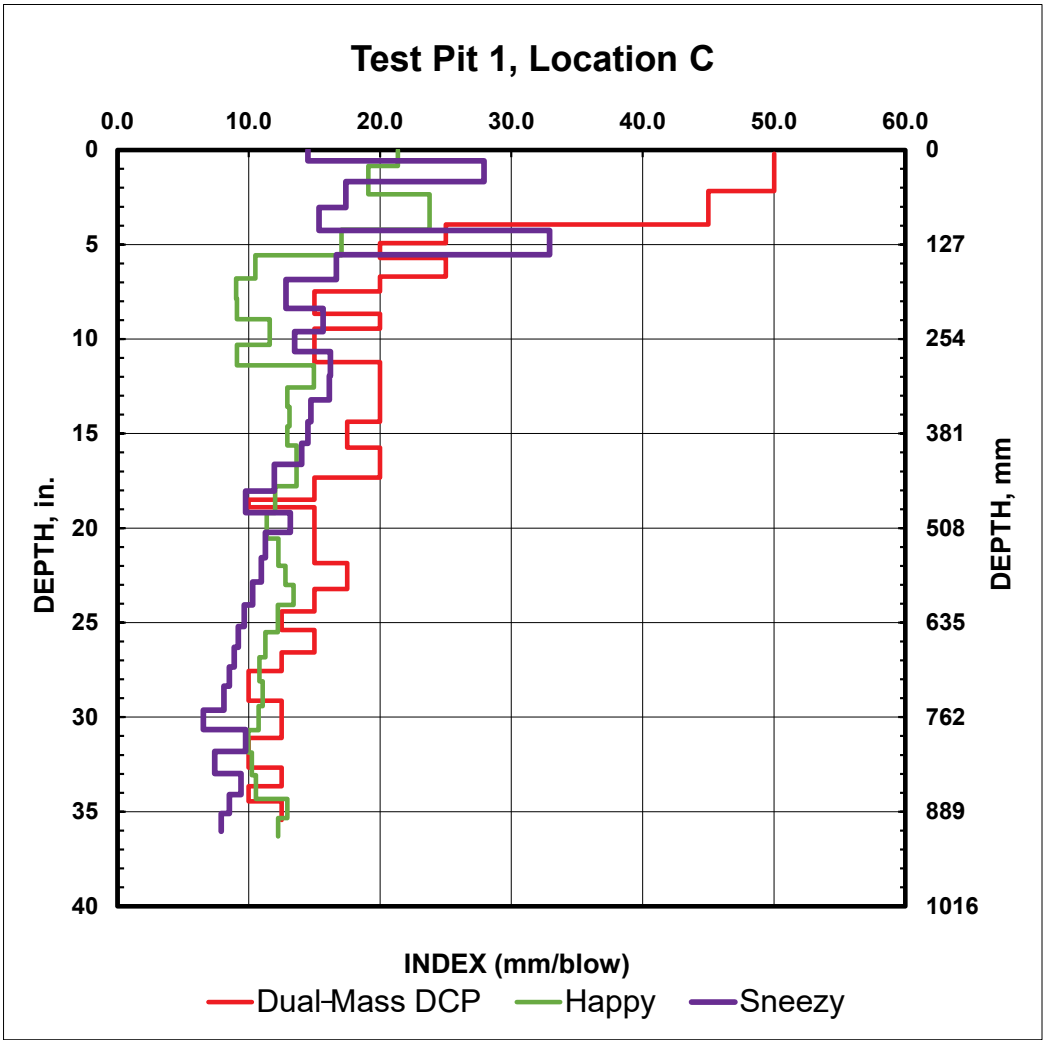

Figure 19 shows the selected Table 3 penetration rates versus in situ CBR. The two A-DCP units, as well as the manual dual-mass DCP, are plotted together in this graph to show the results of the penetration rate-CBR response when compared against the general dual-mass correlation found in literature, which is represented by a solid black line. The next two figures (Figure 20 and Figure 21) illustrate how the data collected during this experiment relate to the historical data points used to develop the DCP-CBR correlation. In Figure 20, the red circles represent the manual dual-mass data collected during this experiment. In Figure 21, the A-DCP data are represented by blue squares and triangles.

As expected, the penetration data collected with the manual dual-mass DCP tended to be closer to the original data used in the correlation than that collected with the A-DCP. The A-DCP data appeared to have a leftward shift when compared to historical data, suggesting that the A-DCP penetration rate was less than that of the dual-mass DCP for each measured CBR value. This suggests that a new penetration rate-CBR correlation will be required for the A-DCP.

Figure 19. Summary of penetration rate for the A-DCP units and the dual-mass DCP.

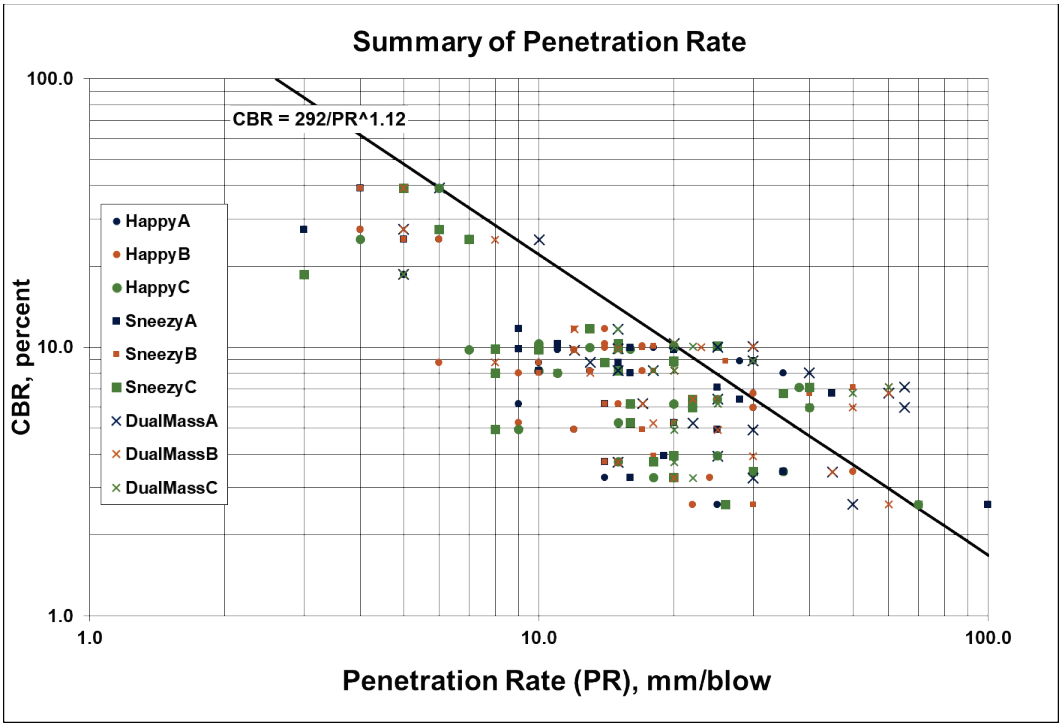

Figure 20. Penetration rate for the historical DCP data and the current DCP data.

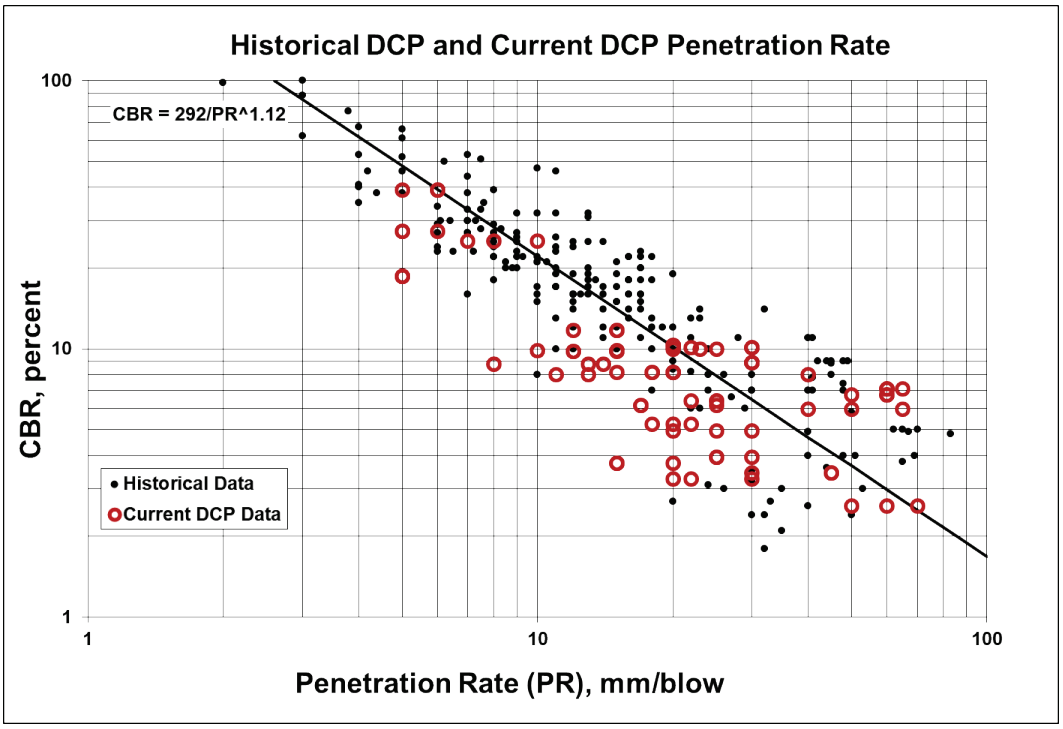

Figure 21. Penetration rate for the historical DCP data and the current A-DCP data.

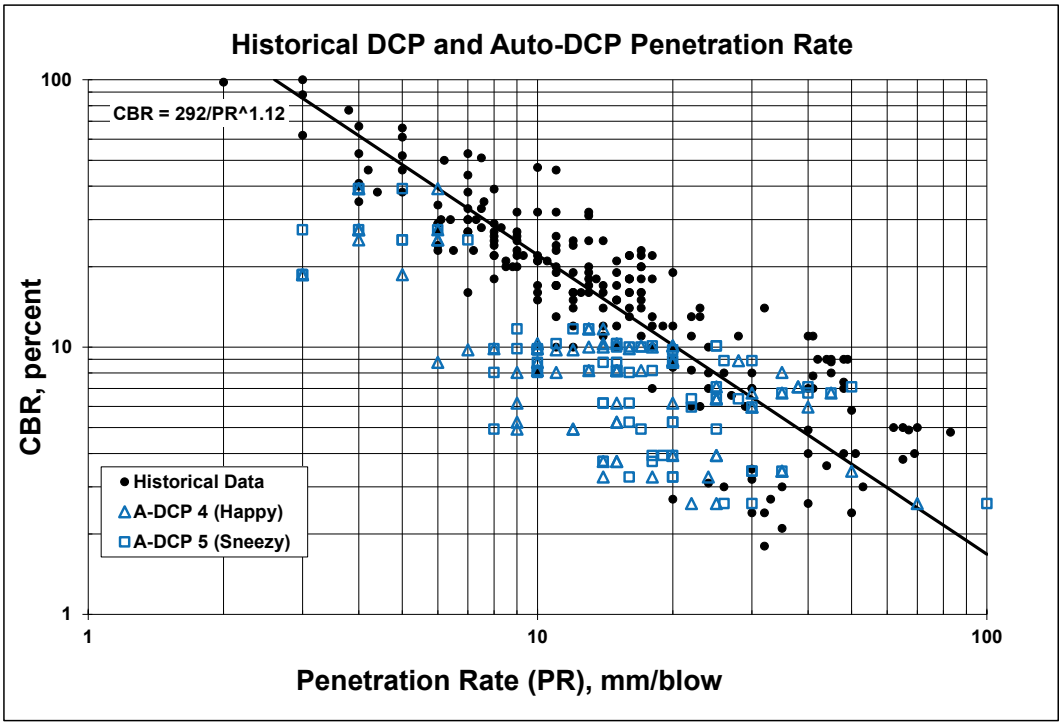

Table 3. Penetration rates for the three devices tested, for each location, A, B, and C.

PIT #	Depth (in.)	Soil Type	CBR Avg	Penetration Rate for Dual-Mass DCP			Penetration Rate for Thumper 4, Happy			Penetration Rate for Thumper 5, Sneezy		
				DCP A	DCP B	DCP C	Happy A	Happy B	Happy C	Sneezy A	Sneezy B	Sneezy C
1	0	Clay Gravel	8.9	30	30	30	28	20	20	30	26	20
1	6	Clay Gravel	10.3	20	20	20	15	14	10	11	15	15
1	12	Sand	10.0	25	23	20	18	14	13	16	17	15
1	30	Sand	8.0	40	13	11	35	9	11	16	10	8
2	0	Crushed Rock	7.1	65	60	60	25	38	38	25	50	40
2	12	Crushed Rock	3.3	30	20	22	14	24	18	16	20	20
2	24	Silt	11.7	15	12	15	13	14	13	9	12	13
2	36	Silt	25.2	10	8	7	6	6	4	5	5	7
3	0	Silt	3.9	25	30	25	20	25	25	19	18	20
3	6	Silt	8.2	18	20	20	13	15	15	15	13	15
3	12	Clay Gravel	3.7	15	15	20	15	14	15	14	14	18
3	18	Clay Gravel	6.2	17	17	25	9	15	20	14	14	16
3	24	Limestone	27.5	5	5	6	4	4	6	3	4	6
3	36	Limestone	18.7	5	5	5	5	3	3	3	3	3
4	0	Limestone	10.1	30	30	22	20	17	20	25	18	25
4	7	Limestone	8.2	15	20	18	15	17	10	10	18	15
4	15	Clay Gravel	5.2	22	18	20	15	9	15	20	20	16
4	21	Clay Gravel	4.9	30	25	20	12	12	9	25	17	8
4	30	Clay	2.6	50	60	70	25	22	70	100	30	26
4	38	Clay	6.0	65	50	40	30	30	40	114	30	22
5	0	Clay	6.7	60	60	50	45	30	35	45	40	35
6	0	Natural	3.4	45	45	30	35	50	35	35	30	30
6	24	Natural	9.8	12	12	15	11	12	7	20	10	10
6	30	Natural	9.9	15	15	10	8	10	16	9	10	8
8	8	Natural	39.2	6	5	6	4	4	6	4	4	5
8	18	Natural	8.8	13	8	14	10	6	20	15	10	14
8	30	Natural	6.4	25	22	25	25	25	25	28	25	22

2.7 Single blow versus automatic mode

Since the cumulative blow-count correlation for the A-DCP and the manual DCP had similar trends but appeared to be offset by a correction factor, a study of the behavior of the A-DCP using its single-blow feature was investigated. The impact loads from the manual DCP and the A-DCP were measured using a floor-mounted load cell, as shown in Figure 22. The rods for each device were threaded into the top of a load cell to provide constant contact with the load cell and to eliminate bounce of the apparatus. Figure 23 reveals that the loads are very similar and do not appear to be meaningfully different.

The single-blow method involved pressing the A-DCP fire button to activate a single blow rather than allowing it to run on its own. The fire button was repeatedly pressed until the A-DCP had penetrated full depth. Test Pit 8, a natural test location, was used to evaluate the effect of utilizing the single-blow mode of operation. Figure 24 and Figure 25 present data from Happy

and Sneezy, respectively. As can be seen in these two graphs, the single-blow method data were similar to the automatic method data.

It was hypothesized that the cumulative penetration drift noted earlier may be due to a mechanical flaw in the manual counter that was used to determine the number of blows induced in the system. By using the single-blow method, each blow could be manually verified such that no false blows were counted. The fact that the two curves showed relatively the same drift from the dual-mass DCP suggested that the drift was likely due to an energy or physical change in the A-DCP system not yet accounted for. This finding further reinforced the observations that the A-DCP required its own correlation to in-situ CBR.

What can be observed but was not quantified sufficiently until the validation study described later in this report is that the manual DCP exhibited a significant rebound of the hammer following the first impact. The secondary and tertiary impacts of the DCP hammer effectively imparted additional energy into the soil, thereby increasing the efficiency of the manual DCP device over the A-DCP. This in turn could explain the greater number of blows required by the A-DCP to achieve full penetration through the soil test pits than the manual dual-mass DCP. Evidence to support this hypothesis is provided in Chapter 5.

Figure 22. Setup of A-DCP on load cell for calibration of single-blow energy.

Figure 23. Load cell measurements.

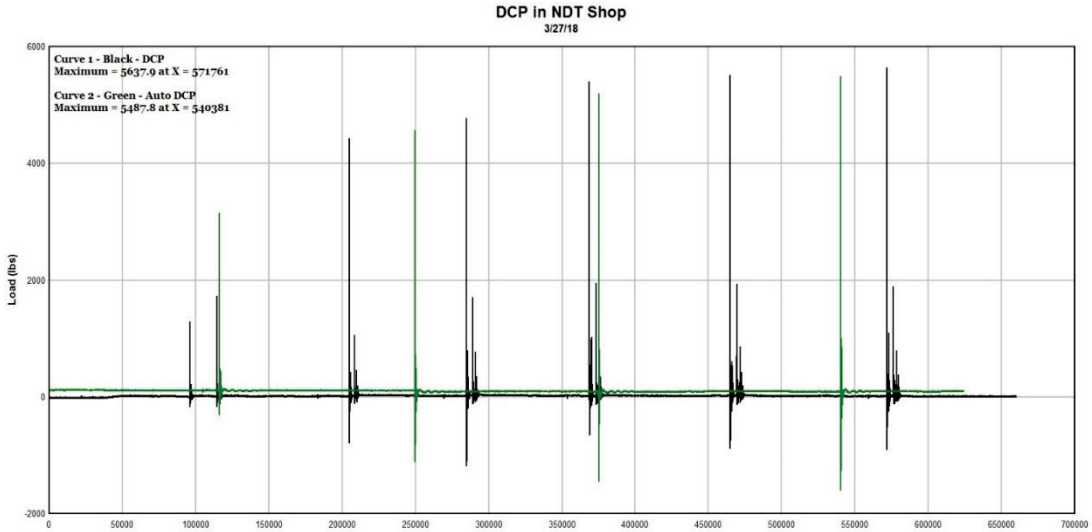

Figure 24. Cumulative blow count plotted by depth for Pit 8, comparing the single blow count and the automatic method for Happy A-DCP.

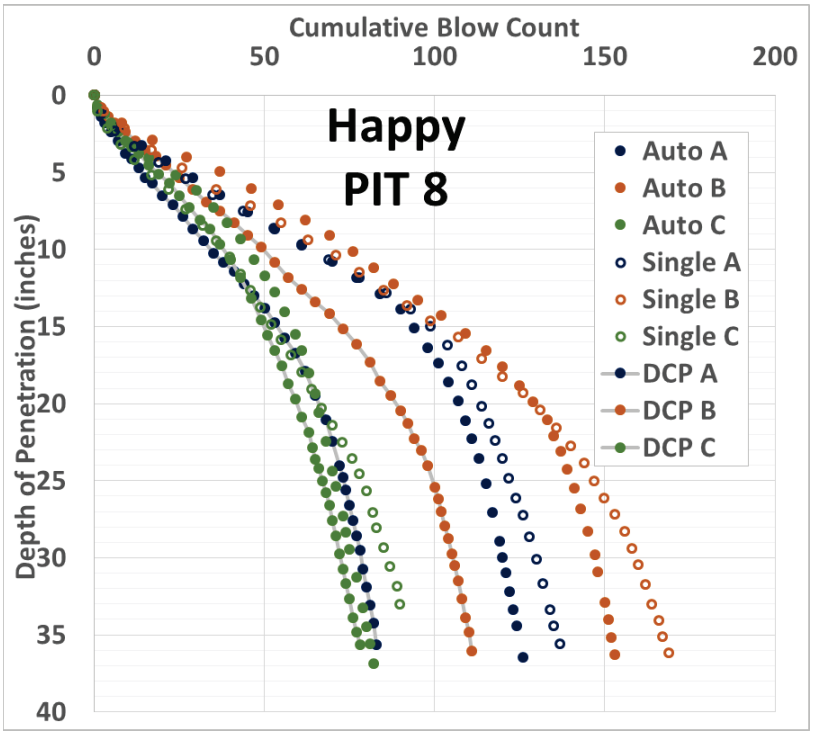

Figure 25. Cumulative blow count plotted by depth for Pit 8, comparing the single blow count and the automatic method for the Sneezy A-DCP.

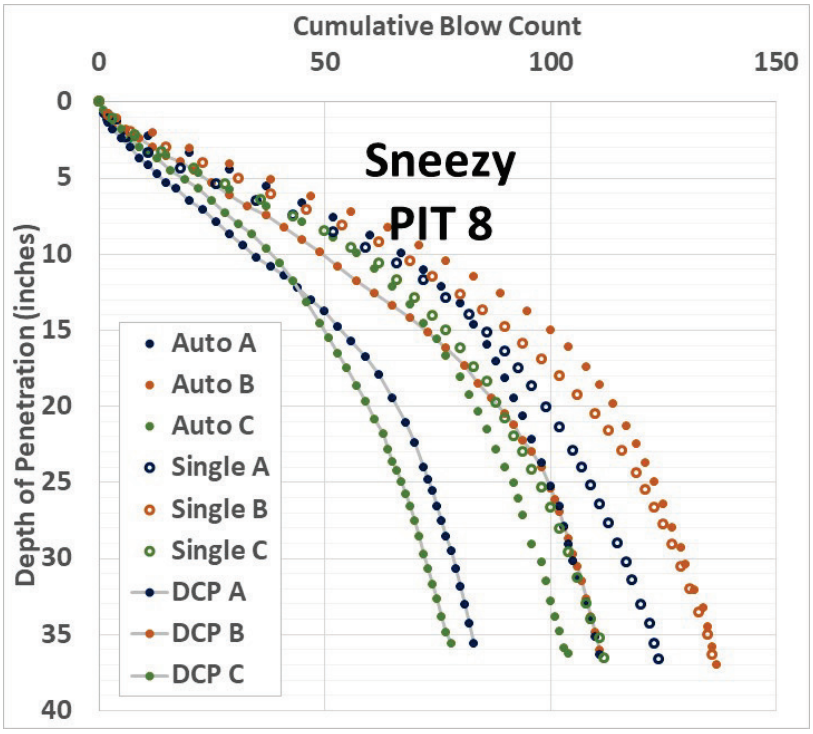

3 Validation of Second Generation A-DCP prototype

In 2020, ERDC was tasked with performing a final validation of the A-DCP device with the goal to develop a calibration curve capable of calculating the in situ CBR value from the A-DCP penetration rate value. To accomplish this research, ERDC established a list of materials representing a range of soil strengths from which to construct homogeneous test sections. In situ CBR tests were performed on each test section to enable correlation of the A-DCP results to the CBR data. A traditional truck-mounted CBR test was used to measure the CBR with depth in each test pit and a manual dual-mass DCP was performed alongside each A-DCP test for comparison.

3.1 Soil selection and test section construction

Evaluation of the A-DCP units was accomplished using a series of 12 test sections. Data from the test sections were used to populate a calibration database that could be used to establish a correlation between the data output of the A-DCP and the in situ CBR. Table 4 summarizes the soil types selected for experimentation. Each soil used in the test sections was analyzed and classified according to the Unified Soil Classification System (USCS) as described in ASTM D2487 (2017a). Modified proctor testing (ASTM 2012) was performed on each soil to determine optimum moisture content and maximum dry density. Sieve analysis (ASTM 2019) was performed on each soil type to determine the gradation of each soil. Specific Gravity (ASTM 2014, 2015) and Atterberg Limit (ASTM 2017c) testing was used in the USCS classification process. All soil testing was performed by the ERDC's Materials Testing Center. Results from soil testing can be found in Appendix A.

CBR values were strategically targeted to encompass a range of strengths to evaluate the A-DCP's performance in various strength ranges. Using modified proctor testing results, the moisture content of each soil was selected to obtain the desired density to achieve the targeted CBR based on laboratory data.

Table 4. Soil properties.

Material	USCS	Optimum Moisture (%)	Maximum Dry Density (pcf)	Specific Gravity	LL	PI
Heavy Clay	CH	17.5	106.1	2.73	74	50
Silt	ML	15.8	109.4	2.76	30	6
Sand	SP	4.5	103.8	2.6	--[a]	--[a]
Limestone	GP-GM	5.3	146.4	2.76	NV[b]	NP[c]
Silty Sand	SM	8.1	131.4	2.65	NV[b]	NP[c]
Clayey Sand	SC	5.0	139.2	2.69	25	14
Lean Clay	CL	13.6	116.8	2.76	34	17

[a]Data were not determined during laboratory testing.

[b]NV denotes a nonviscous material.

[c]NP denotes a nonplastic material.

3.1.1 Heavy clay - CH

A heavy clay (Figure 26) was chosen to achieve a 2, 4, and 6 CBR. This soil was selected to examine the A-DCP's reaction to rod friction that is typically experienced with a manual DCP. As the rod penetrates further into heavy clays, rod friction reduces the penetration rate, resulting in abnormally high CBR readings. The heavy clay used during testing is known as a Vicksburg buckshot clay, which classified as a CH according to the USCS (ASTM 2017a) . The heavy clay had a specific gravity of 2.73 (ASTM 2014). Laboratory CBR testing at multiple moisture contents identified the soil's allowable strength ranges. The optimum mositure content of the CH was found to be 17.5% with a maximum dry density of 106.1 pcf. Because it can be difficult to process and place CH at moisture contents at or below optimum moisture content, it was decided to prepare the CH at moisture contents greater than optimum. The CH was constructed at an average moisture content of 30.4% but post-test moistures at the time of CBR testing revealed an increase in average moisture content to 35.8% likely due to difficulty in achieving uniform soil moisture during processing. The soil was compacted with a pneumatic roller and reached an a dry density between 80 and 83 pcf, which was measured with a nuclear density gauge (ASTM 2017b). Table 5 summarized the measured properties of the heavy clay test section constructed.

Table 5. Heavy clay test section properties.

	Pre-Test	Post-Test
Average Moisture Content (%)	30.4	35.8
Dry Density (pcf)	80.5	83.6
Average CBR		5.0

Figure 26. Heavy clay (CH) during processing.

3.1.2 Silt - ML

Silt (Figure 27) was used to target a CBR of approximately 20. The silt was classified according to USCS as an ML. Silt was constructed in two test sections. The optimum moisture content of the ML was determined to be 15.8% and a maximum dry density of 109.4 pcf. The ML's specific gravity was 2.76. The first test section was constructed at an average moisture content of 16.8% and dry density of 99.5 pcf. The CBR for test section 1 had an average of 20 CBR. The second test section had an average of 21.4% moisture content. The ML was compacted to an average dry density of 97.8 pcf. The material in test section 2 was wet of optimum, and pumping was observed during compaction. An average CBR of 1 was measured for test section 2. Both silt test sections were compacted using the sheepsfoot roller. Table 6 summarizes the measured properties of the silt test sections constructed.

Table 6. Silt test sections properties.

Property	Test Section 1	Test Section 2
Average Moisture Content (%)	16.8	21.4 (22.5)
Dry Density (pcf)	99.5	97.8
Average CBR	20	1

Figure 27. Silt (ML).

3.1.3 Sand - SP

A sand test section (Figure 28) was constructed to determine the A-DCP's interaction with a sandy material. Sand does not have cohesive properties and develops its strength from confinement. On unpaved surfaces, AFSOC discards the DCP data of the top 11 in. collected in sand because it does not accurately represent the strength. The sand used in this experiment was classified as an SP according to the USCS (ASTM 2017a). From the modified proctor test results found in Appendix A, sand has two peaks on the water content versus dry density chart. The first peak, at 4.5% moisture content and a maximum dry density of 103.8 pcf, was targeted for this experiment. Sand tends to exhibit dilative tendencies around the second optimum moisture content. The specific gravity of the sand was 2.6. The average moisture content of the constructed test section was 4.3%. The sand was compacted using a plate compactor to a dry density of 103.3 pcf. Field CBRs were difficult to measure with depth, owing to the cohesionless properties of the material and difficulty in replicating the overburden properly with the surcharge weights. The approximate CBR in the top 12 in. was 6 and in the next 12 in., 11. Table 7 presents the measured properties of the sand test section constructed.

Table 7. Sand test section properties.

Property	Sand
Average Moisture Content (%)	4.3
Dry Density (pcf)	103.3
Average CBR	11

Figure 28. Sand (SP).

3.1.4 Limestone – GP-GM

Two limestone test sections were constructed for this experiment. The limestone (Figure 29) moisture content of the material was determined to be 5.3% at a maximum dry density of 146.4 pcf. The GP-GM had a specific gravity of 2.76. Test Section 1 was constructed at a 5.3% moisture content and compacted using a smooth-wheel vibratory roller to an average dry density of 137.1 pcf. Test Section 1 was allowed to sit for a week before being tested to permit the limestone to stiffen from a reduction in moisture content and cementation of the lime. The goal of Test Section 1

was to achieve a CBR of 100. Test Section 2 was constructed at a moisture content of 4.9% and compacted with a smooth-wheel compactor to a dry density of 135.5 pcf. Test Section 2 was tested immediately following construction so that no stiffening of the material could occur. An average CBR of 38 was achieved on Test Section 2. Table 8 summarized the measured properties of the limestone test sections constructed.

Table 8. Limestone test section properties.

Property	Test Section 1	Test Section 2
Average Moisture Content (%)	5.3	4.9
Dry Density (pcf)	137.1	135.5
Average CBR	100	38

Figure 29. Limestone (GP-GM).

3.1.5 Silty sand - SM

A silty sand (Figure 30) was selected to represent a mid-range CBR between 10 and 20. The silty sand was blended from the sand and silt reported in Sections 3.1.2 and 3.1.3. The silty sand was created using 3 parts sand (SP) and 1 part silt (ML). The silty sand was classified as SM according to the USCS (ASTM 2017a). The SM had a specific gravity of 2.65 and an optimum moisture content of 8.1% at a maximum dry density of 131.4 pcf. Two test sections were constructed. Test Section 1 was constructed near optimum moisture content. The average moisture content for Test Section 1 was

8.8%. The average dry density of Test Section 1 was measured to be 118.9 pcf. CBRs of Test Section 1 averaged around 12. Test Section 2 was constructed at 5.3% moisture content and compacted to a dry density of 121.8 pcf. CBRs of Test Section 2 averaged around 14. Both test sections were compacted using a smooth-wheel vibratory roller. Table 9 describes the measured properties of the silty sand test sections constructed.

Table 9. Silty sand test section properties.

Property	Test Section 1	Test Section 2
Average Moisture Content (%)	8.8	5.3
Dry Density (pcf)	118.9	121.8
Average CBR	12	14

Figure 30. Silty sand (SM).

3.1.6 Clayey sand - SC

Clayey sand, which was classified using the USCS (ASTM 2017a) as SC, obtained CBRs of 8 and 30. The optimum moisture content of the SC was determined to be 5.0% at a maximum dry density of 139.2 pcf. The specific gravity was determined to be 2.69. Figure 31 shows a photograph of the clayey sand. Two test sections were constructed with clayey sand. Test Section 1 was constructed at 8.3% moisture content and was compacted to a dry density of 127.6 pcf. An average of 8 CBR was obtained in Test Section 1. Test Section 2 obtained a 30 CBR. Test Section 2 had an average moisture content of 6.4% and a dry density of 126.1 pcf. Both test sections were compacted with a sheepsfoot roller. Table 10 summarizes the measured properties of the clayey sand test sections constructed.

Table 10. Clayey sand test section properties.

Property	Test Section 1	Test Section 2
Average Moisture Content (%)	8.3	6.4
Dry Density (pcf)	127.6	126.1
Average CBR	8	30

Figure 31. Clayey sand (SC).

3.1.7 Lean clay - CL

Lean clay (Figure 32) was used to obtain CBRs of approximately 10 and 20. The lean clay used classified as a CL, according to the USCS. The optimum moisture content of the CL was 13.6%, and its maximum dry density was 116.8 pcf. The specific gravity was determined to be 2.76. Test Section 1 was constructed at 18.3% moisture content and a maximum dry density of 100.5 pcf. Test Section 1 achieved an average CBR of 10. Test Section 2 averaged a 14.9% moisture content and compacted to a dry density of 105.5 pcf. The CBR of Test Section 2 averaged 20 CBR. Both test sections were compacted using a smooth-wheel vibratory roller. Table 11 summarizes the measured properties of the lean clay test sections constructed.

Table 11. Lean clay test section properties.

	Test Section 1	Test Section 2
Average Moisture Content (%)	18.3	14.9
Dry Density (pcf)	100.5	105.5
Average CBR	10	20

Figure 32. Lean clay (CL).

3.2 Test section construction

3.2.1 Layout

Each test section was constructed to a depth 36 in. below the surface to ensure that the DCP rods always penetrated a prepared layer. The test section had a width of 9 ft and a length of 12 ft, as shown in Figure 33. A 3:1 sloped ramp was constructed on both sides of the main test bed, allowing equipment access, and was filled with the same soil as that used in the main test bed.

Figure 33. Test section design.

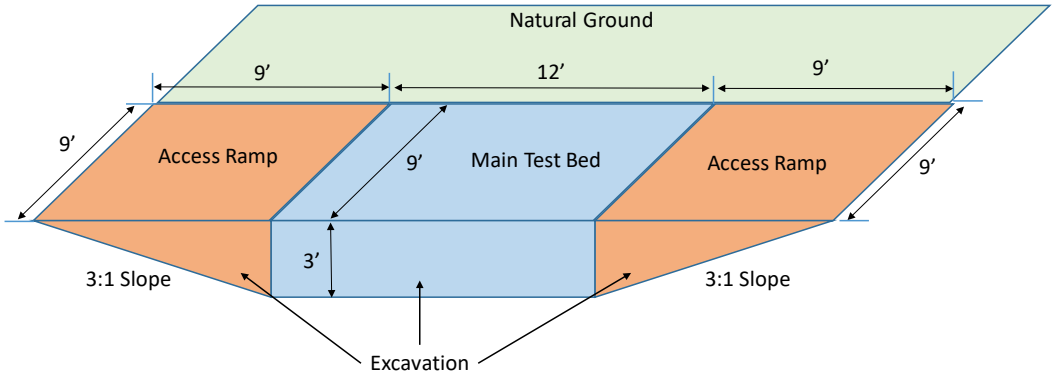

3.2.2 Equipment

3.2.2.1 Multi-terrain loader

A multi-terrain loader (MTL), CAT 277, was used to place and spread the material in each test section. Because of its ease in maneuvering and small size, it was convenient to use the MTL to construct the test section. The tracks allowed the MTL to easily travel in and out of the steep test section during construction, as shown in Figure 34. Specifications for the MTL used in this testing are listed in Table 12.

Figure 34. CAT 277.

Table 12. Caterpillar 277 multi-terrain loader specifications.

Specification Parameter	Caterpillar 277
Net power	74 hp
Operating weight	9,226 lb
Rated operating capacity	2,950 lb
Travel speed	6 mph
Tipping load	5,900 lb
Breakout force, tilt cylinder	5,259 lb
Width over tracks	6.23 ft
Height to top of cab	6.81 ft
Ground clearance	13.9 in.
Length with bucket	12.18 ft

3.2.2.2 Front-end loader

A Komat'su WA 150 front-end loader (Figure 35) was used for moving soil stockpiles and processing large amounts of material before placement. Because of its large bucket, the front-end loader was able to quickly and efficiently bring soil from the processed stockpiles to place in the test section. The specifications of the Komat'su WA 150 front-end loader can be found in Table 13.

Figure 35. Front-end loader.

Table 13. Komat'su WA 150 front-end loader specifications.

Specification Parameter	Komat'su WA 150
Net power	96 hp
Operating weight	16,369 lb
Travel speed	24 mph
Tipping load	14,043 lb
Breakout force, tilt cylinder	16,314 lb
Width over tires	7.5 ft
Height to top of cab	10 ft
Ground clearance	4.3 in.
Length with bucket	20.75 ft
Bucket capacity	2 yd^3

3.2.2.3 Smooth-wheel compactor

A Dynapac CA25 smooth-wheel compactor (Figure 36) was used to apply compaction energy to sandy materials and gravels. Specifications for the Dynapac CA25 are listed in Table 14. The front wheel is a steel drum that can perform vibratory or static compaction. The smooth wheel was used to compact the limestone, silty sand, and lean clay test sections. The number of passes to achieve the desired level of compaction varied by material type. The number of passes was determined by monitoring the dry density with a Troxler nuclear density gauge (Figure 41).

Figure 36. Smooth-wheel roller compactor.

Table 14. Dynapac CA25 smooth-wheel roller specifications.

Specification Parameter	Dynapac CA25
Net power	125 hp
Operating weight	19,800 lb
Travel speed	12 mph
Static linear load	137 lb/in.
Vibratory frequency	1,680 vpm
Drum width	84 in.
Drum diameter	60 in.
Drum shell thickness	0.98 in.
Length	207.09 in.

3.2.2.4 Pneumatic roller compactor

The Ingram 10,000 pneumatic roller compactor (Figure 37) was used to compact the heavy clay test section. Specifications of the Ingram 10,000 roller are listed in Table 15. This compactor has strategically spaced rubber tires to provide a uniform compaction coverage to the material. The number of coverages was determined by monitoring the dry density with a Troxler nuclear density gauge.

Figure 37. Pneumatic roller compactor.

Table 15. Ingram 10,000 pneumatic roller specifications.

Specification Parameter	Ingram 10000
Operating weight	13,200 lb
Length	170 in.

3.2.2.5 Plate compactor

The Northern Industrial JPC-80 plate compactor (Figure 38) was used on the sand test section to apply compaction to achieve density requirements. The smooth-wheel roller was not capable of entering and exiting the test pit during placement of the sand, nor could the sand fully support the weight of the smooth-wheel roller. Therefore, the plate compactor was used as a substitute to the smooth-wheel roller. Compaction using a plate compactor was performed in a circular coverage method. The operator started on the outside and worked inside and then repeated the process. This was considered two coverages. The number of coverages was

determined by monitoring the dry density with a Troxler nuclear density gauge. The specifications for the plate compactor are listed in Table 16.

Figure 38. Plate compactor.

Table 16. Northern Industrial JPC-80 plate compactor specifications.

Specification Parameter	Northern Industries JPC-80
Net power	5.5~6.0 hp
Weight	86 lb
Plate size	21.25 in. x 16.5 in.
Travel speed	65-82 ft/min

3.2.2.6 Sheepsfoot compactor

A CAT CS-433E sheepsfoot compactor (Figure 39) was used on clayey sand and silt test sections. The sheepsfoot compactor had small circular feet on the compaction drum. These feet provide a higher contact pressure with the material. Each section was smoothed with the smooth-wheel compactor after compacting with the sheepsfoot to allow a flat surface for density testing. The number of coverages was determined by monitoring the dry density with a Troxler nuclear density gauge. Specifications for the CAT CS-433E sheepsfoot compactor are listed in Table 17.

Figure 39. Sheepsfoot roller.

Table 17. CAT CS-433E sheepsfoot compactor specifications.

Specification Parameter	CAT CS-433E
Net power	96.6 hp
Operating weight	15,410.4 lb
Max speed	7.2 mph
Static linear load	288.8 lb/in.
Drum width	66 in.
Drum diameter	48.3 in.

3.2.2.7 Mini-excavator

The Bobcat E45 mini-excavator (Figure 40) was used to excavate the CBR test trench and the test section after test completion. The mini-excavator was selected because of its ability to precisely excavate a narrow trench while operating within a confined space. A flat plate was mounted on the bucket, across the teeth, to allow for smooth excavation of the CBR test pit. Specifications of the Bobcat E45 mini-excavator can be found in Table 18.

Figure 40. Mini-excavator.

Table 18. Bobcat E45 mini-excavator specifications.

Specification Parameter	Bobcat E45
Net power	42.7 hp
Operating weight	10,077 lb
Dig depth	10.8 ft
Reach at ground level	18.6 ft
Bucket digging force	7,650 lb-ft

3.3 Testing devices

3.3.1 Nuclear density gauge

A Troxler Model 3440 nuclear density gauge (NDG), shown in Figure 41, was used to evaluate in situ density. The NDG uses a radioactive source to measure the density of a soil. The source rod is lowered into a predrilled hole in the soil, and the NDG counts the amount of radiation that is allowed to pass through the soil to reach the detector tubes, which are located on the opposite side of the radioactive source. With a less dense soil, more gamma rays are transmitted through the soil and counted by the detector tubes, indicating a low density. With higher densities, fewer gamma rays are allowed to pass through the soil. Therefore, they are not able to be counted by the detector tubes, indicating a high density. The NDG's measurable depth is between 4 and8 in. For this experiment, the rod was inserted into the ground at a depth of 4 in.

The NDG also measures the moisture content of the soil by releasing neutrons into the soil. When the neutrons interact with hydrogen

particles, the neutrons slow. The Helium 3 tubes in the NDG can detect only the neutrons that have slowed down their movement after interacting with the hydrogen molecules. Therefore, high neutron counts from the Helium 3 tubes indicate a high moisture count.

The NDG was used for in situ soil moisture and density measurement during test section construction. A soil sample was collected near each NDG test location for oven-dry moisture determination to confirm actual in situ moisture content. The NDG was used between compaction passes on each test section to determine when the material reached the desired dry density.

Figure 41. Troxler nuclear density gauge.

3.3.2 Automatic dynamic cone penetrometer

The Honeybee Robotics Tactical Hammer for User-Manipulated Penetrometer Evaluation and Recording (THUMPER), also referred to as the Automatic Dynamic Cone Penetrometer, was used in this experiment, as shown in Figure 42. The A-DCP uses an electric motor to curl a spiral cam to compress a spring. The spring is released and strikes the hammer, causing energy to transfer through the rod. This pushes the rod through the soil and measures the rod's rate of penetration. The rate of penetration can be used to correlate to a CBR. The electric motor is powered by a 60-volt 9.0 amp-hour lithium-ion battery, which provides approximately 2,000 blows of the A-DCP before recharging is required. Two different A-DCP units (i.e., A-DCP #1 and

A-DCP #2) were used in this experiment, as Happy and Sneezy from the previous experiment had been returned to the manufacturer.

Figure 42. Automatic Dynamic Cone Penetrometer.

3.3.3 Dual-mass dynamic cone penetrometer

The dual-mass dynamic cone penetrometer (DCP) (Figure 43) was used in this experiment to compare to the A-DCP. The DCP is used to approximate soil strength and to approximate the location of soil layers. A metal cone is attached to the steel rod and the cone is driven into the ground by lifting and dropping a weight from a known drop height. The weight generates a force and drives the cone into the ground. A measurement rod is used to measure the penetration rate. A lower penetration rate correlates to a stronger soil with a higher CBR value. As the rod is driven into the soil, the penetration rate changes; through data analysis, soil layers can be determined. The modern DCP-CBR correlation allows operators to perform quick CBR checks.

Figure 43. Conventional dual-mass DCP testing.

3.3.4 Instrumented dynamic cone penetrometer

An instrumented dynamic cone penetrometer was developed at ERDC to measure the influence of force acting on the drive rod. To accomplish this, a load cell was fabricated to fit in line with a manual DCP, adding only a small weight to the overall frame (Figure 44). When the weight of the DCP hammer was dropped, the force generated on the penetration rod was recorded. The intent was to measure the accumulation of force resulting from hammer rebound during testing. The same testing procedure that was used with testing the manual DCP was used for testing the instrumented DCP. However, as shown in Chapter 5, this analysis proved not to be necessary, as a direct comparison of hammer load between the A-DCP and the manual DCP on an instrumented load frame proved sufficient to identify the change in accumulated force.

Figure 44. Instrumented Dynamic Cone Penetrometer.

3.3.5 In situ California Bearing Ratio

The in situ California Bearing Ratio test, shown in Figure 45, was used to establish the true value to correlate to the A-DCP penetration rate. The in situ CBR test was designed to determine the load-carrying capacity of a soil. A test trench was excavated to perform CBR measurements for each lift, as shown in Figure 46. Three CBRs were performed on the surface and each subsequent 6-in. lift. An in situ CBR apparatus was mounted to a 2.5-ton Army truck. Proving rings of specific load ratings were used on each soil. Stiff soils, such as limestone, require proving rings with a higher load rating than proving rings required for clay or silt. A steel plate was placed under the penetration piston to evenly distribute the surcharge reaction. As the depth of the excavation increased, surcharge weights were added to the steel plate to represent the overburden of the soil removed to simulate the conditions the soil experienced while being tested by the devices. This was especially critical when conducting CBR tests at depth for each test pit and on coarse-grained soils, whose strength originates primarily from friction generated from overburden pressures.

Figure 45. Truck-mounted in situ CBR testing.

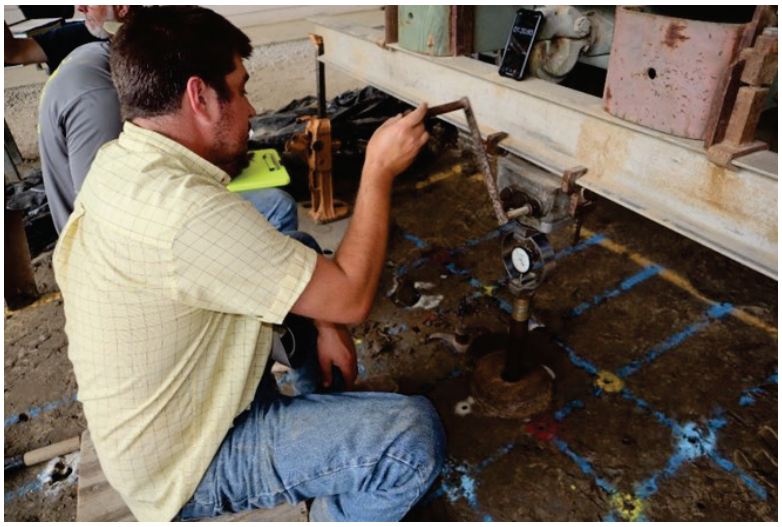

Figure 46. CBR test trench.

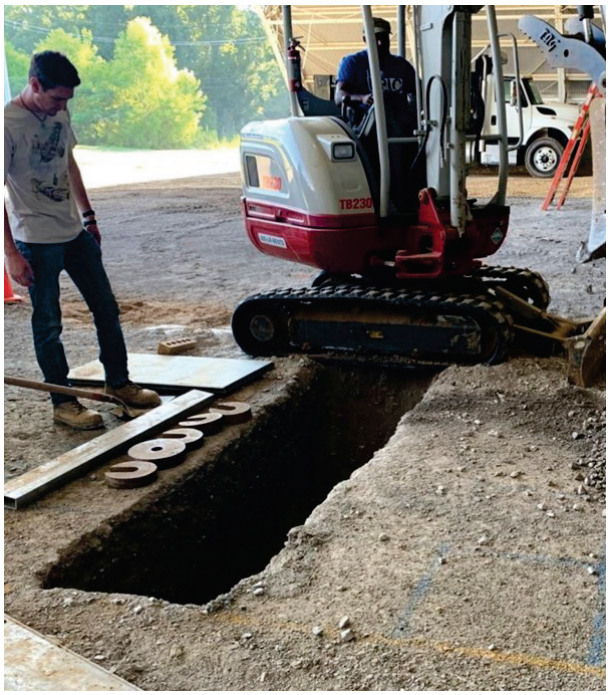

3.3.6 Clegg hammer

A Clegg hammer Model 96051, as shown in Figure 47, was used as a secondary measure to obtain the strength and stiffness of soils. A 4.5-kg (10-lb) Clegg hammer was used for this experiment. The Clegg hammer is located inside a guide tube. To perform a Clegg hammer drop, the hammer is pulled up the tube to the marked drop height and released. The Clegg hammer is equipped with accelerometers to measure the deceleration rate of the hammer upon impact with the soil. The Clegg hammer produces

measurements referred to as Clegg Impact Values (CIV). For this experiment, the Clegg hammer was primarily used as a construction quality control device while the Troxler NDG was undergoing maintenance. Specifically, this device was used on the Silty Sand Test Section #2 between coverages of the smooth-wheel compactor to determine when the maximum strength of the material was reached, signifying approximate achievement of maximum density.

Figure 47. Clegg hammer.

3.4 Data collection layout

After all lifts were constructed, the surface of a completed test section was painted to mark appropriate test locations, as seen in Figure 48. The test locations are shown in Figure 49. Physical testing involved conducting a manual DCP, an instrumented DCP, and two A-DCP devices three times each across each 12-ft x 9-ft test bed at the locations noted in Figure 49. The instrumented manual DCP was used to assess energy accumulation

from the manual DCP during testing. The truck-mounted CBR apparatus involved taking measurements at three unique locations at a cross section cut through the middle of the DCP test field following all testing.

Figure 48. Test section marking.

Figure 49. Test section labeling.

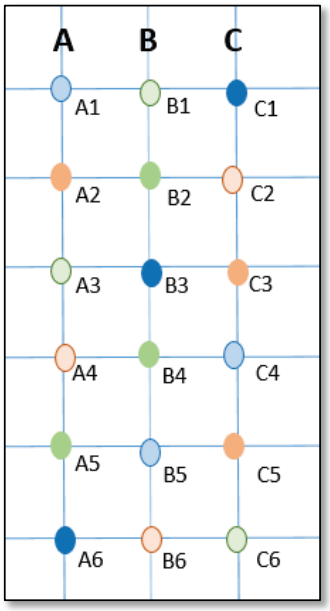

Device	Location
A-DCP #1 (S/N: 001)	A6, B3, C1
A-DCP #2 (S/N: 010)	A1, B5, C4
Manual DCP	A5, B2, B4
Instrumented DCP	A3, B1, C6

A-DCP #1

A-DCP #2

Manual DCP

Instrumented DCP

3.5 Initial performance of the A-DCP

Over the course of the experiment, a number of observations were made by the research team regarding the field performance of the A-DCP units. The observations are summarized below.

1. Battery life for each unit appeared to be sufficient for testing. Batteries were charged prior to every testing event, and a new battery was used for each A-DCP. About 20% of the battery was used during 20 min of testing.
2. Removal of the A-DCP rod was accomplished through manual lifting of the rod, sometimes requiring two people in more plastic soils. The only soil tested where manual extraction was not possible was in the CH clay when the A-DCP rod was inserted to the full 36-in. depth. Extraction of the rod required removal of the head from the rod and a forklift with a chain to extract the rod due to high friction between the clay and the rod (Figure 50).
3. In hard soils with CBR > 80, the A-DCP was able to continue driving into the soil to a full 36-in. depth, moving at small 0.25- to 0.5-in./10 blow increments before high CBR warnings were given. The manual DCP was unable to penetrate the full depth, owing to the lack of reaction force on the rod allowing it to rebound or "bounce" after each blow instead of directing that energy into the soil for greater penetration.
4. The devices recorded each test correctly internally, and the printer was able to produce a hard copy of the test results without fail. Connection time to the printer was slow and incurred a 30-sec lag after connection to print the receipts. A Bluetooth feature was not explored during this experiment.
5. In softer soils, the requirement to stand on the A-DCP led to problems establishing near-surface CBR values due to the heavy weight of the device and the operator placed on the platform. The platform sank into soft soils due to the combined weights of the head and the operator. Initial settlement of the device for low CBR soils ranged from 3 to 6 in. before testing. This could cause problems with assessing soft soils.
6. The presence of high rod friction in the clay soils caused high CBR error messages on the A-DCP, even though the soil CBR remained relatively low.
7. Periodically, the A-DCP apparatus would rebound after the first blow and relock itself, which could be quickly observed by the high pitch of the hammer blows on the immovable head unit.

8. In many cases, the A-DCP screens would display a “motor stalled” error. This was found in testing of sand, silty sand, limestone, and clayey sand. The meaning of this error message was unknown, but an audible change in pitch to the motor could be heard when this condition was approached. Following the motor stalled error message, the A-DCP successfully completed each test.
9. It was critical to ensure the rod was perfectly vertical before starting each test, so, when the testing began, the rod was driven straight into the ground. If the rod was not vertical, a torque was exerted on the nut of the rod that was inserted into the head of the A-DCP. This torque could cause premature failure around the welds (Figure 51).

Figure 50. Forklift used to retrieve mired rod from CH material after testing.

Figure 51. Broken nut on A-DCP.

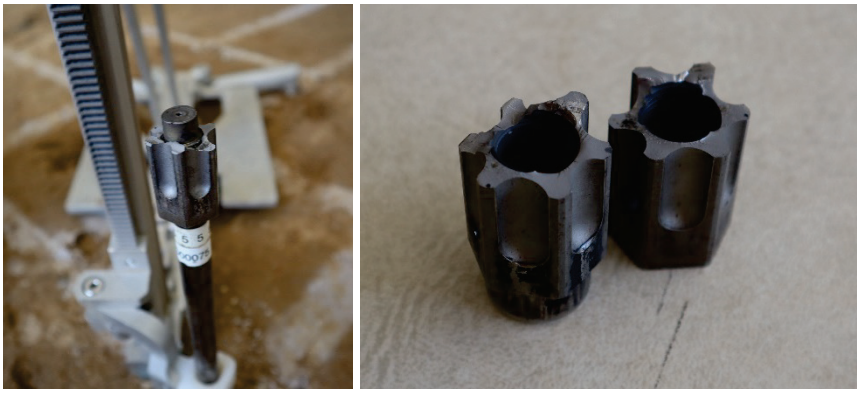

4 Data Analysis for Second Generation A-DCP Prototype

4.1 Data organization

All accumulated data from the 2020 validation study that included the truck-mounted CBR apparatus, the manual DCP device, and the two A-DCP devices were collected and processed in a series of Excel spreadsheets. The following outlines the steps taken to analyze the data to obtain each unique data point found within the correlation charts.

1. A paper copy of the blow count versus depth was obtained from both the A-DCP and DCP following each test and manually entered into an Excel spreadsheet.
2. Using standard DCP conventions, the penetration (mm) per blow was calculated, taking the increment of depth from either the DCP or the A-DCP and dividing by the blows over that range. These values are recorded as the DCP or the A-DCP Index, respectively.
3. To establish the initial depth of the first A-DCP Index value, the initial settlement of the A-DCP rod was added to the first depth value recorded by the A-DCP device. This is similar to marking the initial zero point of the DCP rod when beginning the test.
4. Three truck-mounted CBR data points were collected at each depth (i.e., 0, 6, 12, 18, 24, and 30 in.) within each test section and were denoted as west, center, and east positioning along the cross section of the test pit (Figure 52).
5. The west, center, and east truck CBR values were paired with either the A-DCP or DCP Index value obtained nearest that test location. This made A6, B5, and A5 paired with the west CBR; B3, C4, and B4 with the center CBR; and C1, A1, and B2 with the east CBR.
6. AFSOC has identified certain soil classifications that negatively influence the penetration rate readings of the manual DCP based on the depth in which the readings are taken. Therefore, to determine whether a given soil lift provided suitable DCP and A-DCP data for comparison to the truck CBR, a table was generated comparing the average truck CBR from each layer to the manual DCP CBR value calculated from the standard conversion equation.
7. Since each test pit was nearly uniform in strength and consistency along the entire depth profile, an engineering assessment was made from the CBR-DCP table to eliminate data collected at depths where

there was a significant difference in the truck CBR and the manual DCP-calculated CBR. If a significant difference was observed, it was assumed to occur from either excessive rod friction or lack of penetration depth that would invalidate the readings.

8. Data remaining from the engineering assessment were assumed to be valid for both DCP and A-DCP Index values obtained and represented the final data pairings used to generate the updated regression equation.
9. Variability within remaining data points was expected, noting that there was large data scatter present in the original DCP data. Therefore, only one instance of an outlier data point was identified and removed.

Figure 52. Layout of truck-mounted in situ CBR tests.

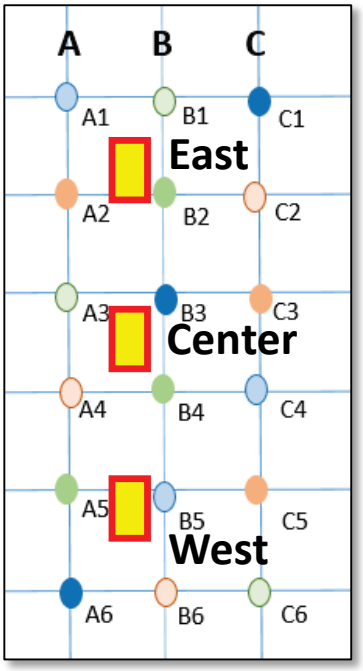

Device	Location
A-DCP #1 (S/N: 001)	A6, B3, C1
A-DCP #2 (S/N: 010)	A1, B5, C4
Manual DCP	A5, B2, B4
Instrumented DCP	A3, B1, C6

A-DCP #1
A-DCP #2
Manual DCP
Instrumented DCP
Truck CBR

4.2 Data distribution

To ensure that validation of the A-DCP was based on a sufficient distribution of data, the distribution of data collected was compared to the legacy experiments of the manual DCP validation in Figure 53 and Figure 54. During the A-DCP experiment, 177 unique data points were collected compared to 211 unique data points acquired during the manual DCP experiment. As shown, the distribution of data points and percentage relationship to the total is similar in both experiments, suggesting sufficient data to enable a valid correlation.

Figure 53. Percentage of unique in situ CBR/A-DCP Index pairs.

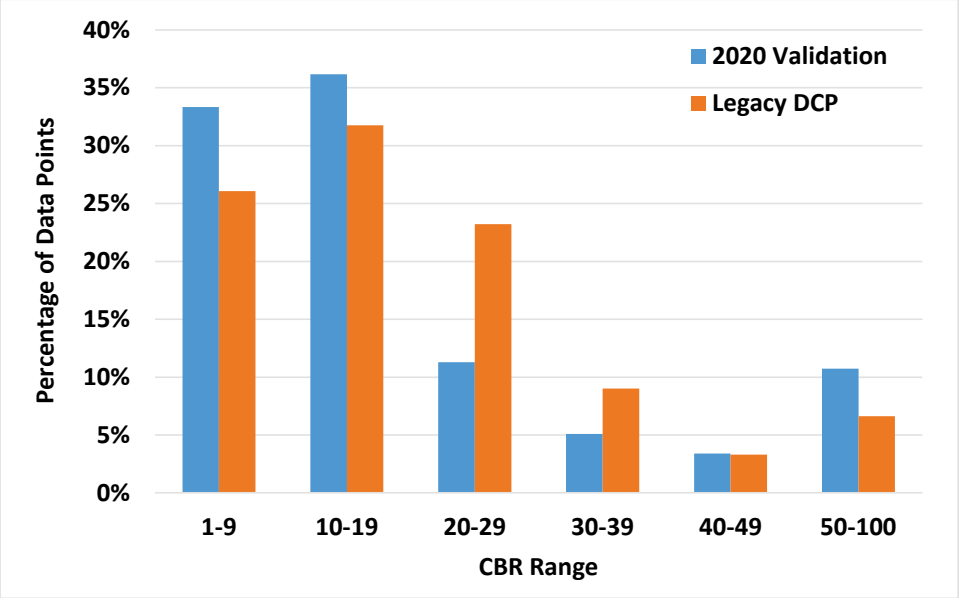

Figure 54. Total number of unique in situ CBR-A-DCP PI pairs.

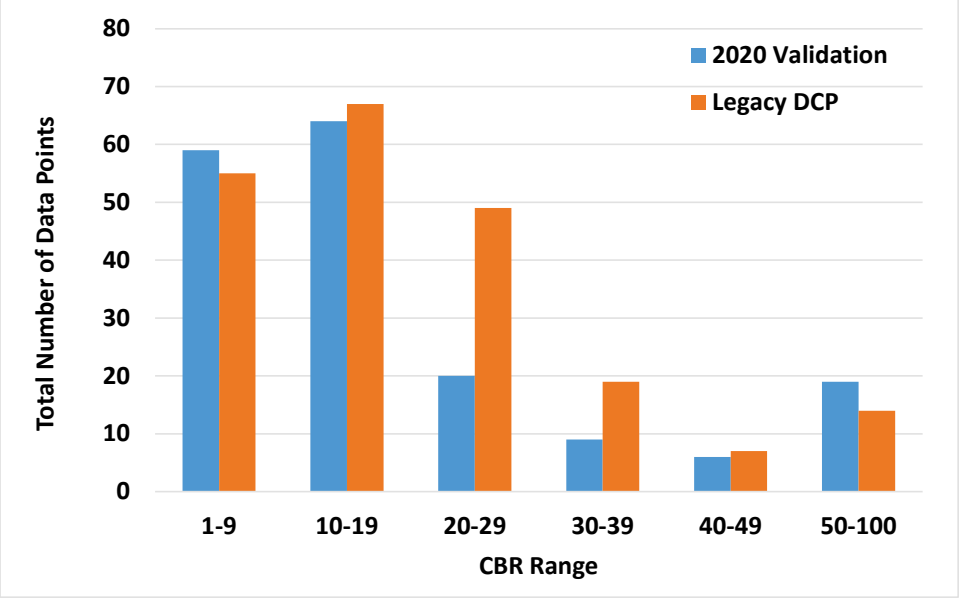

4.3 Selection of valid data points

To determine the viability of data collected from each test section, a comparison was made between the average in situ CBR values and the DCP CBR values. Engineering judgment was used to determine whether the DCP CBR values obtained on a particular lift were representative of the conditions required to obtain a suitable DCP value, as shown in the table in Appendix A. If the in situ CBR values for a given lift of soil differed

considerably from the DCP-derived CBR, then data from that lift were removed from consideration in development of the final A-DCP correlation. In some instances, the A-DCP Index remained consistent throughout the depth profile, even when the DCP CBR value was in error. Data collected on these lifts were included in the A-DCP-CBR correlation but resulted in increasing the error in the DCP-CBR correlation.

Each unique data point used in the regression analysis following the down select from Appendix A is shown in Appendix B. The in-situ CBR for each lift is paired with the A-DCP penetration rate (PR) value for serial number 1 (SN 1) and serial number 5 (SN 5) A-DCP units.

4.4 Regression analysis

In Figure 55, the legacy correlation curves for the DCP versus in situ CBR are presented. What is important to note is that, in the legacy correlations, not one but three curves are required to represent all soils. A separate correlation curve exists for low CBR clayey soils and a second for high plasticity clays. When removing these two data sets, the error present in the correlation for the remaining points decreases. However, this represents a problem for AFSOC personnel because the DCP test is often conducted in an expeditionary manner, where the soil type with depth is unknown and the DCP is relied upon to determine what strengths are present with depth. Therefore, in almost all situations, the standard correlation curve (i.e., $CBR = 292 * PR^{-1.12}$) is selected to convert PR to CBR, thus introducing more risk for error in determining low-strength soils that are not included in the curve. It is the intent of this research to introduce a single correlation curve that does not make a distinction between soil types because this is more often than not the circumstance in which the airmen find themselves.

Figure 55. Legacy in situ CBR versus Penetration Rate correlation.

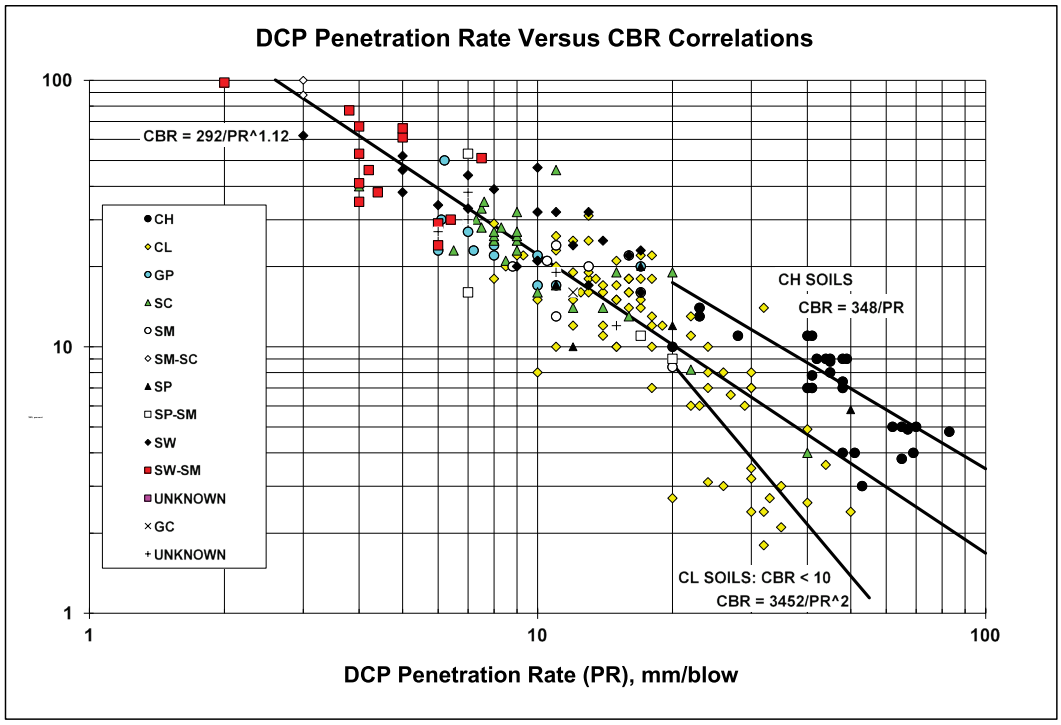

Two types of regression analyses were performed on the A-DCP data. The first used the PR versus in situ CBR data pairs collected from each A-DCP separately, such that a regression expression was obtained for SN1 and SN5 to show variability between devices (Figure 56 and Figure 57). The second combined all collected data pairs from both A-DCP units to create an average correlation curve that will be referred to as the standard curve (Figure 58). All A-DCP correlations relied on the same power regression used in the legacy DCP so that a direct comparison could be made (Table 19) between constants, C, and exponents for the change in PR.

Table 19. Coefficient matrix for A-DCP and DCP regression correlations.

Device	Constant	Exponent	Coefficient Of Determination
A-DCP SN1	105.84	-1.073	0.81
A-DCP SN5	141.09	-1.086	0.75
A-DCP – Combined	118.35	-1.065	0.77
DCP – Current test data	179.09	-1.030	0.72
DCP – Legacy	292	-1.120	
$CBR\ (\%) = C \times PR^{Exponent}$			

The constants have a distinct offset between the A-DCP and the manual DCP, which is a result of an increase in the number of blows with depth to obtain the same CBR. The rationale for this increased number of blows has yet to be pinpointed, but the increase is likely due to the difficulty in applying consistent loading due to the design of the DCP, including variable release points of the hammer, secondary hammer impacts, and operator performance. What is also of significance is that the exponents all fall within a very narrow band, suggesting that the overall performance of the A-DCP is very similar to that of the manual DCP, which was the largest factor concerning its deployment as a DCP replacement tool.

The variation of constants between the two A-DCP units is concerning, as it suggests that the mechanical operation of the devices is not constant and may require a factory calibration prior to deployment. Unfortunately, a third A-DCP unit was unable to be tested to determine which units represented the most repeatable energy. This type of discrepancy was not noted during the initial 2018 study and was not anticipated during this series of experiments. Within this limited data set, it can be seen that SN1 had a better overall R^2 with the collected data than SN5, 81% versus 75% respectively, suggesting a slightly more accurate unit. Any instrument reading in soils approaching an 80% coefficient of determination is considered excellent.

Figure 56. A-DCP SN1 correlation between in situ CBR and penetration rate.

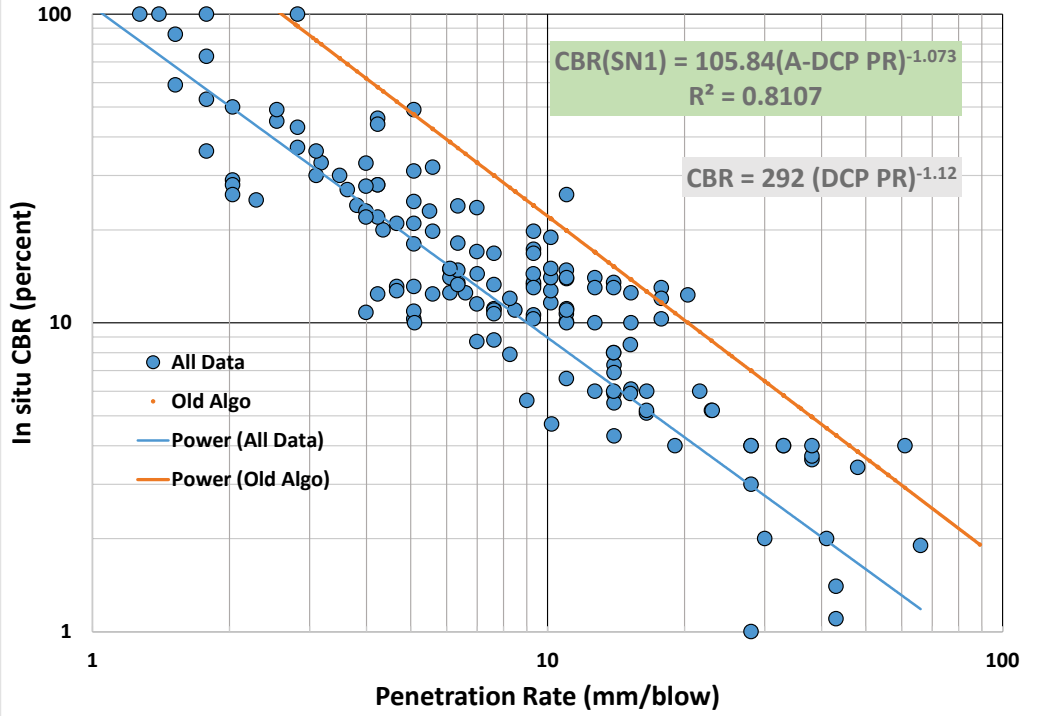

Figure 57. A-DCP SN5 correlation between in situ CBR and penetration rate.

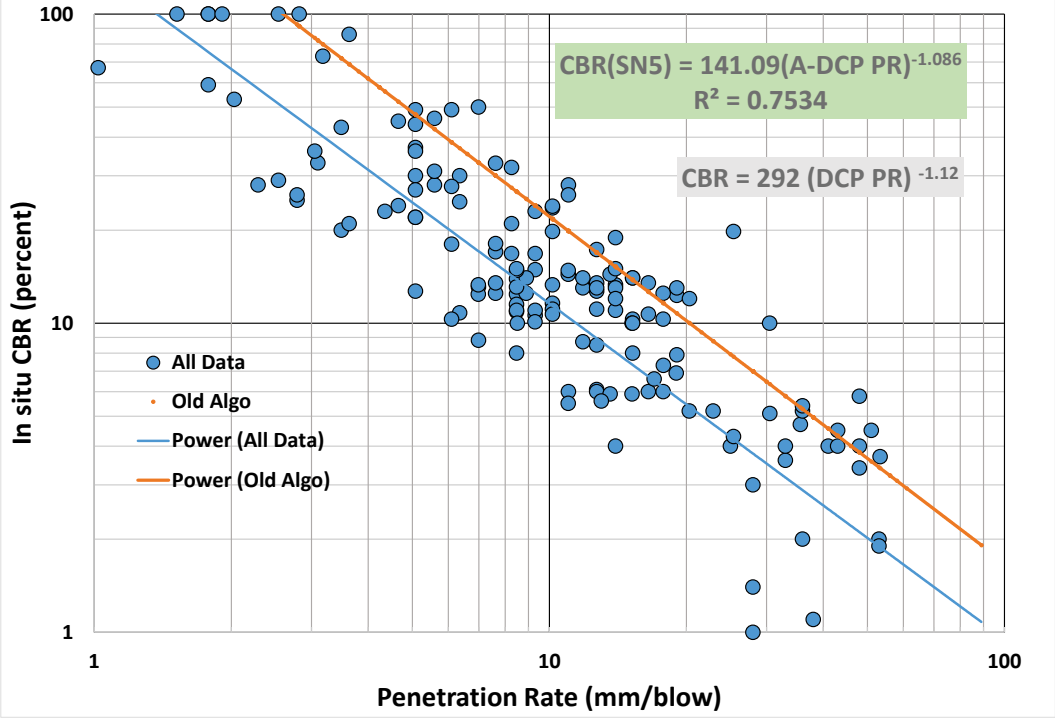

Figure 58. Standard curve for all A-DCP data and ERDC manual DCP data.

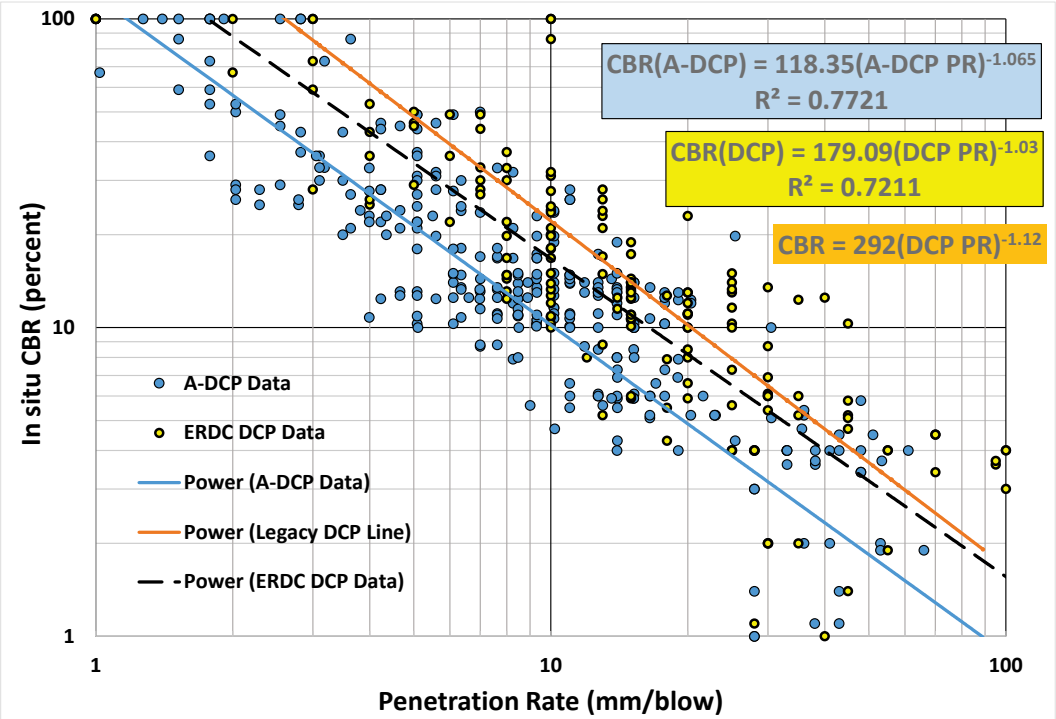

When considering the accuracy of the A-DCP calibration curve, it is useful to understand where the error is occurring. A simple method to visualize the effectiveness of the calibration is comparing the average differential in predicted CBR versus the in situ CBR. Figure 59 shows the absolute value of the average differential that occurred between the measured and predicted CBRs for each A-DCP unit and manual DCP. For this exercise, the manual DCP CBR value is calculated using the standard calibration equation, as it is assumed soil type is unknown prior to testing. Absolute values displayed as relative changes in positive or negative differential are not consistent with any particular soil or device. From Figure 59, the following observations can be made.

1. From CBR < 10, the new regression typically provides a predicted value within 1 CBR, which is consistent with the manual DCP error and suggests very accurate results for low CBR materials. Error rates are similar between SN1 and SN5.
2. For 10 < CBR <20, an error of about 5 CBR is apparent, which falls within the same bounds as the manual DCP; and, while the error is larger, the new regression still distinguishes stronger soils from softer soils. Error remains similar between SN1 and SN5.
3. For 30 < CBR, the error range remains consistent with the manual DCP, which traditionally has exhibited increasing error with CBR value. However, within this CBR range there is a wide separation in error between the two devices. The best response based on unit specific data is within about 5 CBR of the actual value. However, depending on the soil type tested, either the SN1 or SN5 device responded better, with errors sometimes approaching the 15 CBR range.

For the purpose of establishing airfield landing criteria, the A-DCP provides a good approximation of the CBR with depth with error bands in agreement with those of the manual DCP. The two A-DCP units responded to some soil types better than others, with most of the error occurring in the more granular, higher CBR condition soils. This is shown in the series of CBR with depth plots appearing in Appendix C for each soil condition tested. These plots illustrate the shift in CBR from a CBR value predicted using the old DCP algorithm and that of the new average A-DCP algorithm. While it would be ideal to have a calibration curve for each device, this is not feasible; therefore, an average response must account for variability between all devices.

Even given the CBR error represented in Figure 59, the A-DCP will still provide a sufficient approximation of soil strength with depth.

Figure 59. Absolute value of average differential in predicted CBR for each A-DCP unit tested.

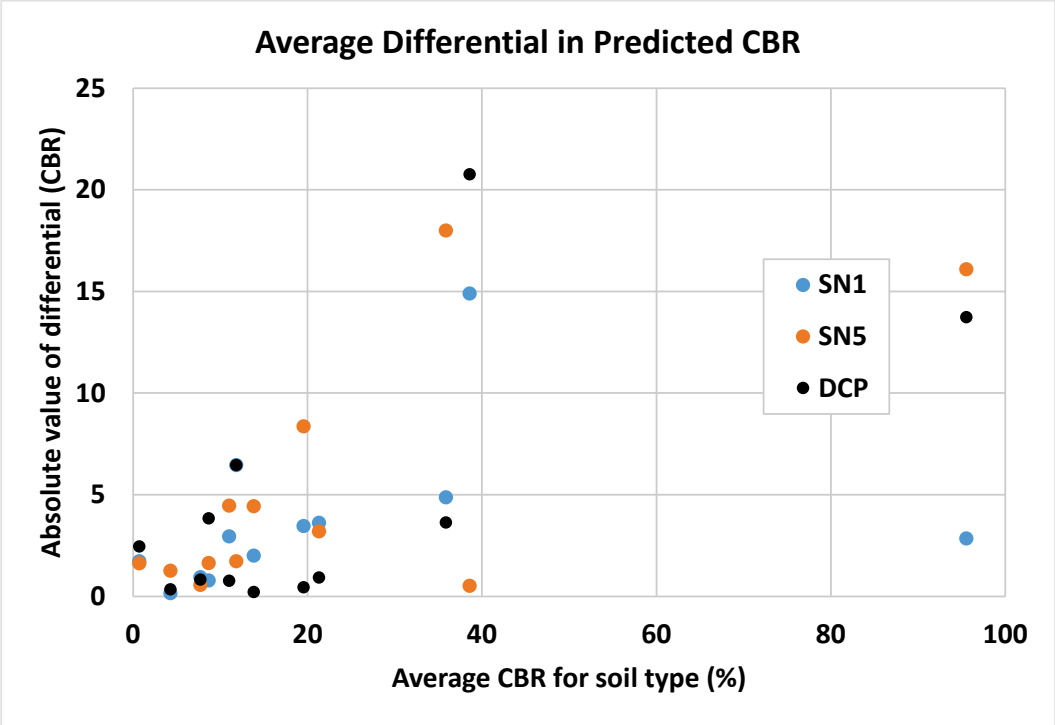

5 Energy Analysis

During the course of experimentation with the A-DCP, it was noticed that one unit seemed to consistently record a greater blow count than the other for each test section encountered. This behavior was supported during the analysis portion of the research where the calibration curves relating CBR to penetration rate varied between the two units. Also, it was shown that the manual DCP exhibited a higher CBR per penetration rate curve than was obtained with the A-DCP devices that necessitated this research to establish a new calibration curve for the A-DCP.

To determine why a discrepancy existed not only between the A-DCP and the manual dual-mass DCP but also between A-DCP units, an energy experiment was conducted in February 2021. This experiment involved securing the penetration rod from either the A-DCP or the manual DCP to a load plate using a screw adapter to ensure a continuous connection through the steel rod between the excitation load (i.e., the hammer) and the load plate, as shown in Figure 60.

Figure 60. Force-Impulse experimental setup.

The load plate consisted of three distinct load cells secured by the large hex screws in the top plate, as seen in Figure 60, each of which recorded

a portion of the total force imparted by the DCP hammer. The data recorded from all three load cells were summed to provide the total load on the system. A data recorder was set up to record data at several thousand cycles per second to ensure that the complete load-time curve was captured for the initial impact and any subsequent impacts resulting from rebound of the hammer. To isolate the system from the concrete floor, the entire apparatus was seated on a foam block equivalent to a 4 CBR for consistency. Table 20 details the sequence of experiments conducted with the two A-DCP devices (SN 5 and SN 1), the instrumented DCP, and the standard manual DCP.

Data recording began just prior to dropping or application of the hammer blow and quickly stopped following impact. This created a plot of force versus time for each experiment. To analyze this data, two values were extracted from the data.

1. The maximum force experienced during the course of a single blow or repeated blows.
2. The approximate area under the force-time curve for each blow or rebound blow experienced during the hammer drop representing the impulse occurring during impact.

These data were used to determine the force and impulse differential occurring between each A-DCP device and with respect to the manual DCP device.

To compare this load cell evaluation to the data recorded during the soil experimentation phase of the research, a parameter was established for each unique test conducted in the field. The total number of blows required of each device was determined and divided by the total depth of penetration of the test. This is referred to as the total blows per depth (TB/D). The idea behind this parameter is the assumption that soil exhibiting a uniform strength throughout a uniform depth for two devices that are identical in all respects would require the same number of blows to penetrate the full depth. If there is a difference between devices, this would reveal itself in a change to the total number of blows recorded, which is indeed what was observed.

Table 20. Series of hammer blow experiments performed with each test device.

Impulse Experiments Run					
Test #	Unit	Type	Test #	Unit	Type
1	S/N #5	Single	21	Inst DCP	Single
2		Single	22		Single
3		Single	23		Single
4		Single	24		Single
5		Single	25		Single
6		5 blows	26		Single
7		10 blows	27		Single
8		10 blows	28		Single
9		10 blows	29		Single
10	S/N #1	Single	30		Single
11		Single	31	Man DCP	Single
12		Single	32		Single
13		Single	33		Single
14		Single	34		Single
15		5 blows	35		Single
16		10 blows	36		Single
17		10 blows	37		Single
18		10 blows	38		Single
19		10 blows	39		Single
20*		10 blows	40		Single

** For this experiment operator did not stand on support apparatus.*

5.1 Field blow-count analysis

For each unique soil condition prepared during the field study, three tests were performed with each A-DCP: SN 5, SN 1, and the manual DCP. For each of these tests, the total blows per depth were computed, and the results then averaged for each device. Table 21 shows the total number of blows per meter to penetrate each unique soil condition. In all instances, the total number of blows is highest for SN 1, then for SN 5, with the lowest being for the manual DCP. To quantitatively compare the two devices to each other or to the manual DCP, a differential was calculated between the average blow response per soil according to the following expression.

$$Differential\ (\%) = (Device\ A_{blows} - Device\ B_{blows})/(0.5*(Device\ A_{blows} + Device\ B_{blows})) \times 100$$

Evaluating the behavior of all test sections together, SN 1 required 25% more blows per soil tested on average than did SN 5, suggesting that SN 1 has a lower energy per hammer blow. SN 5 and SN 1 required 60% to 80% more blows, respectively, than did the DCP. This suggests a much greater energy per blow for the DCP unit. It will be shown later that this blow differential is more closely related to the additional impact energy of the rebound occurring with the manual DCP than the actual force of the first hammer impact.

Table 21. Average total blows per meter to penetrate each soil test section by device and associated differential.

	Average Response of Devices (Total blows per meter depth)				Average Blow Differential Between Tests			
	SN #5	SN #1	DCP		SN1:SN5	SN1:DCP	SN5:DCP	Average Soil CBR
GC-Opt	178	267	122	GC-Opt	40%	75%	38%	36
GC-Wet	92	123	49	GC-Wet	29%	86%	61%	9
ML-Wet	26	33	10	ML-Wet	24%	109%	91%	1
ML-Opt	168	194	66	ML-Opt	14%	98%	87%	21
CL-Dry	109	149	78	CL-Dry	31%	63%	33%	20
CL-Opt	62	88	40	CL-Opt	34%	74%	43%	11
GW	936	1131	675	GW	19%	51%	32%	96
GW Quick	302	417	182	GW Quick	32%	79%	50%	40
SM 5	88	129	55	SM 5	38%	81%	47%	14
SM-Opt	100	141	48	SM-Opt	34%	98%	70%	12
SP	104	120	45	SP	14%	92%	80%	8
CH	122	134	25	CH	9%	137%	132%	4
Tensar CH	75	104	67	Tensar CH	33%	44%	11%	2
Mat CH	68	71	27	Mat CH	4%	90%	86%	5
	Average Differential by Device Type:				**25%**	**83%**	**60%**	

Another observation, which is as yet unexplained, is that as the soil tested becomes softer, the discrepancy in performance between the DCP and the A-DCP becomes larger. This is not a well-defined correlation, but as seen in Figure 61, the energy change between the two A-DCP units remains relatively constant across all soil types, whereas the DCP tends to show a larger blow differential percentage as the soil CBR drops below 20 CBR.

Figure 61. Total blows per meter differential between A-DCP and DCP devices by average soil strength tested.

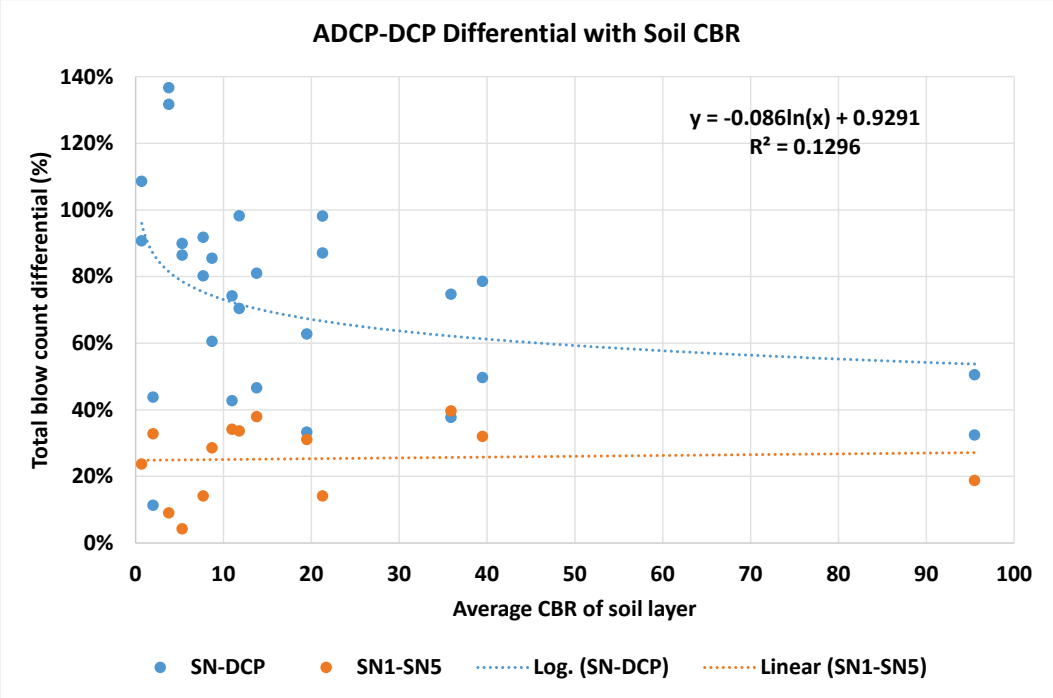

5.2 Force analysis

To begin to understand the mechanical relationship between the two A-DCP units, a series of experiments was performed. The force of the hammer blow generated within the A-DCP housing was recorded on a load cell as described earlier. Given that the mechanisms generating the hammer blow are identical between the two A-DCP units and there is negligible rebound in the system following impact of the hammer, a simple comparison between the two devices was assumed to be the maximum force generated upon impact. Therefore, the maximum force was measured for each blow on SN 5 and SN 1, including the five single-blow tests and each of the 10 blows accumulated during the automatic setting of each device. These values are recorded in Table 22. To provide a direct comparison between the devices, an average maximum force was calculated from all blows recorded, as shown in the Table 22. To compare the two forces, a differential was computed according to the following expression.

$$Differential\ (\%) = (Device\ A_{force} - Device\ B_{force})/(0.5*(Device\ A_{force} + Device\ B_{force})) \times 100$$

On average, the SN 5 unit provided 16% more force per blow than did SN 1. This supports the earlier field study blow-count findings, which showed that SN 5 consistently required 25% fewer blows per test section than did SN 1.

Table 22. Maximum force produced per hammer blow from each A-DCP unit.

Maximum force (lb) per hammer blow on load plate											
			SN #5					SN #1			
Blow	Tests 1-5*	Test 6	Test 7	Test 8	Test 9	Tests 10-14*	Test 15	Test 16	Test 17	Test 18	Test 19
1	4,021	5,237	3,142	3,300	2,559	3,609	2,873	4,059	1,792	3,857	3,300
2	4,773	4,883	4,079	3,657	3,825	3,828	4,237	2,535	1,950	2,860	3,657
3	3,806	4,830	4,014	2,227	2,824	3,567	4,360	3,779	3,138	2,976	2,227
4	3,749	2,995	4,053	2,983	4,166	4,211	4,022	4,314	2,215	2,633	2,983
5	5,050	2,035	4,652	3,593	4,339	2,941	2,509	3,719	2,869	2,875	3,593
6			4,428	3,390	4,187			3,358	1,980	2,242	3,390
7			4,163	3,353	3,221			3,031	2,869	2,481	3,353
8			4,241	3,174	3,447			4,108	3,336	3,117	3,174
9			4,358	2,572	4,335			4,355	2,289	2,855	2,572
10			2,975	3,577	4,502			3,137	3,146	3,901	3,577
Average	**4,280**	**3,996**	**4,011**	**3,183**	**3,741**	**3,631**	**3,600**	**3,640**	**2,558**	**2,980**	**3,183**
Average force per blow of all combined tests:					**3,768**	**Average force per blow of all combined tests:**					**3,195**
Maximum force differential between ADCPs:					**16%**						

**Test 1-5 and Test 10-14 were individual blows recorded on ADCP and not multiple-blow sets.*

5.3 Impulse analysis

When applying the maximum force analysis to the DCP response, there was poor agreement with the change in observed blow differential from the A-DCP during the field soil testing. This is because the DCP, while having a similar maximum force, has a rebound effect not found in the A-DCP unit that contributes additional energy to the system. To capture this phenomenon from the force experiments, the area under the force-time curve, known as the impulse or change in momentum over time, was calculated. An illustration of impulse behavior is shown in Figure 62 next to the impulse plot obtained from an A-DCP impact.

Figure 62. Illustration of ideal impulse force-time plot and typical force-time plot from A-DCP experiment.

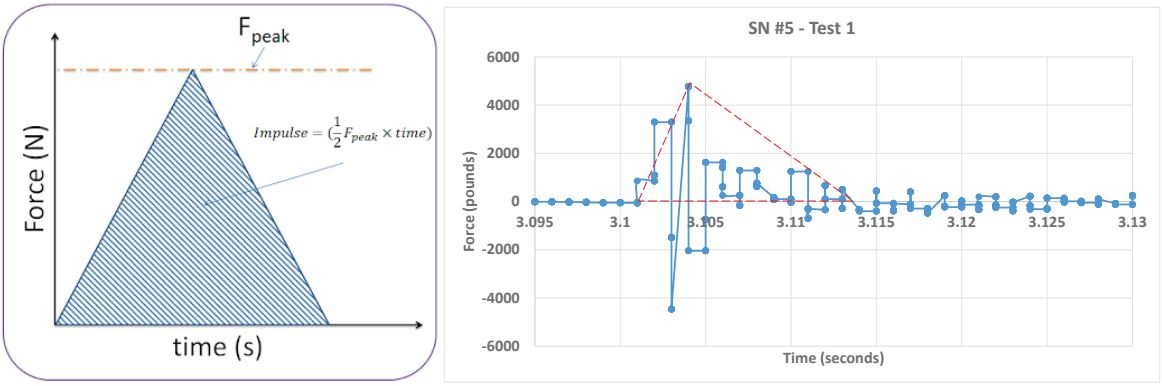

The impulse was determined for each single-blow event that included Tests 1-5 (SN 5), Tests 10-14 (SN 1), and 10 individual blows associated with the manual DCP (Tests 31-40). The impulse was manually determined by overlaying a triangular force distribution across a plot of force versus time, ignoring the reverberation experienced by the rod immediately following impact (Figure 62). In the case of the manual DCP, the hammer lifted off the rod two additional times due to the rebound effect of the hammer drop, resulting in a second and third hit (Figure 63).

Figure 63. Typical impact and rebound response of manual DCP test.

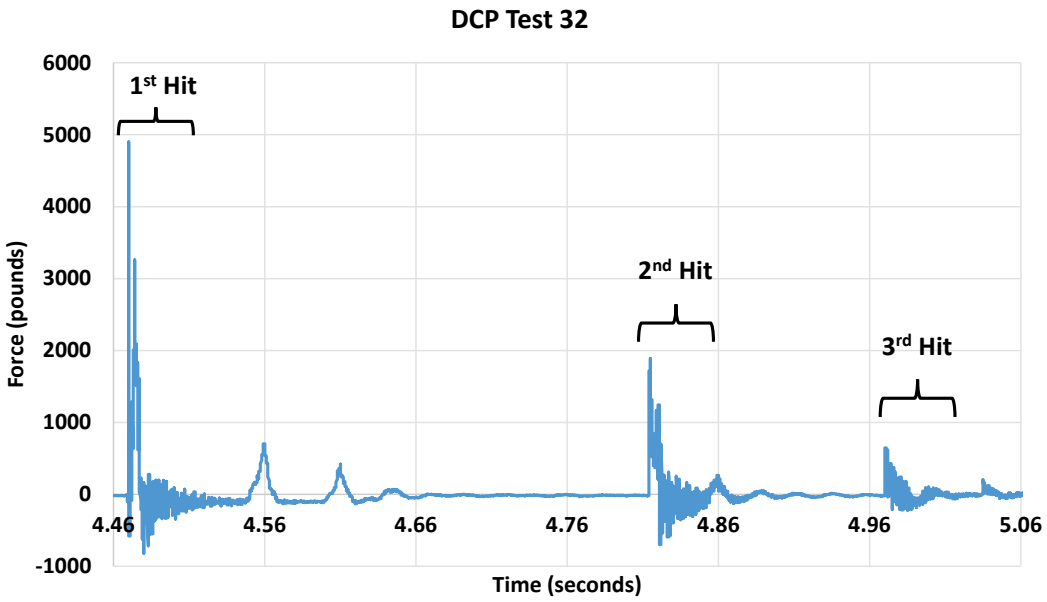

These DCP impulse values were calculated as 1st hit, 2nd hit, and 3rd hit because the accumulated effect of these additional hits is hypothesized to be the reason for the lower DCP blow count for a given soil. The magnitude of the area underneath each force-time triangle derived from each blow within each test is illustrated in Figure 64.

Figure 64. Calculation of impulse for each hit on a manual DCP test using triangular force distributions.

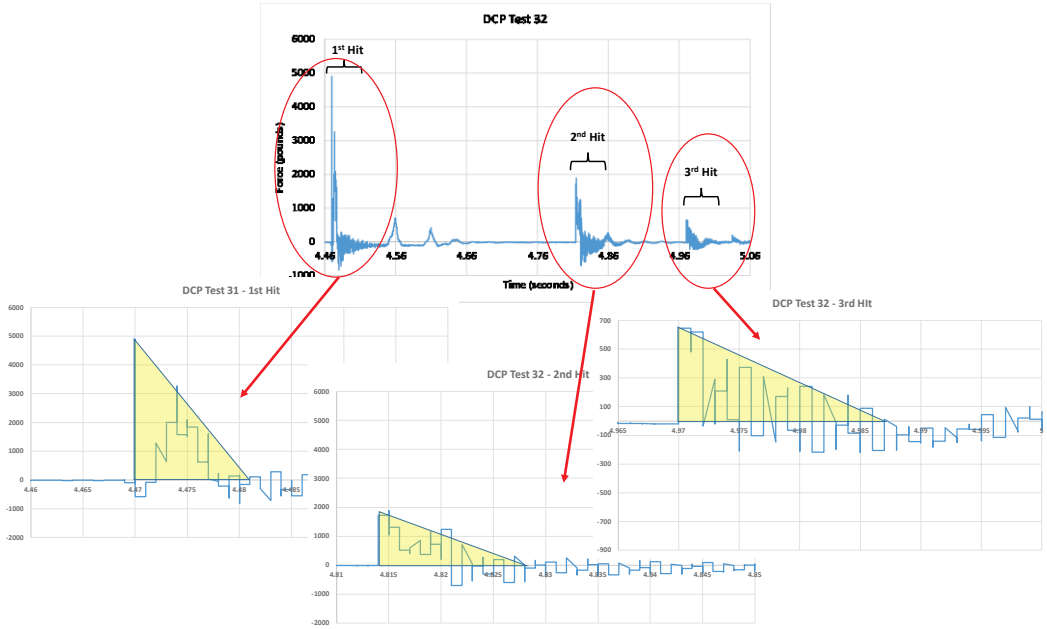

A summary of impulse magnitude for each blow for each test device is shown in Table 23. To compare the impulse between devices, a differential was calculated according to the following expression.

$$Differential\ (\%) = (Device\ A_{impulse} - Device\ B_{impulse})/(0.5*(Device\ A_{impulse} + Device\ B_{impulse})) \times 100$$

Table 23. Impulse recorded for each single blow experiment for A-DCP and manual DCP devices.

	Impulse magnitude for individual blows						Total
	SN #1	SN #5		DCP			DCP
Test	Single	Single	Test	1st Hit	2nd Hit	3rd Hit	Impulse
1 and 10	22.5	25.8	31	46.5	27.2	8.2	81.9
2 and 11	22.3	28.3	32	27.0	12.1	5.6	44.8
3 and 12	22.5	27.9	33	29.9	11.0	4.2	45.0
4 and 13	20.5	21.8	34	45.2	6.5	2.6	54.3
5 and 14	21.3	30.5	35	25.8	6.2	2.2	34.2
Avg. Impulse:	**21.8**	**26.9**	36	32.1	12.2	3.8	48.0
Impulse Diff between ADCP		**21%**	37	31.8	11.4	6.0	49.2
			38	40.0	9.3	1.8	51.1
			39	44.6	12.1	2.7	59.4
			40	33.1	7.7	2.5	43.3
Average DCP Impulse:				**35.6**	**11.6**	**4.0**	**51.1**
Impulse Diff. with Respect to DCP							
	80%	**62%**					

What can be observed is that the impulse is 21% greater for SN 5 than for SN 1, which supports the similarly observed 16% increase in maximum force and 25% fewer blows per soil. Some variability exists between these findings, but all support the same trend in response and are within a reasonable band of error for soil experimentation. When considering the impulse accumulation from all three hits of the manual DCP, the impulse differential between SN 1 and SN 5 is 80% and 62%, respectively, which compares favorably with the 83% and 60% decrease in number of blows required per soil tested.

5.4 Summary of energy study

From the three analyses undertaken (i.e., total blow count, maximum force, and impulse) the following correlations can be derived.

For the two A-DCP units SN 1 and SN 5, the following was observed.

A. Total blow-count differential = 25% (SN 5 < SN 1)
B. Maximum force per blow differential = 16% (SN 5 > SN 1)
C. Impulse magnitude differential = 21% (SN 5 > SN 1)

This illustrates a consistent agreement between test approaches that there is an approximately 20% difference in an assumed energy* between the devices, which leads to the increase in blow counts for SN 1 over SN 5.

When determining the effect between the manual DCP and SN 5, the following was observed:

A. Total blow-count differential = 60 % (DCP < SN 5)
B. Impulse magnitude differential = 62 % (DCP > SN 5).

And for SN 1,

A. Total blow-count differential = 83 % (DCP < SN 1)
B. Impulse magnitude differential = 80 % (DCP > SN 1).

This illustrates a consistent agreement between test approaches that the DCP delivers on average 60% more energy than SN 5 and 80% more energy* than SN 1, leading to the much lower blow count observed in the field study and the dramatic difference in the CBR-penetration rate correlation curves.

**It should be noted that in the conclusions, the term "energy" is used to summarize the rationale for observed blow differential between devices but is not a parameter directly measured. Force and impulse could be determined from the experiments conducted, but energy cannot be derived from these terms. An assumption is made that the increase in impulse correlates with an increase in energy. This may not be accurate but seems to support the concept of relative changes in device response between A-DCP and DCP devices.*

6 Conclusions and Recommendations

6.1 Conclusions

6.1.1 Feasibility study (2018)

In 2018, two A-DCP devices were tested within a number of constructed soil test pits to evaluate their performance in estimating the CBR of the soil. Overall, the A-DCP units showed promise for being simple to use and far more expedient than the manual DCP. However, the CBR value obtained from the A-DCP's penetration rate varied substantially from the CBR obtained from the manual DCP PR. It was observed that the A-DCP required a significantly greater number of blows to penetrate the soil test pit than did the manual DCP, leading to the CBR differential. This differential could be quantified by an average multiplier of 1.6. When the multiplier was applied, reduction of the number of cumulative blows of the A-DCP shifted the A-DCP response closer to the manual DCP data. It was hypothesized that this correction factor represented an energy correction based on the limited single-blow results obtained with the A-DCP, which was investigated in the subsequent research. However, a simple correction factor would not provide confidence in the performance of the new device. This confidence could be established only through a more rigorous experimental study to capture the variances between these two technologies and establish a new correlation equation unique to the A-DCP that would relate A-DCP penetration rate to CBR.

6.1.2 Validation study (2020)

6.1.2.1 General findings

In 2020, the second experimental study was conducted on two new A-DCP devices modified slightly from their 2018 counterparts to validate their performance and establish a unique correlation between penetration rate and CBR. The original A-DCP units had their hand-crank manual mode removed due to its inefficiency and were operated only with the battery-powered hammer system. A more rigorous field experiment was conducted using 13 different soil test pits, consisting of a wide range of soil types and moisture contents to represent CBR values between 1 and 100. Coarse- and fine-grained soils and soil mixtures were included to ensure that the A-DCP would function in any soil environment. Some key findings of the validation study are given below.

1. The A-DCP represented a durable test apparatus, with minimal breakdowns over the course of 5 months of testing in high heat and humidity conditions over 40 tests and several thousand blows.
2. The A-DCP met the mission goals of being operated by a single individual and completed its test within approximately 1 min. Operators found the device easier to use in stiff soils compared to weaker soils.
3. The validation study produced results similar to those of the feasibility study with the number of blows with depth greater for the A-DCP devices than for the manual DCP. Owing to the large amount of test data collected, a new correlation between A-DCP penetration rate and CBR was generated as follows.

$$CBR\ (\%) = 118.35 \times (\text{A-DCP Penetration Rate})^{-1.065}$$

This correlation equation represents an average of the differing responses between A-DCP SN1 and SN5, as SN1 had a greater number of blows per soil layer than SN5. The correlation had a coefficient of determination of 78%, which is similar in error to the manual DCP. A single equation encapsulating all soil types is presented rather than including a set of secondary equations for clayey soils as with the manual DCP. This is desirable because airmen will not have prior knowledge of the soil classification during testing.

6.1.2.2 Impulse findings

Of note was that the slopes of the correlation curves are very similar between each A-DCP unit and the manual DCP (Figure 58). The constant, representing the energy offset, varies between units, as first discovered in the feasibility study. To understand why a differential in blow count and CBR correlation occurred between the units, formal study of the impulse response between devices was undertaken. Each device was secured to an instrumented load cell to record both the initial force and impulse (area under force-time curve) of each device along with any subsequent hammer impacts from rebound. This study showed the following.

1. There was a 16% decrease in force and 21% decrease in impulse from A-DCP SN 1 to SN 5, which correlated to a 25% increase in number of blows from SN 1 to SN 5.
2. The manual DCP had a 62% greater impulse due to multiple impacts of the hammer over A-DCP SN 5, which correlated to 60% fewer blows required than SN 5.
3. The manual DCP had an 80% greater impulse due to multiple impacts of the hammer over A-DCP SN 1, which correlated to 83% fewer blows required than SN 1.
4. The correlation between the constant in the PR-CBR equation and the impulse of each device blow is equal to 1 (Figure 65).

Figure 65. Correlation between PR-CBR equation and impulse of each device.

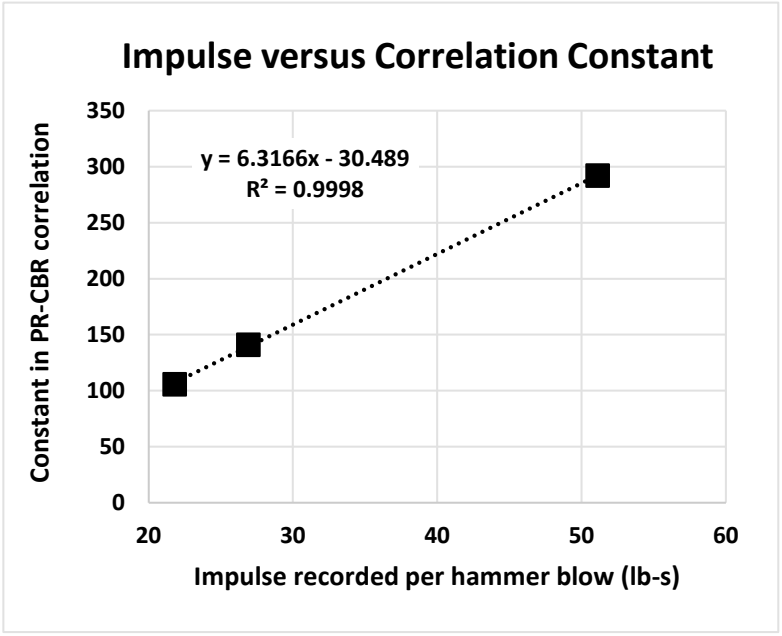

Device	Constant	Impulse
SN#1	105.84	21.8
SN#5	141.09	26.9
Legacy DCP	292	51.1

These differentials can be explained by the following ideas.

1. Operator error in conducting the manual DCP, including improper hammer drops and deviation of rod penetration from the vertical position.
2. Improper calibration of spring response in A-DCP being of lower energy than necessary to match the manual DCP.

3. The rebound effect of the manual DCP hammer, with accumulating impulse occurring from secondary and tertiary blows versus the single-blow effect of the A-DCP.

It is assumed that the blow-count differential is due to energy variation between devices, but this was not a parameter directly measured. Force and impulse were directly measured, but energy cannot be derived from these terms. An assumption is made that the increase in impulse correlates with an increase in energy.

6.2 Recommendations

The following recommendations are made to improve the consistency of the A-DCP units and to ensure accurate measurements of CBR with an electronically operated system.

1. A test needs to be constructed that will allow for calibration of each A-DCP unit to establish a uniform energy distribution between devices. It would be severely problematic to allow a variance in energy between A-DCP units, since that would require a unique correlation coefficient for every device. While this would allow the specific A-DCP to provide the correct CBR, the raw blow-count data could never be used in a stand-alone program to reconstruct the CBR profile. This CBR estimation would be tied to the specific A-DCP unit in which the data were collected.
2. An internal study of the spring coefficient and its possible degradation with repeated testing should be undertaken to ensure that the spring constant is consistent between devices. Further, this will help define the point at which factory recalibration is necessary to ensure consistent data with continued use. The aforementioned calibration test could also be used not only in the manufacture of the A-DCP but also in the maintenance of the A-DCP as stated.
3. The swivel system that holds the rod to keep it from bending during testing should be improved to make the A-DCP more robust for field use. Perhaps a locking mechanism to ensure that the rod is set in a vertical position relative to the head would be beneficial and prevent error in the initial setting of the unit. This would prevent premature rod fatigue and failure and improve the consistency of the blow-count results.

References

American Society for Testing and Materials International (ASTM). 2012. *Standard test methods for laboratory compaction characteristics of soil using modified effort*. Designation: D1557. West Conshohocken, PA: ASTM International.

_____. 2014. *Standard test method for specific gravity of soil solids by water pycnometer*. Designation: D854-14. West Conshohocken, PA: ASTM International.

_____. 2015. *Standard test method for relative density (specific gravity) and absorption of coarse aggregate*. Designation: C127. West Conshohocken, PA: ASTM International.

_____. 2017a. *Standard practice for classification of soils for engineering purposes (United Soil Classification System)*. Designation: D2487. West Conshohocken, PA: ASTM International.

_____. 2017b. *Standard test methods for in-place density and water content of soil and soil aggregate by nuclear methods (shallow depth)*. Designation: D6938. West Conshohocken, PA: ASTM International.

_____. 2017c. *Standard test methods for liquid limit, plastic limit, and plasticity index of soils*. Designation: 4318. West Conshohocken, PA: ASTM International.

_____. 2019. *Standard test methods for sieve analysis of fine and coarse aggregates*. Designation: C136/C136-M19. West Conshohocken, PA: ASTM International.

Anderton, G. L., E. S. Berney IV, J. K. Newman, T. A. Mann, C. Gartrell, and D. K. Miller. 2021. *Joint Rapid Airfield Construction (JRAC) program 2004 demonstration project--Fort Bragg, North Carolina*. ERDC/GSL TR-21-8. Vicksburg, MS: U. S. Army Engineer Research and Development Center.

Parker, F., M. Hammons, and J. Hall. 1998. *Development of an automated dynamic cone penetrometer for evaluating soils and pavement materials*. FHA TR- 199903. Tallahassee, FL: Federal Highway Administration.

Scala, A. J. 1956. Simple methods of flexible pavement design using cone penetrometers. *New Zealand Engineering* 11(2):34-44.

Webster, S. L., R. H. Grau, and T. P. Williams. 1992. *Description and application of dual mass dynamic cone penetrometer*. Instruction Report GL-92-3. Vicksburg, MS: U. S. Army Engineer Waterways Experiment Station.

Appendix A: Soil Properties

Details of soil used for the first- and second-generation A-DCP testing are shown in this appendix.

First Generation A-DCP Prototype Testing – Heavy Clay (CH)

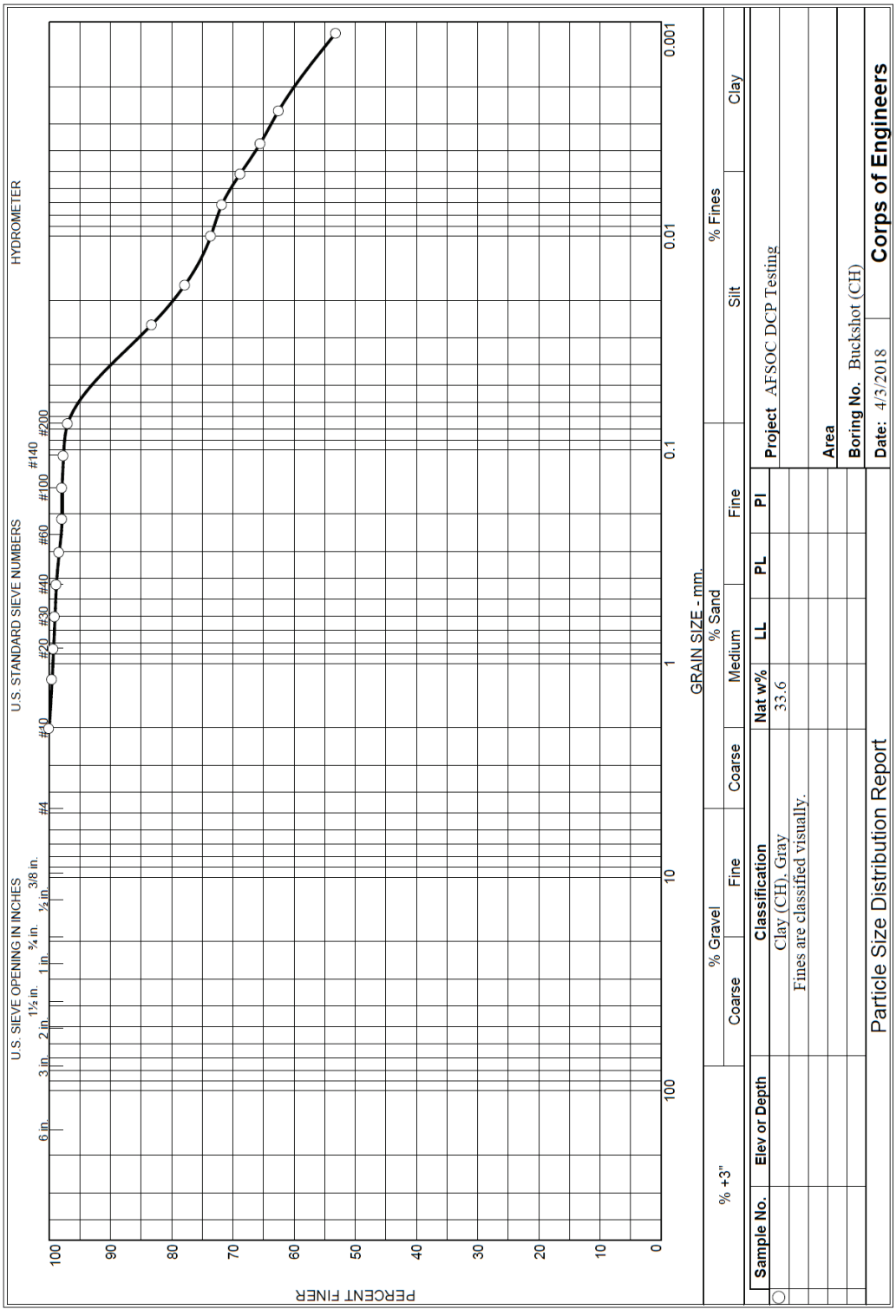

First Generation A-DCP Prototype Testing – Silt (ML)

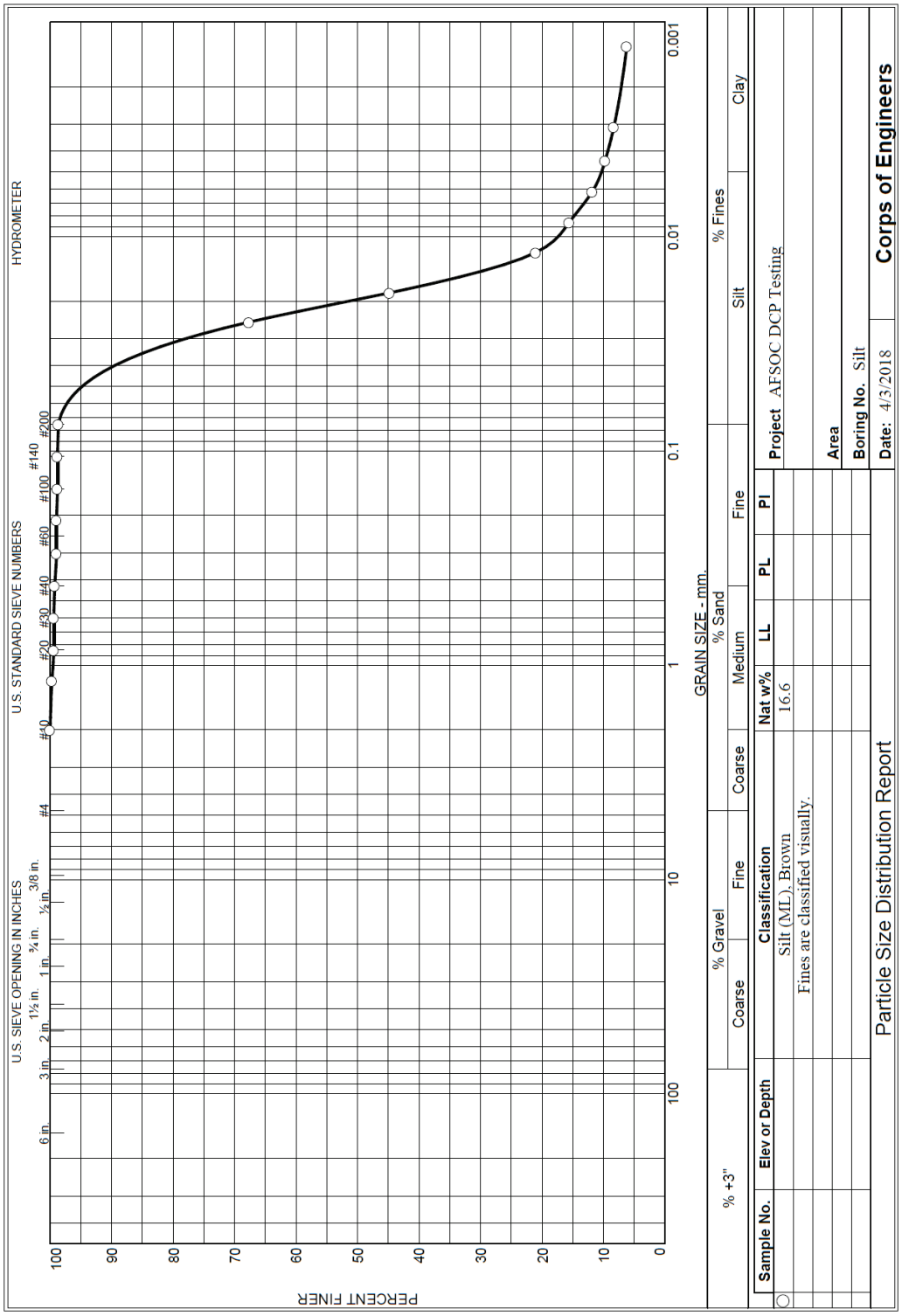

First Generation A-DCP Prototype Testing – Sand (SP)

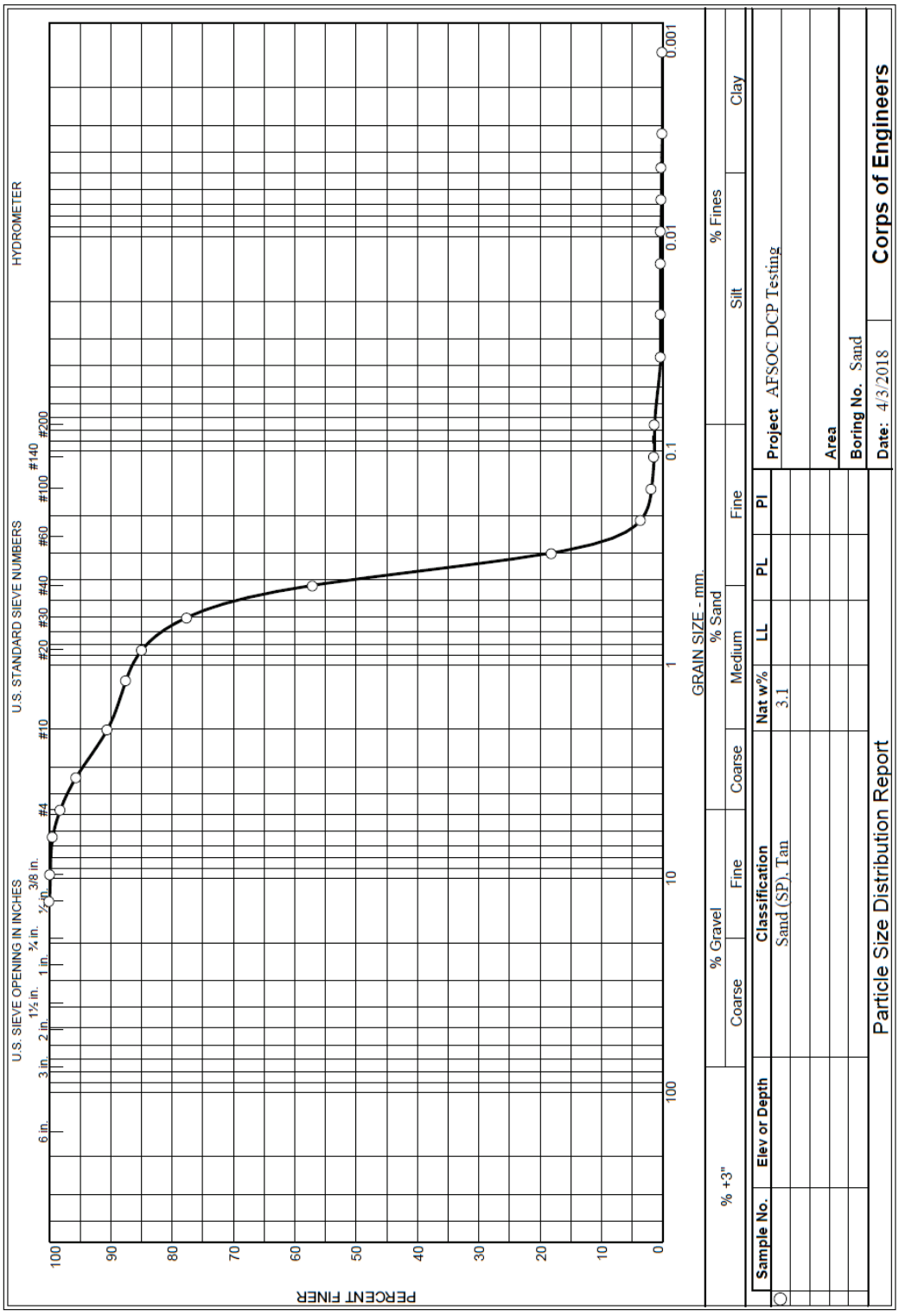

First Generation A-DCP Prototype Testing – Limestone (GW)

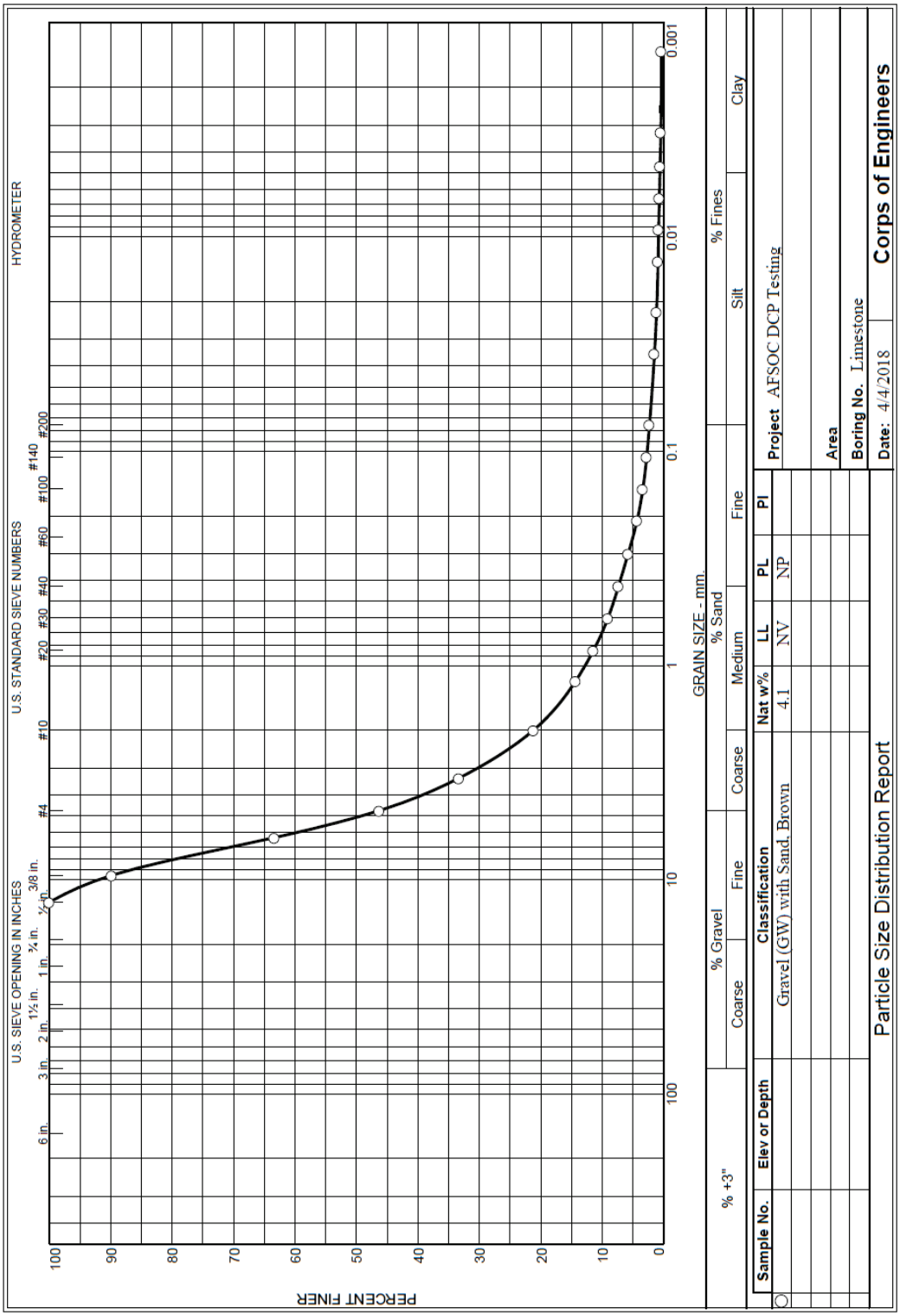

First Generation A-DCP Prototype Testing – Clay Gravel (GP)

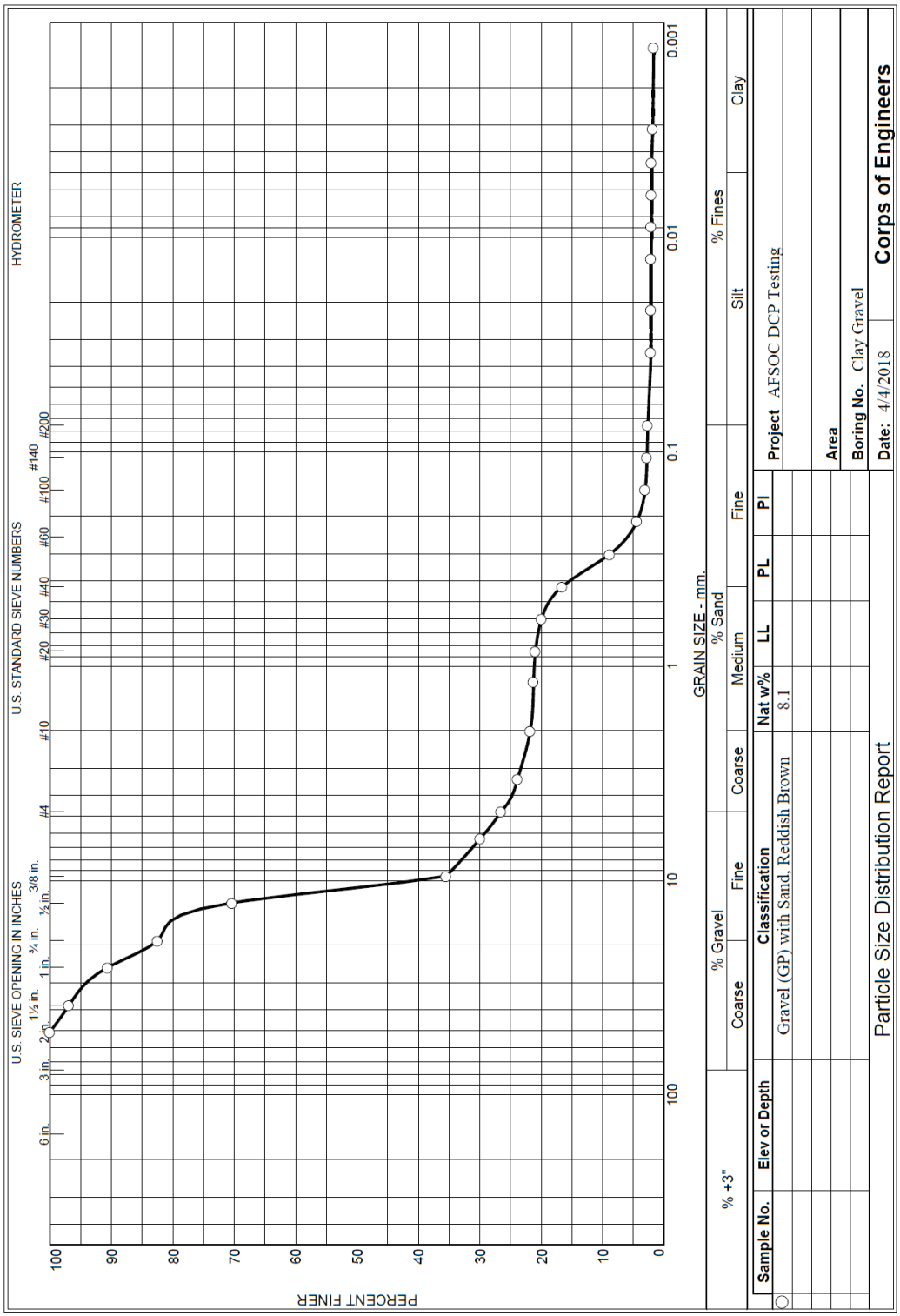

First Generation A-DCP Prototype Testing – Crushed Rock (GM)

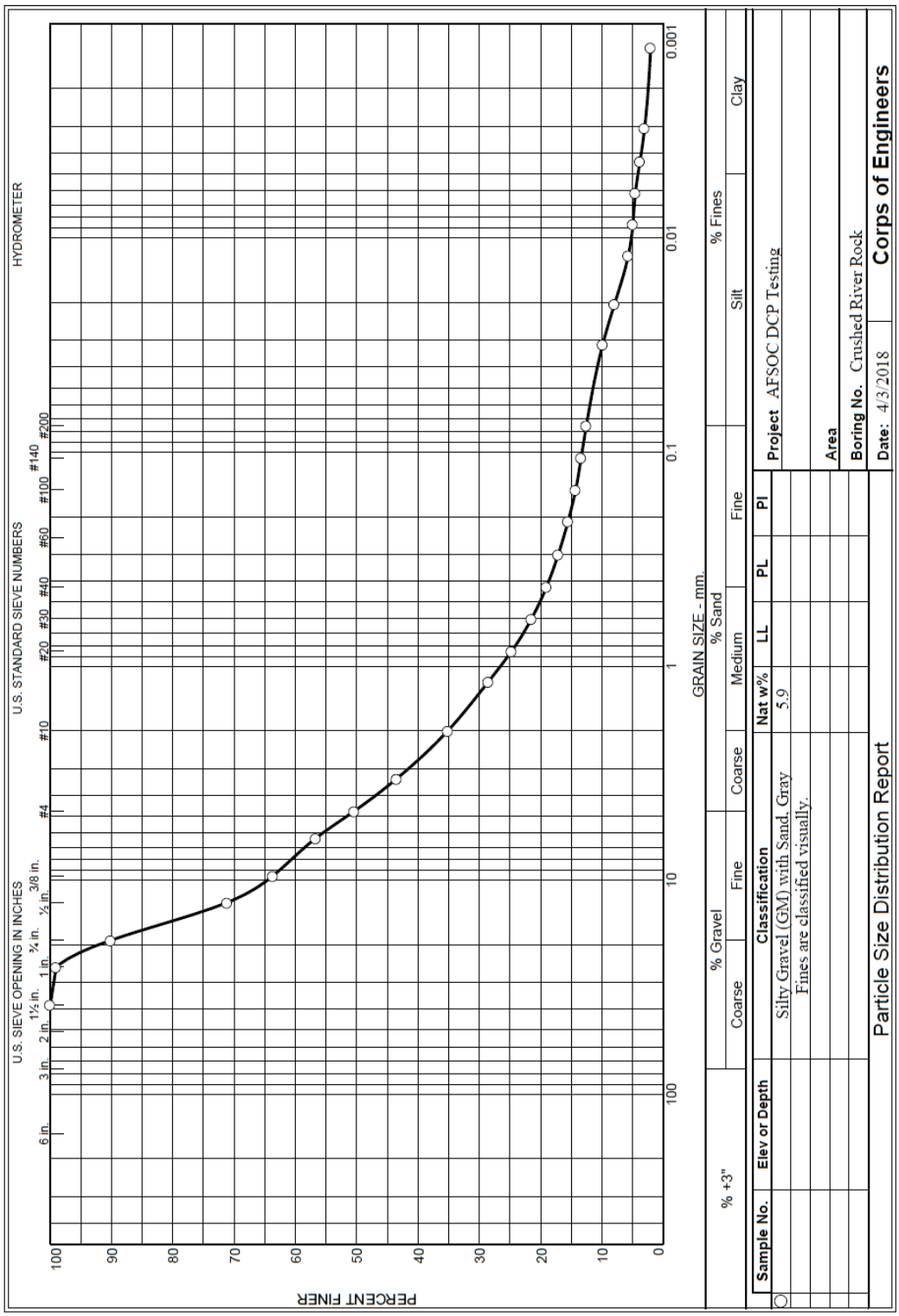

Second Generation A-DCP Prototype Testing - Heavy Clay (CH)

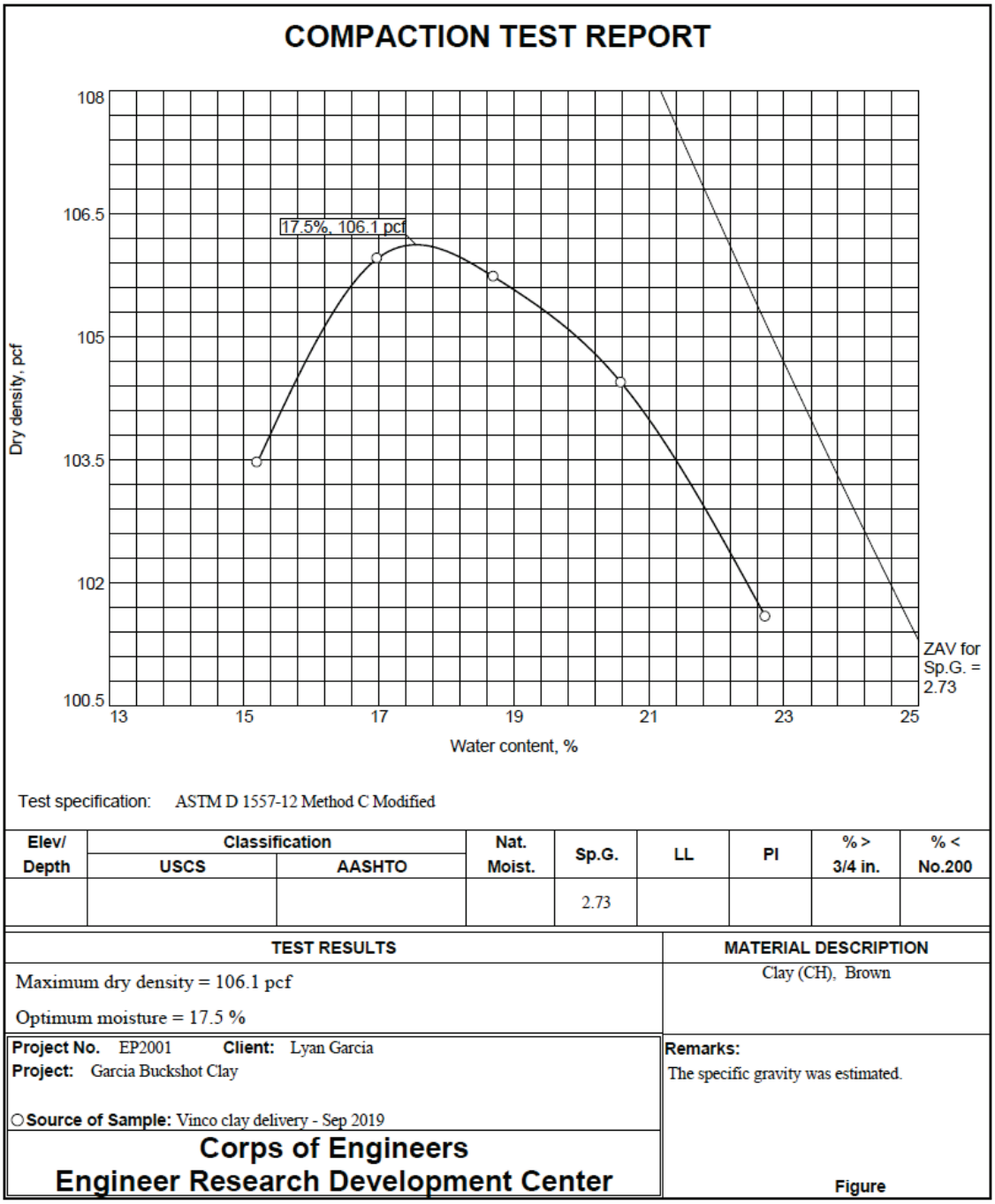

Second Generation A-DCP Prototype Testing- Heavy Clay (CH)

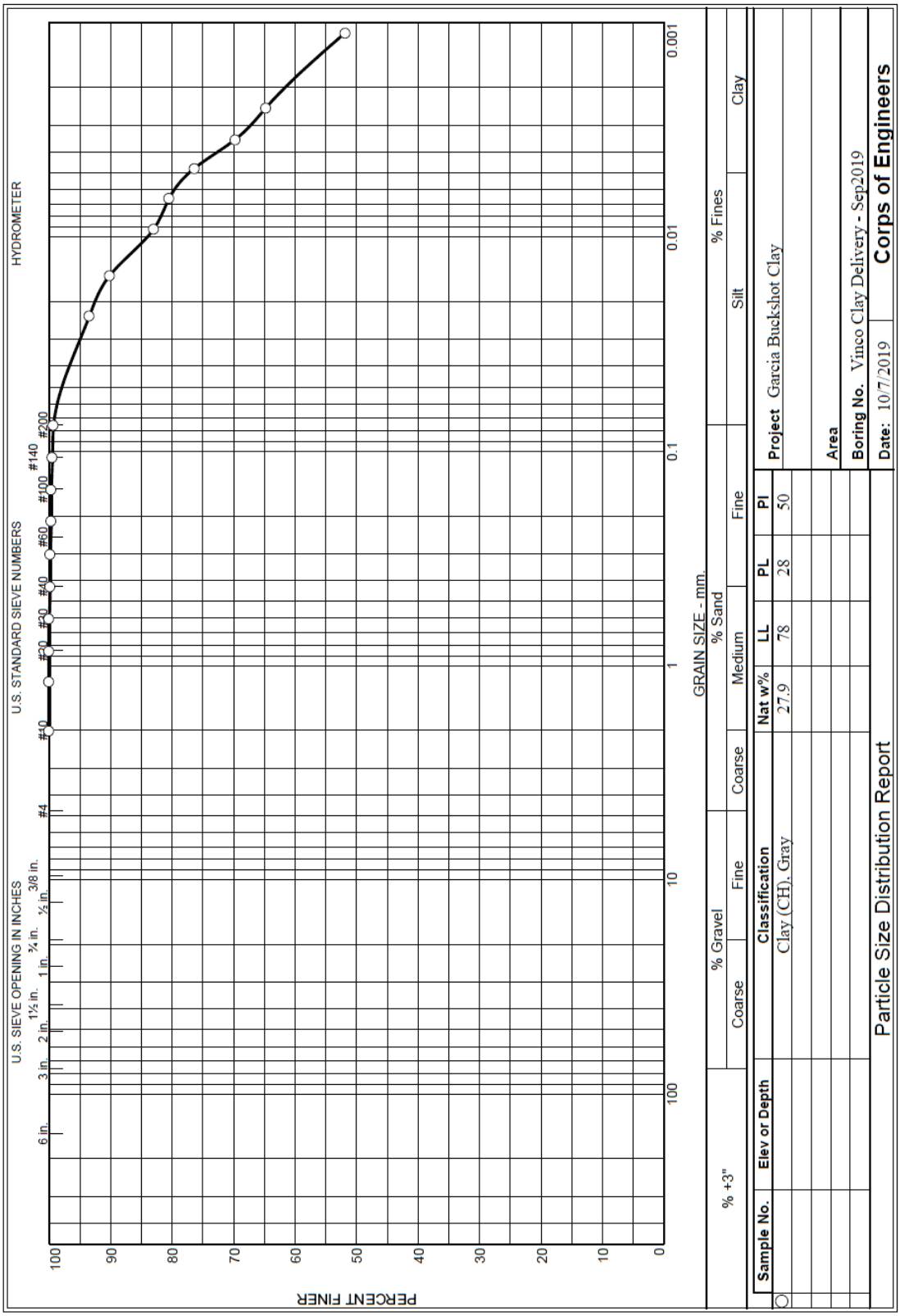

Second Generation A-DCP Prototype Testing- Heavy Clay (CH)

Section Label	Soil Type	Depth in	Truck CBR	Clegg Impact Value CIV	Moisture Content %	Wet Density pcf	Dry Density pcf
CH Wet	CH	0	4	2.8	41.58	111.2	78.5
	CH	0	4	3.3	43.21	110.6	77.2
	CH	0	3	2.3	38.23	109.9	79.5
	CH	6	4	1.9	34.66	109.1	81.0
	CH	6	4	2.3	40.07	106.6	76.1
	CH	6	4	3.0	34.50	109.4	81.3
	CH	12	5	2.8	32.24	112.5	85.1
	CH	12	4	2.6	36.81	109.2	79.8
	CH	12	4	3.1	34.81	105.9	78.6
	CH	18	5	2.6	33.52	111.5	83.5
	CH	18	5	3.0	32.51	112.7	85.1
	CH	18	5	2.4	34.88	112.6	83.5
	CH	24	5	1.9	33.19	103.4	77.6
	CH	24	6	2.3	31.18	107.1	81.6
	CH	24	4	2.8	34.96	102.7	76.1
	CH	30	5	2.4	--	110.3	77.9
	CH	30	6	2.6	--	108.5	76.7
	CH	30	6	2.4	--	112.2	81.4

‘

Second Generation A-DCP Prototype Testing- Silt (ML)

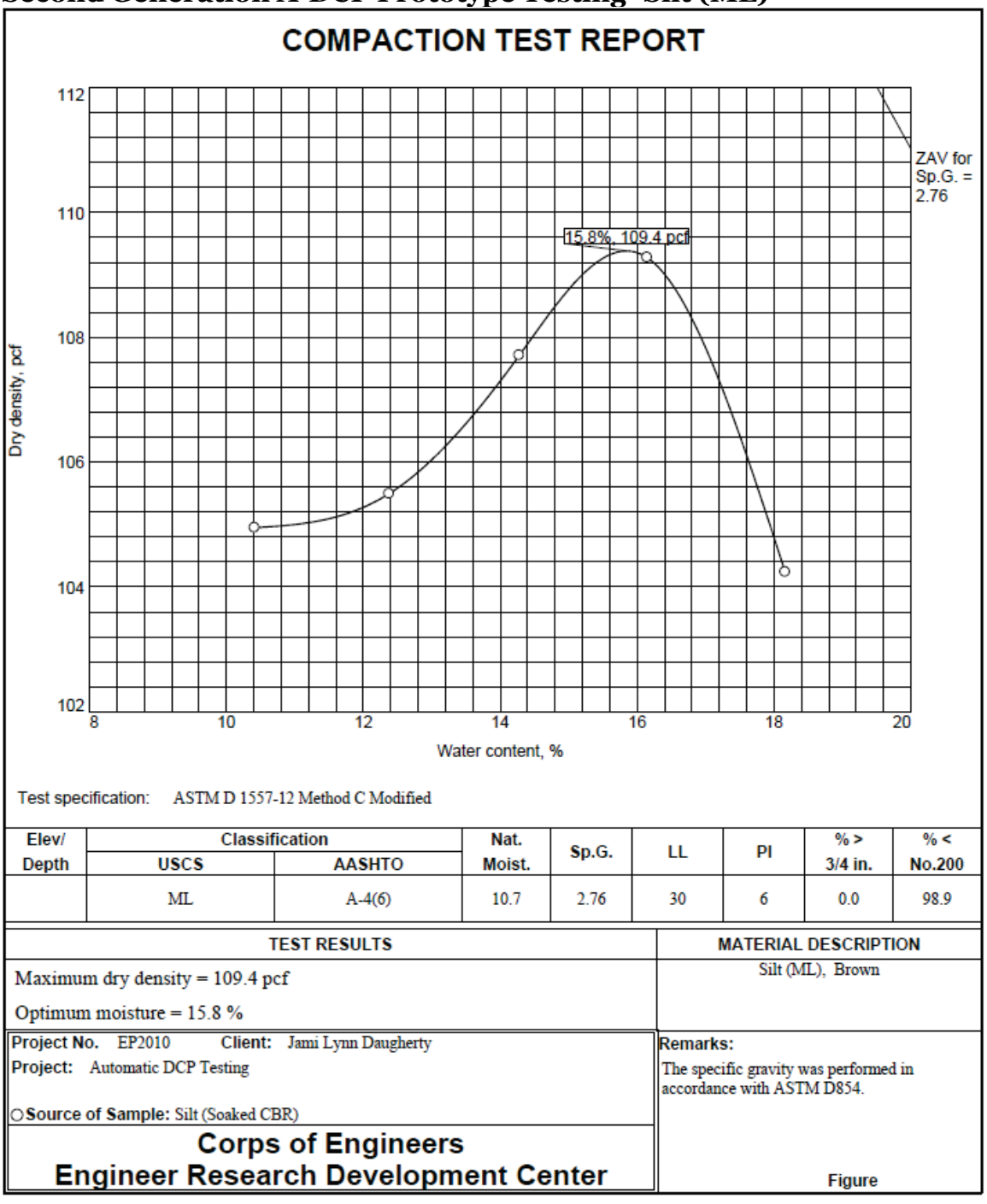

Second Generation A-DCP Prototype Testing- Silt (ML)

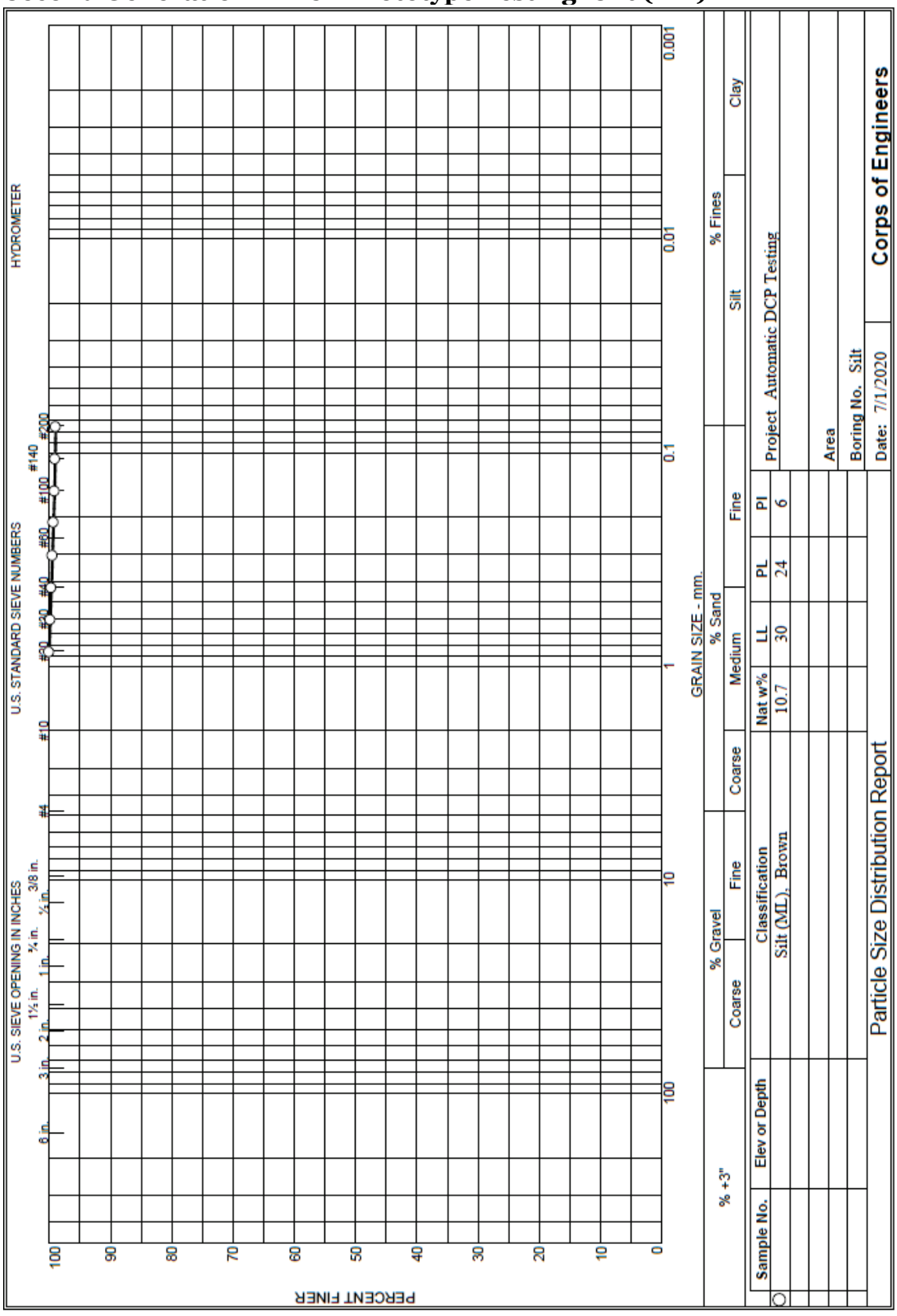

Second Generation A-DCP Prototype Testing- Silt (ML)

Section Label	Soil Type	Depth in	Truck CBR	Clegg Impact Value CIV	Moisture Content %	Wet Density pcf	Dry Density pcf
ML Wet	ML	0	0.6	2.6	25.53	120.5	96.0
	ML	0	0.6	3.3	22.55	120.5	98.3
	ML	0	0.5	3.5	22.78	121.1	98.6
	ML	6	0.6	--	23.81	119.8	96.8
	ML	6	0.6	--	22.77	120.1	97.8
	ML	6	0.6	--	21.90	119.0	97.6
	ML	12	0.5	--	23.55	111.4	90.2
	ML	12	0.7	--	21.93	122.8	100.7
	ML	12	0.6	--	23.10	121.9	99.0
	ML	18	0.7	--	22.13	119.4	97.8
	ML	18	0.6	--	21.64	122.3	100.5
	ML	18	0.6	--	22.57	116.2	94.8
	ML	24	0.7	--	22.28	121.6	99.4
	ML	24	0.7	--	21.95	121.7	99.8
	ML	24	0.7	--	22.13	123.4	101.0
	ML	30	1.4	--	20.95	117.9	97.5
	ML	30	1.1	--	22.21	117.0	95.7
	ML	30	1	--	22.32	121.1	99.0

Second Generation A-DCP Prototype Testing- Silt (ML)

Section Label	Soil Type	Depth in	Truck CBR	Clegg Impact Value CIV	Moisture Content %	Wet Density pcf	Dry Density pcf
ML Opt	ML	0	14	10.5	16.41	118.3	101.6
	ML	0	17	8.6	16.01	118.4	102.1
	ML	0	14	10.8	17.03	119.8	102.4
	ML	6	23	--	16.44	116.2	99.8
	ML	6	20	--	--	117.0	101.6
	ML	6	24	--	16.42	120.8	103.8
	ML	12	22	--	16.87	119.0	101.8
	ML	12	21	--	16.79	120.2	102.9
	ML	12	18	--	16.86	119.1	101.9
	ML	18	18	--	17.24	118.4	101.0
	ML	18	21	--	17.05	119.0	101.7
	ML	18	18	--	17.03	120.4	102.9
	ML	24	13	--	16.61	125.5	107.6
	ML	24	12	--	16.32	127.0	109.2
	ML	24	13	--	16.21	122.7	105.6
	ML	30	7	--	15.88	120.3	103.8
	ML	30	7	--	16.09	116.2	100.1
	ML	30	7	--	16.52	118.6	101.8

Second Generation A-DCP Prototype Testing- Sand (SP)

COMPACTION TEST REPORT

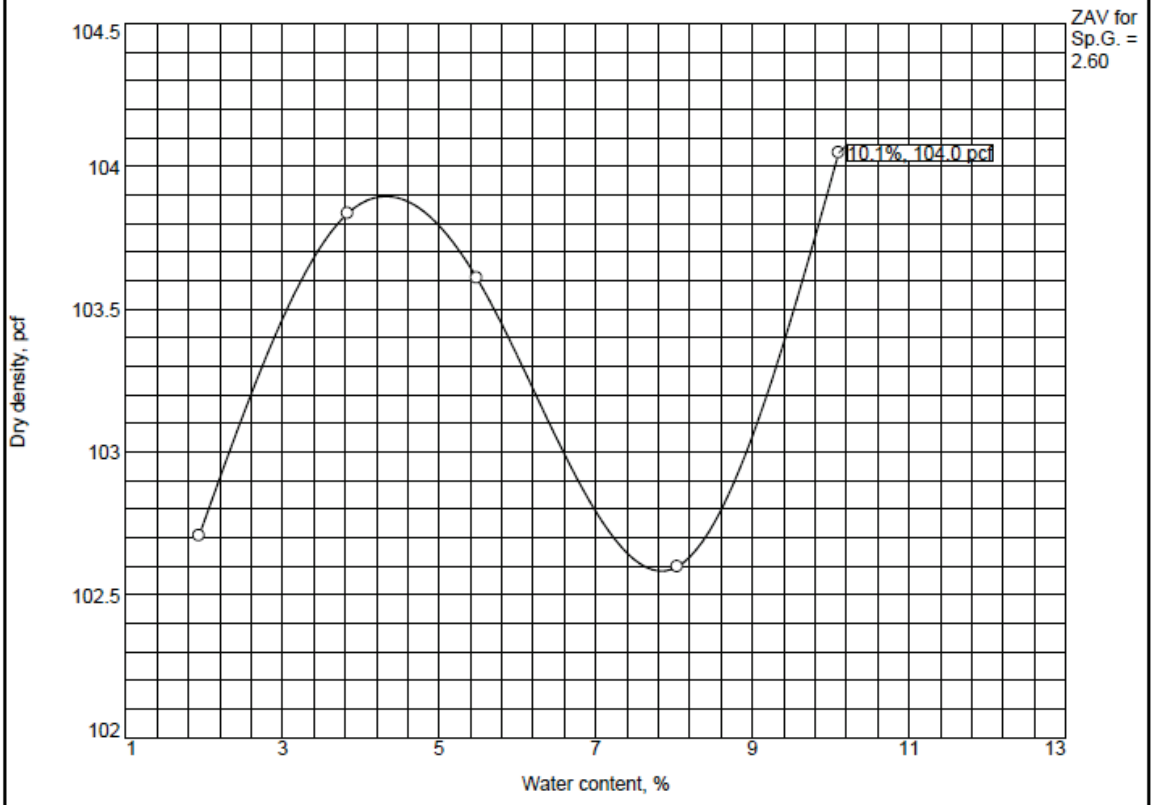

Test specification: ASTM D 1557-12 Method C Modified

Elev/ Depth	Classification		Nat. Moist.	Sp.G.	LL	PI	% > 3/4 in.	% < No.200
	USCS	AASHTO						
	SP			2.60			0.0	0.6

TEST RESULTS	MATERIAL DESCRIPTION
Maximum dry density = 104.0 pcf Optimum moisture = 10.1 %	Sand (SP), Tan

Project No. EP1910 **Client:** Lulu Edwards
Project: E-ADR Backfill Sand Stockpile

○ **Source of Sample:** Sand Stockpile

Remarks:
The specific gravity was estimated. The zero air voids curve for the gravity does not plot on the curve with this water contenr scale.

Corps of Engineers
Engineer Research Development Center

Figure

Second Generation A-DCP Prototype Testing- Sand (SP)

Section Label	Soil Type	Depth in	Truck CBR	Clegg Impact Value CIV	Moisture Content %	Wet Density pcf	Dry Density pcf
SP	SP	0	3.7	4.1	5.05	107.9	102.7
	SP	0	4	3.8	4.95	108.3	103.2
	SP	0	3.6	3.5	3.75	106.3	102.5
	SP	6	6.1	--	4.34	108.5	104.0
	SP	6	6	--	4.33	106.8	102.4
	SP	6	6	--	4.66	107.2	102.4
	SP	12	11	2.8	3.88	107.2	103.2
	SP	12	11.1	4.3	3.94	106.6	102.6
	SP	12	10.6	4.3	1.74	105.6	103.8
	SP	18	11	3.3	3.93	106.7	102.7
	SP	18	10.7	2.4	4.27	106.7	102.3
	SP	18	8.8	3.6	4.39	104.5	100.1
	SP	24	--	3.8	4.19	109.1	104.7
	SP	24	--	4	4.35	106.4	102.0
	SP	24	--	3.8	4.38	102.7	98.4
	SP	30	--	2.3	5.45	103.6	98.2
	SP	30	--	3.8	5.21	110.8	105.3
	SP	30	--	3.3	5.80	101.9	96.3

Second Generation A-DCP Prototype Testing- Limestone (GW)

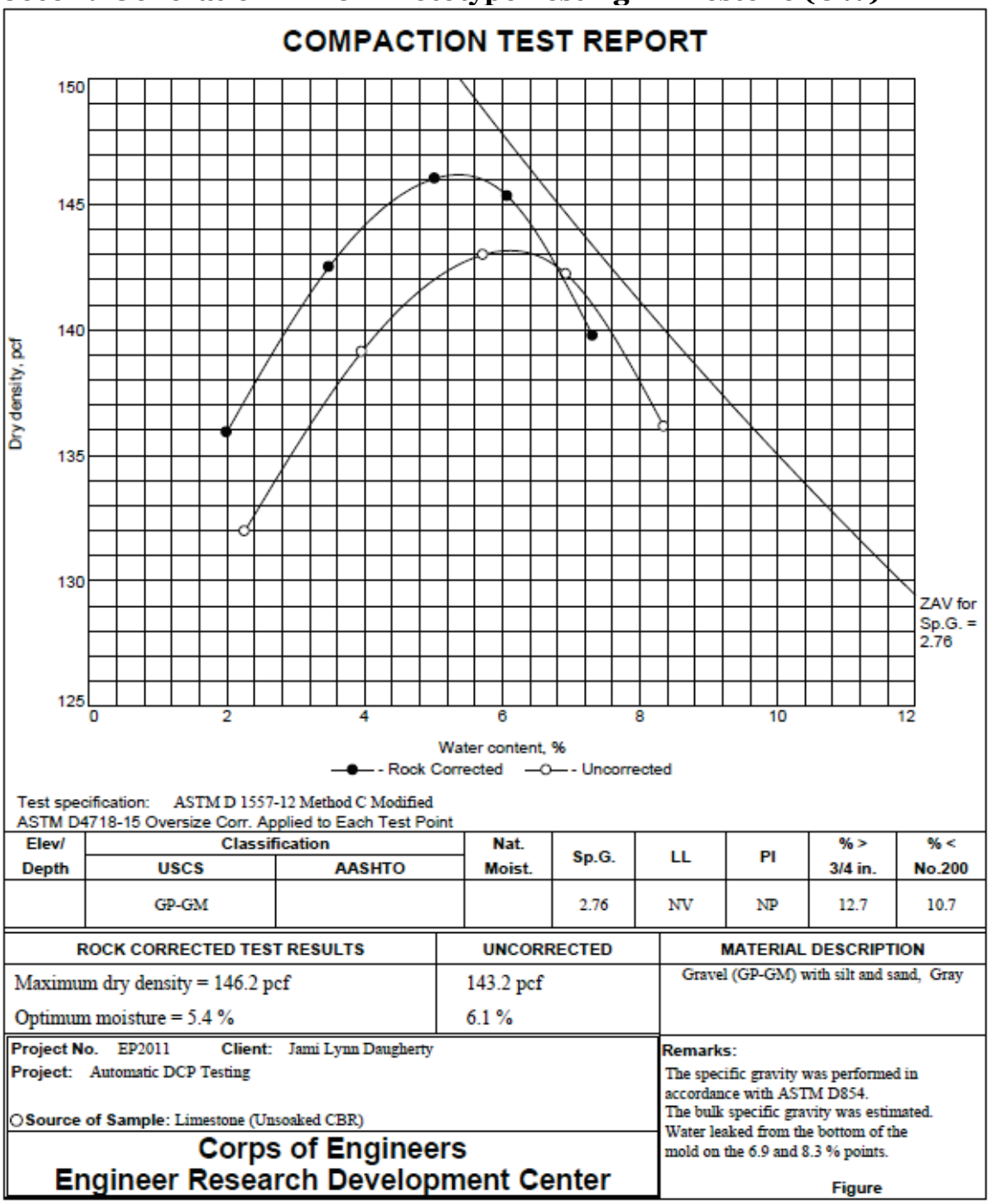

Elev/ Depth	Classification USCS	Classification AASHTO	Nat. Moist.	Sp.G.	LL	PI	% > 3/4 in.	% < No.200
	GP-GM			2.76	NV	NP	12.7	10.7

ROCK CORRECTED TEST RESULTS	UNCORRECTED	MATERIAL DESCRIPTION
Maximum dry density = 146.2 pcf	143.2 pcf	Gravel (GP-GM) with silt and sand, Gray
Optimum moisture = 5.4 %	6.1 %	

Project No. EP2011 **Client:** Jami Lynn Daugherty
Project: Automatic DCP Testing

○ **Source of Sample:** Limestone (Unsoaked CBR)

Corps of Engineers
Engineer Research Development Center

Remarks:
The specific gravity was performed in accordance with ASTM D854.
The bulk specific gravity was estimated.
Water leaked from the bottom of the mold on the 6.9 and 8.3 % points.

Figure

Second Generation A-DCP Prototype Testing- Limestone (GW)

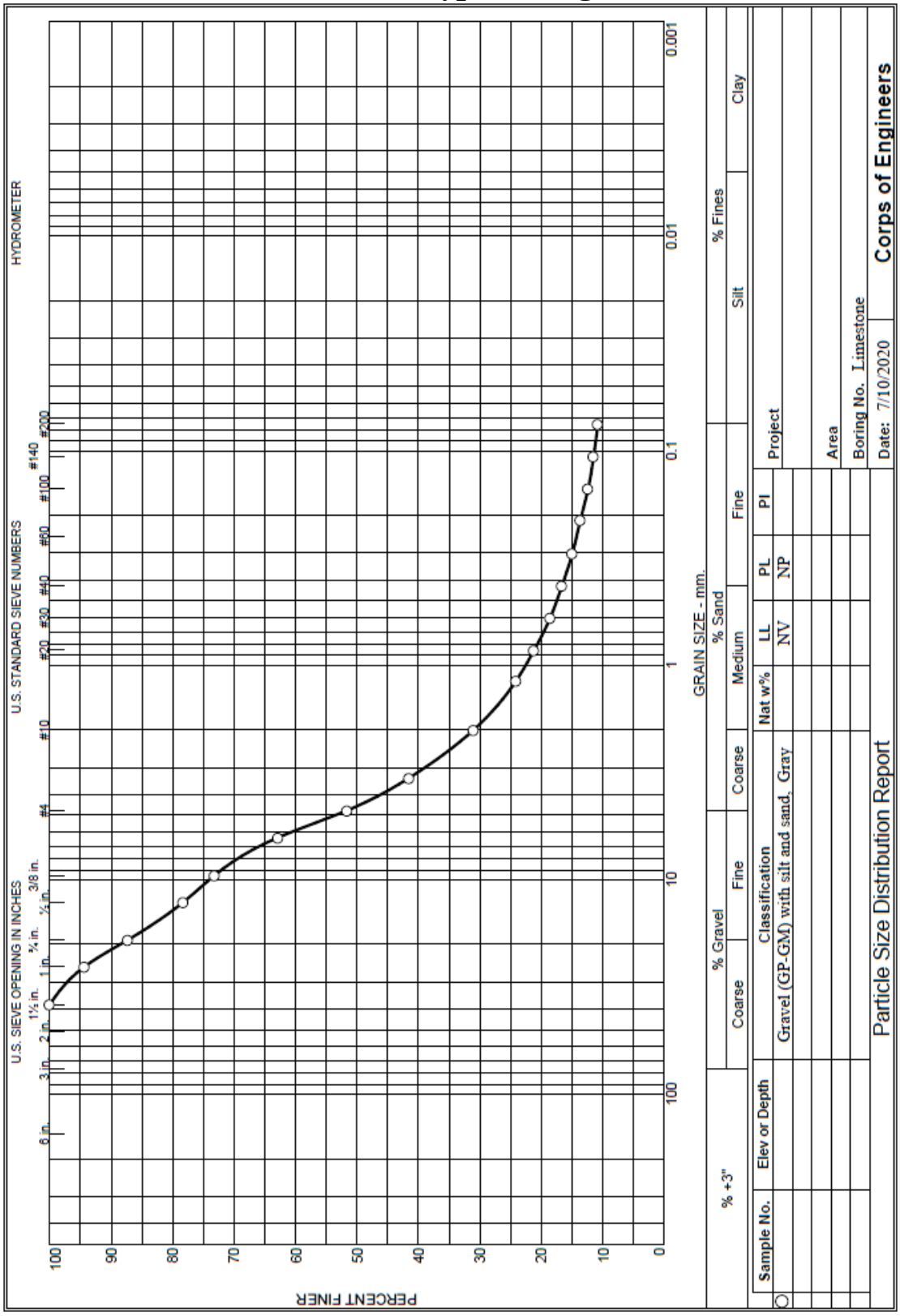

Second Generation A-DCP Prototype Testing- Limestone (GW)

Section Label	Soil Type	Depth in	Truck CBR	Clegg Impact Value CIV	Moisture Content %	Wet Density pcf	Dry Density pcf
GW Opt	GW	0	86	31.9	2.91	137.8	133.9
	GW	0	100	44.6	2.24	137.1	134.1
	GW	0	100	33.3	2.59	136.5	133.1
	GW	6	100	54.1	2.17	138.7	135.8
	GW	6	100	46.1	2.63	139.3	135.7
	GW	6	100	51.6	3.23	143.9	139.4
	GW	12	100	51.1	2.85	133.0	129.3
	GW	12	67	36.6	2.48	130.2	127.0
	GW	12	100	47.3	2.47	120.9	118.0
	GW	18	100	42.9	3.22	135.5	131.3
	GW	18	100	36.4	3.08	136.5	132.4
	GW	18	100	50.9	2.88	133.4	129.7
	GW	24	80	50.7	3.54	138.0	133.3
	GW	24	100	37.5	3.36	140.5	135.9
	GW	24	100	47.5	3.70	140.8	135.8
	GW	30	72	31.6	3.58	136.9	132.2
	GW	30	69	32.5	4.15	139.3	133.7
	GW	30	56	36.7	3.40	132.0	127.7

Second Generation A-DCP Prototype Testing- Limestone (GW)

Section Label	Soil Type	Depth in	Truck CBR	Clegg Impact Value CIV	Moisture Content %	Wet Density pcf	Dry Density pcf
GW Quick	GW	0	38.5	22.4	3.85	140.5	135.3
	GW	0	31.4	24.8	4.08	138.7	133.3
	GW	0	--	21.0	4.85	145.0	138.3
	GW	6	28	29.6	4.72	138.9	132.6
	GW	6	30	23.4	4.39	135.3	129.6
	GW	6	33	24.3	4.71	136.8	130.6
	GW	12	43	27.0	3.69	141.2	136.2
	GW	12	25	29.0	3.68	130.1	125.5
	GW	12	29	27.9	3.20	131.0	126.9
	GW	18	73	43.2	3.17	133.9	129.8
	GW	18	53	31.3	3.20	134.1	129.9
	GW	18	59	33.3	3.16	133.6	129.5
	GW	24	28	29.2	3.68	126.2	121.7
	GW	24	26	29.7	3.14	126.8	122.9
	GW	24	36	27.0	3.05	125.2	121.5
	GW	30	--	21.7	2.92	130.2	126.5
	GW	30	--	25.1	2.87	135.8	132.0
	GW	30	--	19.2	2.98	131.0	127.2

Second Generation A-DCP Prototype Testing- Silty Sand (SM)

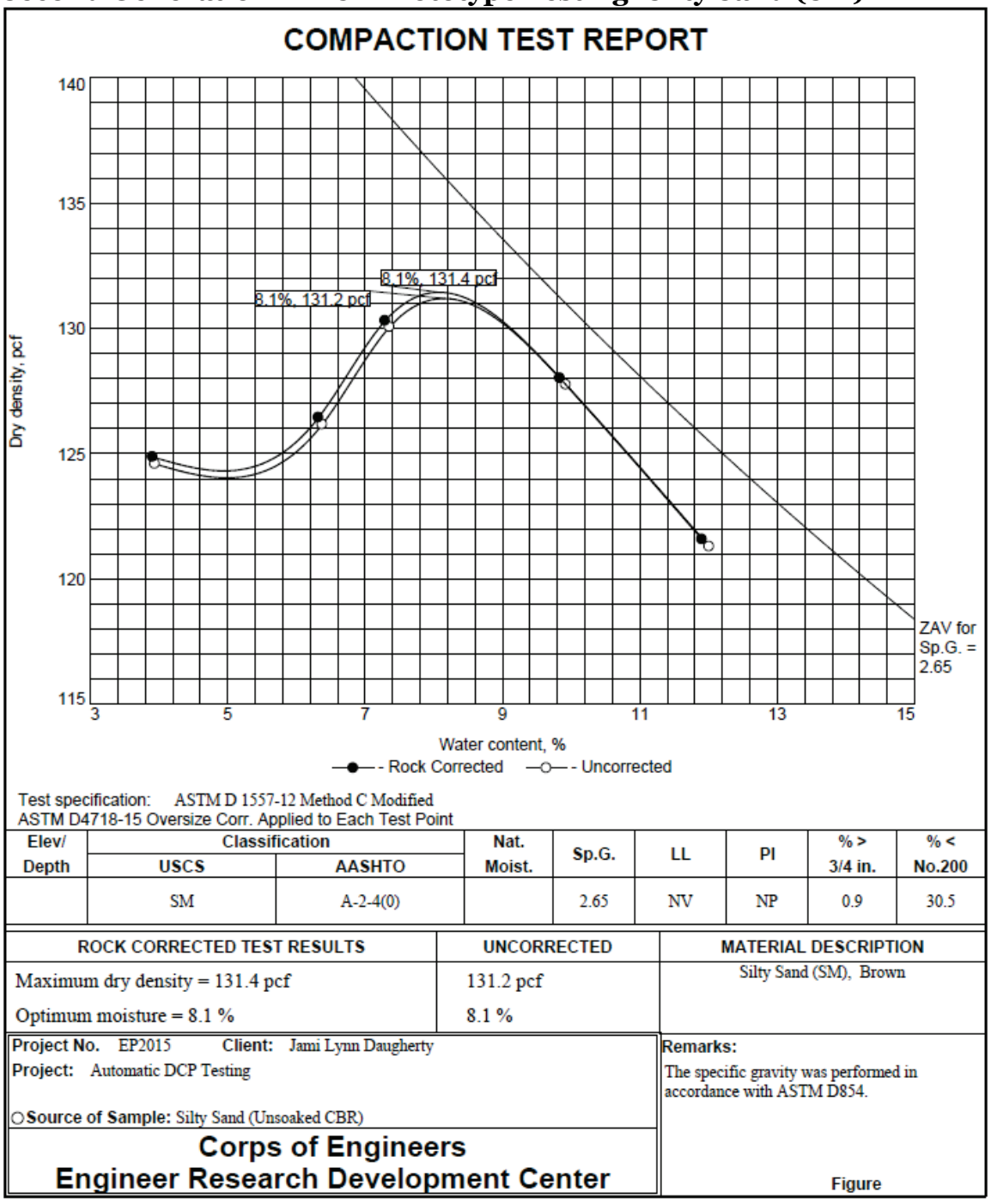

Test specification: ASTM D 1557-12 Method C Modified
ASTM D4718-15 Oversize Corr. Applied to Each Test Point

Elev/ Depth	Classification		Nat. Moist.	Sp.G.	LL	PI	% > 3/4 in.	% < No.200
	USCS	AASHTO						
	SM	A-2-4(0)		2.65	NV	NP	0.9	30.5

ROCK CORRECTED TEST RESULTS	UNCORRECTED	MATERIAL DESCRIPTION
Maximum dry density = 131.4 pcf	131.2 pcf	Silty Sand (SM), Brown
Optimum moisture = 8.1 %	8.1 %	

Project No. EP2015 **Client:** Jami Lynn Daugherty
Project: Automatic DCP Testing

○ **Source of Sample:** Silty Sand (Unsoaked CBR)

Corps of Engineers
Engineer Research Development Center

Remarks:
The specific gravity was performed in accordance with ASTM D854.

Figure

Second Generation A-DCP Prototype Testing- Silty Sand (SM)

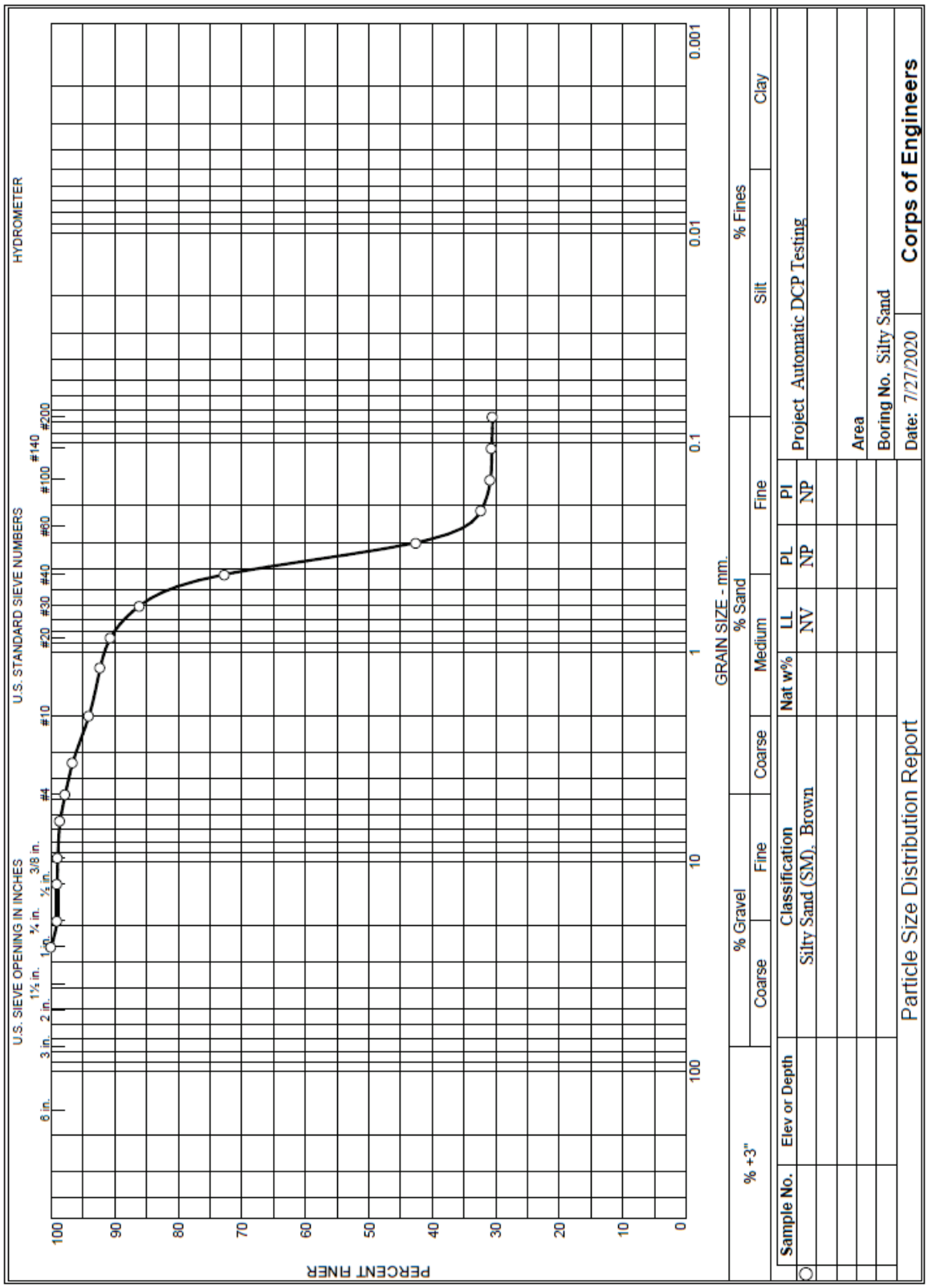

Second Generation A-DCP Prototype Testing- Silty Sand (SM)

Section Label	Soil Type	Depth in	Truck CBR	Clegg Impact Value CIV	Moisture Content %	Wet Density pcf	Dry Density pcf
SM Opt	SM	0	10.2	8.8	8.07	130.2	120.5
	SM	0	10.5	5.3	--	130.3	120.9
	SM	0	9.7	6.7	--	129.4	120.1
	SM	6	12.9	9.4	8.65	130.8	120.4
	SM	6	15.4	12.8	--	131.8	120.9
	SM	6	15.6	9.1	8.13	130.0	120.2
	SM	12	12.7	11.3	8.19	128.4	118.7
	SM	12	11.1	10.5	8.90	126.8	116.4
	SM	12	11.6	10.8	8.63	127.1	117.0
	SM	18	11.5	9.6	8.32	124.6	115.0
	SM	18	12.5	9.4	8.61	127.7	117.6
	SM	18	12.4	8.9	8.70	126.0	115.9
	SM	24	12.4	12.3	8.13	136.9	126.6
	SM	24	12.7	11.3	8.69	134.9	124.1
	SM	24	13.1	15.2	8.62	134.4	123.7
	SM	30	10.3	8.2	8.65	130.8	120.4
	SM	30	10.9	7.0	9.49	132.6	121.1
	SM	30	10.8	13.2	8.49	133.4	123.0

Second Generation A-DCP Prototype Testing- Silty Sand (SM)

Section Label	Soil Type	Depth in	Truck CBR	Clegg Impact Value CIV	Moisture Content %	Wet Density pcf	Dry Density pcf
SM - 5%	SM	0	10.3	10.3	5.34	126.2	119.8
	SM	0	12.5	11.7	5.61	128.5	121.7
	SM	0	12.3	11.7	4.95	124.2	118.4
	SM	6	13.5	11.5	5.27	131.1	124.5
	SM	6	13.3	10.8	5.25	131.1	124.6
	SM	6	17.3	10.8	5.48	136.0	129.0
	SM	12	13.3	10.5	5.64	127.2	120.4
	SM	12	12.5	7.6	--	--	--
	SM	12	14.9	11.3	5.67	130.7	123.7
	SM	18	13.5	12.5	5.25	126.6	120.3
	SM	18	13.5	6.5	--	--	--
	SM	18	17	11.1	5.25	124.5	118.3
	SM	24	16.8	9.8	5.27	134.2	127.5
	SM	24	13.1	7.9	--	--	--
	SM	24	13.9	9.9	5.03	130.2	124.0
	SM	30	15.2	8.9	5.39	124.5	118.1
	SM	30	12.7	9.1	3.64	130.7	126.1
	SM	30	12	10.5	5.58	119.8	113.5

S

Second Generation A-DCP Prototype Testing- Clayey Sand (SC)

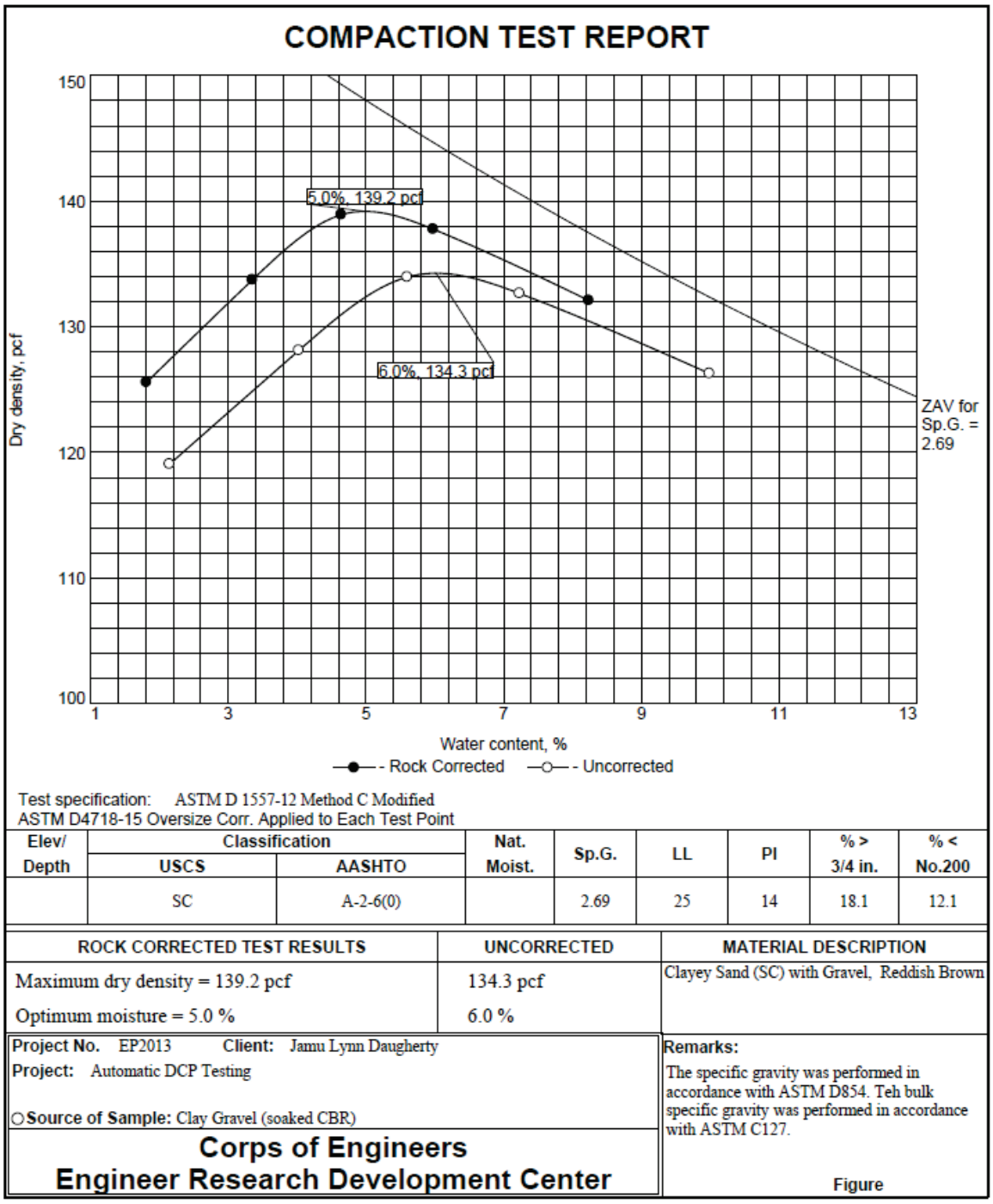

Elev/ Depth	Classification		Nat. Moist.	Sp.G.	LL	PI	% > 3/4 in.	% < No.200
	USCS	AASHTO						
	SC	A-2-6(0)		2.69	25	14	18.1	12.1

ROCK CORRECTED TEST RESULTS	UNCORRECTED	MATERIAL DESCRIPTION
Maximum dry density = 139.2 pcf	134.3 pcf	Clayey Sand (SC) with Gravel, Reddish Brown
Optimum moisture = 5.0 %	6.0 %	

Project No. EP2013 **Client:** Jamu Lynn Daugherty
Project: Automatic DCP Testing

○ **Source of Sample:** Clay Gravel (soaked CBR)

Corps of Engineers
Engineer Research Development Center

Remarks:
The specific gravity was performed in accordance with ASTM D854. Teh bulk specific gravity was performed in accordance with ASTM C127.

Figure

Second Generation A-DCP Prototype Testing- Clayey Sand (SC)

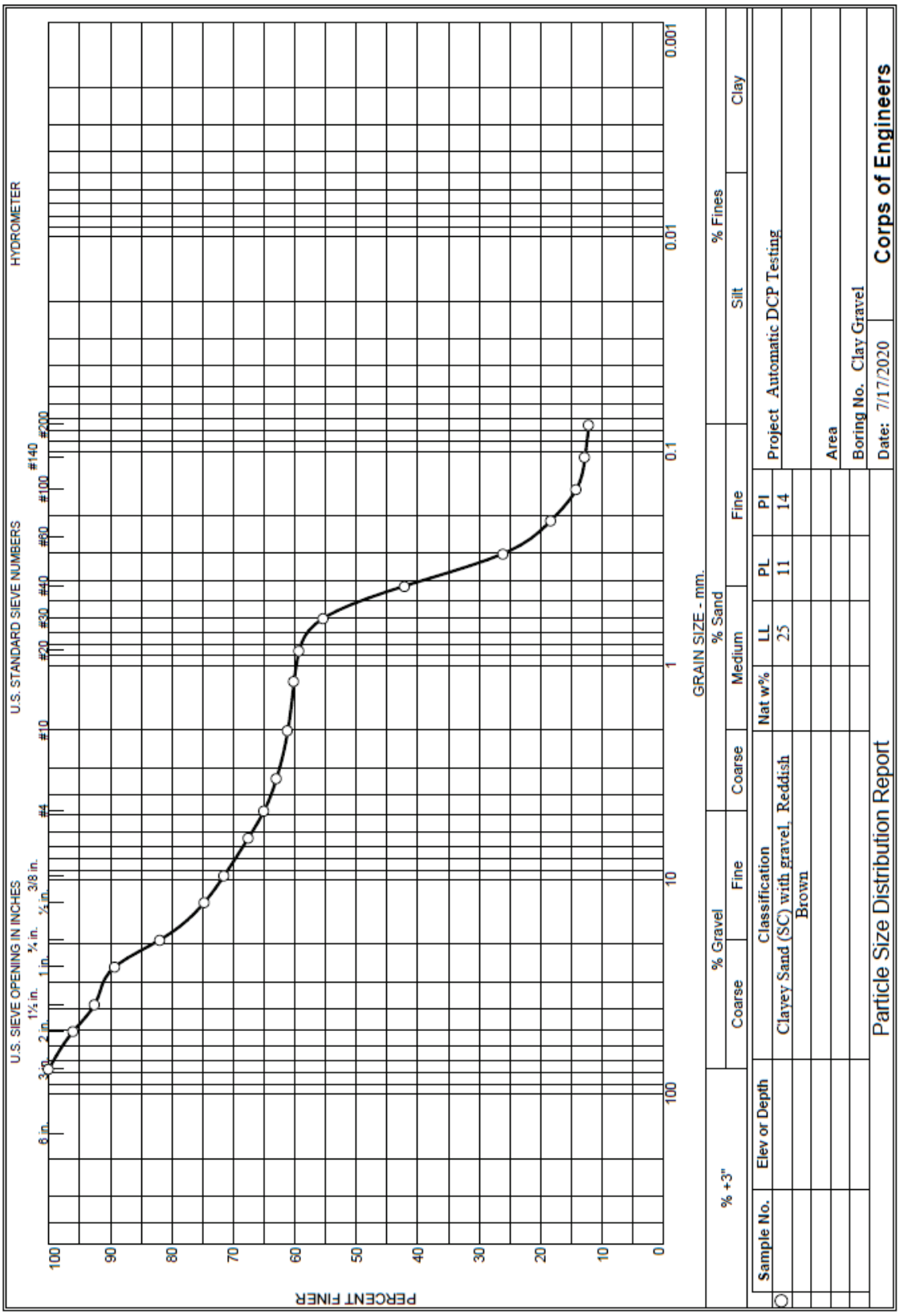

Second Generation A-DCP Prototype Testing- Clayey Sand (SC)

Section Label	Soil Type	Depth in	Truck CBR	Clegg Impact Value CIV	Moisture Content %	Wet Density pcf	Dry Density pcf
SC Opt	GC	0	41	30.9	6.03	137.1	129.3
	GC	0	49	25.6	6.04	139.6	131.6
	GC	0	44	25.1	4.47	133.4	127.7
	GC	6	46	22.4	7.32	136.1	126.8
	GC	6	44	26.1	6.61	138.1	129.5
	GC	6	49	21.9	6.92	136.7	127.9
	GC	12	49	24.6	6.19	136.9	128.9
	GC	12	50	27.0	7.51	136.2	126.7
	GC	12	45	28.5	6.32	137.2	129.0
	GC	18	36	22.9	6.27	133.2	125.3
	GC	18	30	24.6	6.15	127.6	120.2
	GC	18	37	25.8	6.97	130.6	122.1
	GC	24	27	21.5	6.10	132.0	124.4
	GC	24	31	21.4	7.00	132.5	123.8
	GC	24	22	23.6	6.46	131.6	123.6
	GC	30	28	18.0	5.48	133.7	126.8
	GC	30	21	27.2	4.92	134.1	127.8
	GC	30	23	18.6	6.52	131.4	123.4

Second Generation A-DCP Prototype Testing- Clayey Sand (SC)

Section Label	Soil Type	Depth in	Truck CBR	Clegg Impact Value CIV	Moisture Content %	Wet Density pcf	Dry Density pcf
SC Wet	GC	0	5.1	15.6	5.79	137.4	129.9
	GC	0	4.7	7.9	7.43	140.4	130.7
	GC	0	5.2	10.8	8.40	138.5	127.8
	GC	6	7.3	10.5	8.05	137.9	127.6
	GC	6	5.2	12.7	8.18	136.8	126.5
	GC	6	5.9	19.7	8.64	137.5	126.6
	GC	12	5.5	13.4	7.77	138.5	128.5
	GC	12	4.3	8.8	7.29	137.3	128.0
	GC	12	5.9	12.2	6.96	139.3	130.2
	GC	18	14.4	12.8	9.34	137.6	125.8
	GC	18	10	15.4	8.32	136.3	125.8
	GC	18	10.1	10.5	8.72	137.8	126.7
	GC	24	14.8	13	6.74	134.8	126.3
	GC	24	14	8.9	6.22	134.8	126.9
	GC	24	14.4	16.3	5.97	132.2	124.8
	GC	30	10.7	12.5	7.86	135.8	125.9
	GC	30	8.5	6.4	8.84	135.1	124.1
	GC	30	10.3	8.6	9.37	136.6	124.9

Second Generation A-DCP Prototype Testing- Lean Clay (CL)

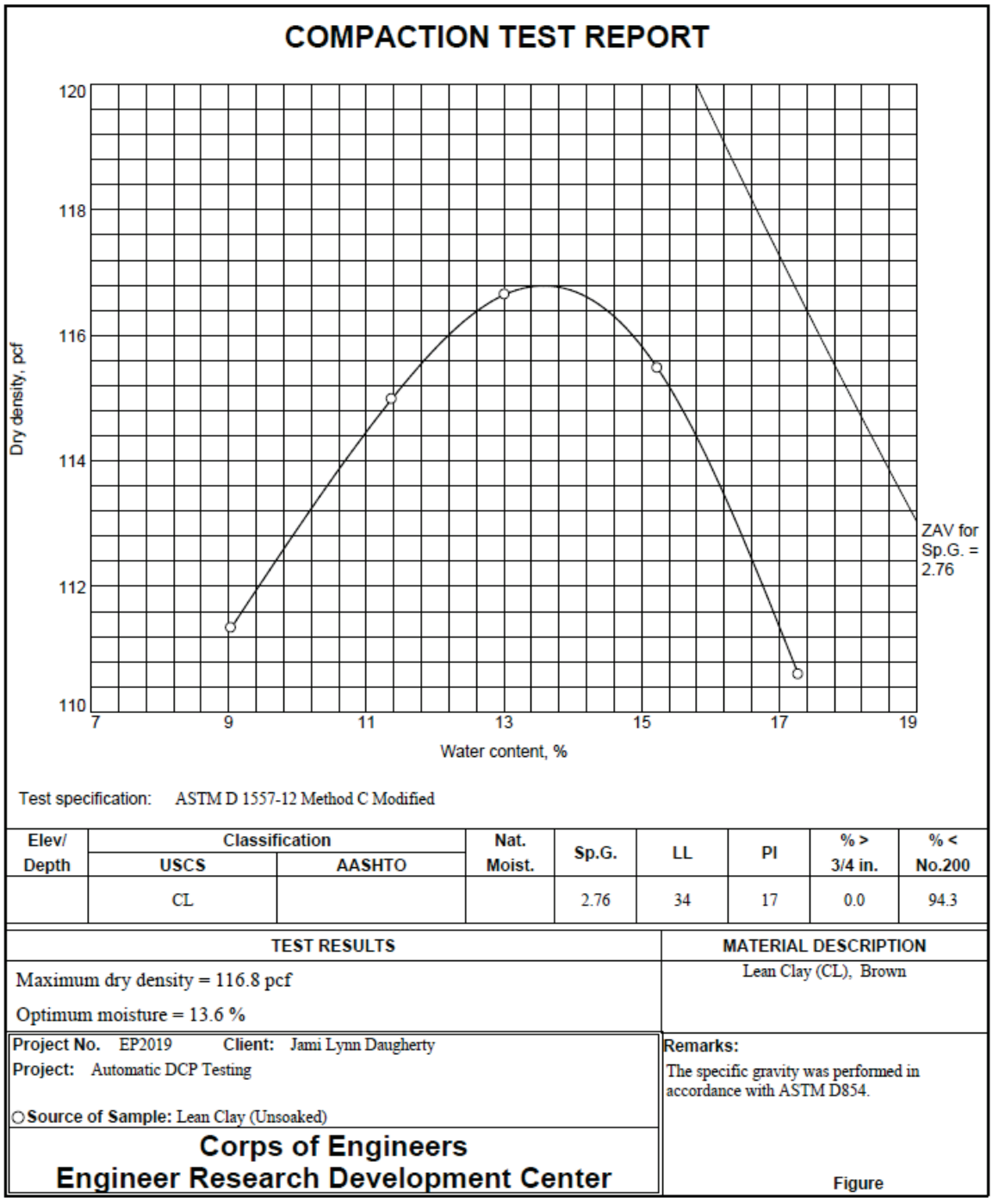

Second Generation A-DCP Prototype Testing- Lean Clay (CL)

Second Generation A-DCP Prototype Testing- Lean Clay (CL)

Section Label	Soil Type	Depth in	Truck CBR	Clegg Impact Value CIV	Moisture Content %	Wet Density pcf	Dry Density pcf
CL Opt	CL	0	14	7.6	18.5	120.3	101.5
	CL	0	10	8.8	17.4	117.7	100.3
	CL	0	6	8.6	17.2	119.5	102.0
	CL	6	13	9.9	17.4	113.3	96.5
	CL	6	12	12.8	17.2	116.9	99.7
	CL	6	14	9.9	17.6	119.8	101.9
	CL	12	8	10.5	17.9	108.9	92.4
	CL	12	10	8.4	22.4	114.8	93.8
	CL	12	13	10.1	17.5	118.8	101.1
	CL	18	13	11.1	18.1	123.7	104.7
	CL	18	11	9.1	17.5	121.0	103.0
	CL	18	14	9.4	18.4	124.5	105.2
	CL	24	6	9.6	19.6	120.2	100.5
	CL	24	4	10.3	17.8	120.3	102.1
	CL	24	10	9.1	18.5	119.6	100.9
	CL	30	13	12.3	18.0	123.9	105.0
	CL	30	15	11.3	18.7	122.3	103.0
	CL	30	12	11.7	19.5	120.9	101.2

Second Generation A-DCP Prototype Testing- Lean Clay (CL)

Section Label	Soil Type	Depth in	Truck CBR	Clegg Impact Value CIV	Moisture Content %	Wet Density pcf	Dry Density pcf
CL Dry	CL	0	31.9	14.9	14.36	123.5	108.0
	CL	0	32.9	17.1	15.75	124.5	107.6
	CL	0	27.7	16.3	15.29	123.5	107.1
	CL	6	23.9	17.1	12.32	125.8	112.0
	CL	6	26	16.9	14.68	121.8	106.2
	CL	6	23.6	14.9	14.03	125.6	110.1
	CL	12	14.8	16.1	13.92	120.7	106.0
	CL	12	15	14.0	14.58	121.7	106.2
	CL	12	24.7	10.1	16.22	121.3	104.4
	CL	18	19.8	15.4	15.12	122.5	106.4
	CL	18	18.1	15.6	15.38	124.4	107.8
	CL	18	16.8	15.7	17.87	124.8	105.9
	CL	24	19.8	14.0	15.05	118.0	102.6
	CL	24	13.3	14.9	14.43	117.8	102.9
	CL	24	18.9	11.3	15.23	118.0	102.4
	CL	30	8	6.4	15.05	117.5	102.1
	CL	30	7.9	9.9	14.98	116.2	101.1
	CL	30	8.7	10.8	14.80	116.4	101.4

Appendix B: Second Generation A-DCP Field Data

Following is the blow count with depth data recorded for each test conducted during the field experimentation. These data were used in the calculation of the penetration rate and correlated to CBR at 6-in. intervals throughout each test section. The following figure restates the position in which each test was taken.

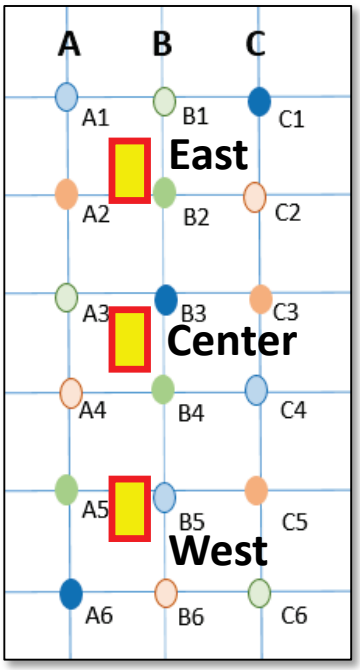

Device	Location
A-DCP #1 (S/N: 001)	A6, B3, C1
A-DCP #2 (S/N: 010)	A1, B5, C4
Manual DCP	A5, B2, B4
Instrumented DCP	A3, B1, C6

A-DCP #1

A-DCP #2

Manual DCP

Instrumented DCP

Truck CBR

Soil Type: CH

Thumper SN #1						Thumper SN #5						Manual DCP					
A6		C1		B3		B5		A1		C4		A5		B2		B4	
No. of Blows	Accum. Penetration (mm)	No. of Blows	Accum. Penetration (mm)	No. of Blows	Accum. Penetration (mm)	No. of Blows	Accum. Penetration (mm)	No. of Blows	Accum. Penetration (mm)	No. of Blows	Accum. Penetration (mm)	No. of Blows	Accum. Penetration (mm)	No. of Blows	Accum. Penetration (mm)	No. of Blows	Accum. Penetration (mm)
1	84	1	104	1	99	1	25	1	81	1	96	0	0	0	0	0	0
1	112	1	137	1	160	1	53	1	121	1	121	1	100	1	100	1	100
1	157	1	173	1	187	2	91	1	149	1	159	1	190	1	165	1	165
1	185	1	206	2	220	3	127	1	198	1	202	1	245	1	215	1	220
2	216	2	234	2	251	3	152	2	228	1	235	1	290	1	255	1	260
2	244	3	264	2	276	3	180	2	256	1	261	1	330	1	290	1	300
3	274	3	295	3	307	4	206	2	281	2	296	1	365	1	320	1	335
3	302	3	325	3	340	4	231	3	320	2	324	1	400	1	350	1	365
3	332	3	351	3	368	4	259	3	347	2	350	1	435	1	375	1	390
3	360	3	378	4	398	4	284	2	378	3	383	1	465	1	400	1	415
3	388	4	409	4	426	4	310	3	403	3	411	1	490	1	420	1	440
4	414	4	437	4	452	5	340	3	431	3	436	1	515	1	445	1	465
3	444	4	462	4	480	5	371	3	457	2	464	1	540	1	465	1	485
4	472	4	488	5	507	5	399	4	487	3	492	1	565	1	490	1	505
4	503	4	516	5	538	5	429	4	518	3	517	1	580	1	510	1	525
4	528	4	541	5	563	5	457	4	548	3	545	1	600	1	530	1	540
4	556	4	566	5	591	5	485	4	579	3	576	1	620	1	550	2	575
4	584	5	597	5	617	5	511	4	607	3	601	1	635	1	570	2	610
4	609	4	622	5	642	5	536	4	637	3	629	1	650	1	585	2	640
5	640	5	653	5	662	5	564	4	665	3	655	2	680	1	605	2	670
5	670	5	683	5	695	6	592	4	690	3	680	2	710	1	620	2	705
5	701	5	711	5	721	5	620	4	718	4	708	2	735	1	635	2	735
5	729	5	742	6	751	6	648	4	744	4	741			2	665		
5	759	5	767	6	782	6	676	4	769	4	766			2	695		
5	787	5	792	6	812	6	704	5	800	3	794			2	720		
5	815	6	823	6	840	6	734	5	830	4	825						
5	840	6	851	5	868	5	759	5	861	4	853						
6	868	9	879	5	896	5	785	5	886	4	881						
9	896	10	904	6	922	6	813	5	911	4	906						
9	922	9	930	4	939	8	841	6	934	5	939						
6	942	2	937			7	869			1	944						
						6	892										

Soil Type: SC-OPT

Thumper SN #1						Thumper SN #5								Manual DCP					
A6		C1		B3		B5		A1		C4		C4		A5		B2		B4	
No. of Blows	Accum. Penetration (mm)	No. of Blows	Accum. Penetration (mm)	No. of Blows	Accum. Penetration (mm)	No. of Blows	Accum. Penetration (mm)	No. of Blows	Accum. Penetration (mm)	No. of Blows	Accum. Penetration (mm)	No. of Blows	Accum. Penetration (mm)	No. of Blows	Accum. Penetration (mm)	No. of Blows	Accum. Penetration (mm)	No. of Blows	Accum. Penetration (mm)
4	30	10	8	4	43	2	28	2	31	1	39	1	41	0	0	0	0	0	0
6	58	3	31	5	68	6	56	5	61	3	67	4	74	1	15	1	20	1	25
7	84	5	59	5	96	5	81	6	89	4	92	4	105	2	40	1	35	1	35
8	112	5	87	10	121	5	109	6	117	4	120	4	130	2	65	2	50	2	50
7	137	6	115	6	149	5	137	5	148	7	145	4	158	2	75	2	70	3	70
5	163	7	143	6	175	5	168	5	173	5	173	4	186	3	100	2	85	3	95
5	188	6	168	7	200	5	193	6	204	4	201	4	214	3	125	3	115	3	120
7	216	6	194	9	228	5	221	5	232	4	229	6	239	3	150	3	145	3	140
8	244	10	221	9	256	4	246	5	257	5	257	7	267	3	170	3	170	3	160
8	272	8	249	8	284	6	272	5	282	6	282	7	295	3	195	3	185	3	180
9	297	7	275	7	309	5	302	4	315	5	313	5	321	3	215	4	205	3	200
8	323	9	303	10	335	6	330	4	343	5	338	5	346	3	235	4	225	3	220
10	348	10	321	10	355	7	358	5	374	7	369	5	374	3	250	4	250	3	240
10	371	10	341	10	375	6	384	5	402	6	394	6	402	4	265	4	270	3	255
9	396	9	369	10	398	7	409	6	430	5	422	9	427	5	285	4	295	3	265
7	424	7	394	10	424	6	437	7	460	4	453	8	455	5	300	4	320	4	280
7	450	8	420	9	449	5	470	4	486	5	478	7	481	6	330	4	345	5	305
7	475	6	448	8	477	5	495	4	511	6	506	7	511	6	355	4	365	5	330
9	500	6	473	9	505	7	523	5	539	9	531	7	539	6	385	4	385	5	355
7	526	8	501	7	530	8	551	6	567	7	559	6	564	6	425	4	415	5	385
9	554	6	526	8	558	6	584	6	597	6	587	7	592	4	455	4	445	5	420
6	579	7	552	7	586	4	612	5	625	5	618	6	620	4	485	4	470	4	455
7	605	6	577	6	614	5	638	4	653	5	643	6	648	4	515	4	500	3	480
7	632	6	608	7	640	7	665	3	681	5	669	6	676	4	535	4	530	3	500
7	658	5	633	7	670	6	691	3	707	5	696	5	707	4	550	4	555	3	530
8	686	5	661	7	695	5	721	3	737	4	724	4	737	5	575	3	575	3	555
6	714	5	689	6	723	4	749	3	765	3	752	3	765	5	595	3	600	3	585
5	739	5	714	4	751	3	780	3	798	4	785	3	801	5	625	3	620	2	605
7	765	4	742	4	777	3	808	4	829	4	813	3	829	5	640	3	645	2	625
6	798	4	770	5	802	4	841	6	854	4	841	2	859	6	675	3	670	2	640
5	823	6	796	4	830	9	869	5	884	5	872	4	884	1	700	3	695	3	660
8	851	7	826	9	858	10	894	5	915	5	900	6	912	2	725	3	720	3	685
9	876	7	854	10	886	6	917	2	925	5	930	5	938	2	765	3	755	2	700
8	904	8	882	8	911					1	938			2	805	3	795	3	725
5	919	7	907	9	929											2	810	2	750
		4	925															2	775
																		2	805

Soil Type: SC-Wet

Thumper SN #1						Thumper SN #5						Manual DCP					
A6		C1		B3		B5		A1		C4		A5		B2		B4	
No. of Blows	Accum. Penetration (mm)	No. of Blows	Accum. Penetration (mm)	No. of Blows	Accum. Penetration (mm)	No. of Blows	Accum. Penetration (mm)	No. of Blows	Accum. Penetration (mm)	No. of Blows	Accum. Penetration (mm)	No. of Blows	Accum. Penetration (mm)	No. of Blows	Accum. Penetration (mm)	No. of Blows	Accum. Penetration (mm)
2	33	3	62	3	52	1	38	1	35	1	30	0	0	0	0	0	0
2	78	2	95	3	83	2	79	1	66	1	66	1	45	1	45	1	45
2	114	2	120	2	113	2	117	1	93	2	101	1	80	1	75	1	85
2	149	2	151	2	151	3	150	1	126	2	147	1	110	1	105	1	110
2	180	2	184	2	179	3	191	2	170	2	182	1	135	1	135	1	135
2	205	2	224	3	212	2	234	2	215	3	218	1	155	1	160	1	150
2	233	2	257	3	240	2	264	2	253	2	256	1	165	1	185	1	165
4	264	2	285	2	271	2	297	2	287	2	289	1	180	1	205	2	190
3	297	3	318	4	306	2	325	2	325	2	314	2	210	1	220	2	235
3	325	2	346	3	331	2	356	1	350	3	347	2	250	1	245	1	250
2	353	3	377	2	359	3	386	2	383	3	375	1	270	1	270	1	265
2	380	4	407	2	395	3	417	3	408	3	403	1	285	1	285	2	305
2	416	3	433	2	420	2	445	5	439	3	436	1	310	1	300	2	340
3	454	4	458	3	448	3	472	3	464	3	469	1	330	1	310	1	360
3	487	5	483	3	476	4	500	3	502	3	500	1	350	2	345	1	375
3	520	5	514	3	504	4	531	3	538	3	528	1	370	2	395	1	395
2	551	4	542	3	535	3	569	3	568	4	561	1	385	1	410	1	415
3	579	4	575	3	565	1	594	3	599	3	591	1	400	1	430	1	430
4	607	5	603	4	596	3	630	3	624	3	622	1	410	1	440	1	445
4	634	5	633	3	629	3	671	4	660	3	655	2	435	2	460	1	465
4	670	5	661	5	659	2	699	2	688	2	685	2	460	2	490	1	485
4	695	5	689	4	687	2	726			3	721	2	490	2	520	1	500
7	723	5	717	3	715	2	762			4	751	1	505	2	545	1	520
6	749	3	745	3	751	1	790			3	789	2	530	2	565	1	545
4	774	4	773	2	781	1	815			3	828	2	550	2	580	1	575
3	802	3	806	2	812	2	846			2	861	2	575	2	595	1	590
5	830	3	844	2	839	2	876			3	894	2	600	3	620	1	605
6	855	2	872	2	867	2	907			3	922	2	615	3	645	2	635
8	881	2	902	2	903	1	922					3	640	3	675	1	655
8	909	5	933	3	928							3	660	2	695	1	670
4	919	1	941	3	944							3	700	2	730	1	685
												2	730	2	760	2	725
												1	755	2	790	1	750
														2	820	1	770
														1	850	1	805
																1	850

Soil Type: CL-Dry

Thumper SN #1						Thumper SN #5						Manual DCP					
A6		C1		B3		B5		A1		C4		A5		B2		B4	
No. of Blows	Accum. Penetration (mm)	No. of Blows	Accum. Penetration (mm)	No. of Blows	Accum. Penetration (mm)	No. of Blows	Accum. Penetration (mm)	No. of Blows	Accum. Penetration (mm)	No. of Blows	Accum. Penetration (mm)	No. of Blows	Accum. Penetration (mm)	No. of Blows	Accum. Penetration (mm)	No. of Blows	Accum. Penetration (mm)
3	27	2	27	3	29	3	20	2	28	3	29	0	0	0	0	0	0
7	55	5	55	7	55	4	48	4	58	5	59	1	10	1	15	1	10
7	83	5	83	7	83	5	79	4	91	4	90	2	25	3	45	3	35
5	110	5	114	7	110	4	109	3	119	3	118	3	45	3	85	3	60
4	141	4	147	5	141	3	140	3	152	2	146	3	75	3	125	3	100
4	171	3	177	4	171	3	175	3	188	2	179	3	105	2	160	2	140
4	199	3	210	4	197	3	206	3	221	3	209	3	145	2	185	2	175
4	225	3	238	6	225	4	234	4	249	5	240	2	170	2	205	2	200
6	255	4	266	5	253	4	262	4	279	5	270	2	190	2	220	2	215
4	281	4	294	5	281	4	287	4	312	4	306	2	210	3	245	3	240
5	309	4	322	4	306	4	318	3	338	3	331	2	225	3	270	3	265
5	334	5	352	4	331	4	343	3	363	3	357	3	250	3	300	3	295
5	362	4	380	4	359	4	371	3	393	3	385	3	275	3	325	3	325
4	387	4	408	4	385	4	404	3	424	3	420	3	300	3	345	3	355
5	418	5	441	4	415	3	437	4	452	3	448	3	330	3	365	3	395
5	446	5	469	3	443	3	465	5	485	3	479	3	360	3	390	3	435
5	471	4	495	4	471	4	498	4	515	3	509	3	395	3	420	2	455
4	502	4	528	5	499	3	526	3	546	3	534	3	425	3	445	2	480
5	530	3	558	5	527	3	554	3	574	2	570	3	450	3	470	2	500
4	560	2	586	4	558	3	587	2	604	2	613	3	475	3	495	2	525
3	588	2	616	3	588	2	622	3	635	1	639	3	500	3	525	2	555
3	616	4	642	2	613	2	650	4	663	2	666	3	530	3	560	2	610
3	646	5	670	3	641	4	681	4	688	3	694	3	565	2	590	1	635
4	677	5	695	4	669	5	709	4	724	3	722	3	610	2	625	1	650
5	705	4	723	7	697	5	742	3	754	3	755	2	640	2	645	2	675
4	733	3	756	6	725	4	775	3	782	2	783	2	660	2	675	2	700
4	763	2	784	4	751	3	810	3	807	2	821	2	675	2	695	2	720
4	791	2	809	4	784	3	838	3	835	2	852	3	700	3	725	2	745
5	819	4	840	3	817	2	866	3	863	3	880	3	725	3	755	2	770
5	845	3	865	3	850	3	892	2	891	4	913	3	750	3	790	2	805
5	870	3	891	3	878	3	917	3	922	1	923	1	780	3	815	2	840
6	903	3	924	3	903							2	810				
5	921			2	923												

Soil Type: CL-Opt

Thumper SN #1						Thumper SN #5						Manual DCP					
A6		C1		B3		B5		A1		C4		A5		B2		B4	
No. of Blows	Accum. Penetration (mm)	No. of Blows	Accum. Penetration (mm)	No. of Blows	Accum. Penetration (mm)	No. of Blows	Accum. Penetration (mm)	No. of Blows	Accum. Penetration (mm)	No. of Blows	Accum. Penetration (mm)	No. of Blows	Accum. Penetration (mm)	No. of Blows	Accum. Penetration (mm)	No. of Blows	Accum. Penetration (mm)
7	64	3	28	3	32	1	25	1	39	2	40	0	0	0	0	0	0
2	91	3	61	2	63	2	58	2	70	2	68	1	20	1	30	1	25
3	122	3	92	4	103	2	89	2	100	1	96	1	35	1	55	1	50
3	147	3	125	2	131	2	127	2	128	2	132	1	55	1	90	1	70
3	178	3	155	2	167	2	155	2	174	2	160	1	75	1	125	1	95
3	203	4	188	1	195	2	185	2	215	2	187	1	95	1	150	1	125
3	234	3	214	2	220	3	216	2	243	2	215	1	115	1	170	1	145
3	264	4	247	3	251	2	244	3	281	2	241	1	135	1	190	1	165
2	295	2	272	3	276	3	274	3	311	3	279	1	150	1	210	1	185
4	323	4	298	3	307	3	307	2	342	2	309	1	170	1	230	1	200
3	351	3	328	2	335	3	343	2	377	2	340	1	185	1	250	1	220
3	376	3	361	2	368	2	373	1	405	2	365	1	205	1	270	1	235
3	406	2	389	2	403	2	411	1	431	2	403	1	220	1	285	1	255
3	445	3	425	2	436	2	445	2	471	2	429	1	235	1	310	1	275
2	472	3	455	2	464	2	470	2	499	2	457	1	250	1	330	1	290
2	498	3	483	2	492	3	505	2	525	2	482	1	260	1	360	1	310
3	528	3	516	2	540	2	538	2	552	2	510	2	290	1	390	1	330
3	554	2	542	1	566	2	572	2	588	2	543	2	320	1	420	1	350
4	587	2	577	1	591	2	617	2	626	2	579	2	350	1	440	1	375
3	617	2	608	2	627	1	648	2	654	2	617	2	400	1	455	1	405
3	655	2	646	2	660	1	678	2	692	2	652	1	425	1	475	1	430
3	691	2	681	2	690	2	732	2	738	2	680	1	445	1	495	1	445
3	724	2	712	2	723	1	767	2	779	2	708	1	460	1	515	1	465
3	765	2	737	2	754	2	795	2	817	2	739	1	475	1	525	1	480
2	800	3	770	3	784	2	833	2	852	2	769	1	495	1	550	1	495
3	828	2	796	3	812	2	861	2	885	2	797	1	515	1	580	1	510
4	859	4	826	3	843	3	894	2	923	3	833	1	535	1	615	2	545
4	889	3	854	3	870	2	919	1	931	2	858	1	555	1	645	2	590
4	922	3	882	2	898					2	886	1	570	1	670	1	620
4	953	3	912	2	919					2	919	1	595	1	695	1	645
												1	615	1	715	1	675
												2	635	1	735	1	700
												2	655	1	765	1	725
												2	675	1	790	1	755
												2	695	1	810	1	780
												2	725	1	825	1	795
												2	745	1	845	1	810
														1	860		
														1	880		
														1	895		

Soil Type: GW

Thumper SN #1						Thumper SN #5						Manual DCP					
A6		C1		B3		B5		A1		C4		A5		B2		B4	
No. of Blows	Accum. Penetration (mm)	No. of Blows	Accum. Penetration (mm)	No. of Blows	Accum. Penetration (mm)	No. of Blows	Accum. Penetration (mm)	No. of Blows	Accum. Penetration (mm)	No. of Blows	Accum. Penetration (mm)	No. of Blows	Accum. Penetration (mm)	No. of Blows	Accum. Penetration (mm)	No. of Blows	Accum. Penetration (mm)
4	29	10	36	10	25	2	20	2	32	4	29	0	0	0	0	0	0
9	55	10	51	10	43	9	46	7	58	10	54	1	10	1	10	1	10
9	85	10	76	10	60	7	74	6	86	8	85	2	20	3	25	3	25
9	110	9	104	10	78	7	102	8	111	8	113	3	30	3	40	3	40
10	133	10	124	10	99	9	127	10	131	9	141	6	50	3	50	3	50
10	146	20	150	10	116	10	145	20	167	10	151	6	70	6	85	6	85
20	174	20	175	20	144	10	160	20	205	10	169	6	90	6	120	6	115
20	204	20	201	20	160	20	196	20	235	10	186	6	110	6	135	6	140
20	235	20	229	20	177	20	236	20	258	10	207	6	125	10	150	6	150
20	258	20	251	20	198	20	267	20	274	10	232	8	140	10	175	10	175
20	276	20	269	20	218	20	282	20	291	10	255	10	155	10	205	10	205
20	291	20	282	20	238	20	297	20	312	20	278	10	175	10	230	10	235
20	309	20	297	20	259	20	315	20	332	20	301	10	190	10	260	10	260
20	326	20	312	20	274	20	333	20	355	20	331	10	205	10	270	10	280
20	349	20	328	20	289	20	356	20	378	20	369	10	230	15	290	10	285
20	370	20	345	20	302	20	376	20	406	20	407	10	255	15	305	15	295
20	390	20	358	20	317	20	394	20	428	20	433	10	265	15	325	20	315
20	413	20	376	20	337	20	411	20	446	20	453	10	270	15	345	20	355
20	433	20	391	20	363	20	419	20	464	20	471	15	285	15	375	20	390
20	451	20	404	20	386	20	427	20	482	20	489	15	295	15	395	20	425
20	466	20	417	20	408	20	437	20	500	20	504	20	310	15	420	20	445
20	484	20	427	20	426	20	442	20	515	20	519	20	320	15	435	20	460
20	499	20	437	20	439	20	452	20	533	20	537	20	345	20	450	20	470
20	517	20	445	20	449	20	467	20	548	20	555	20	365	20	465	20	485
20	535	20	455	20	462	20	480	20	563	20	573	20	395	20	475	20	500
20	550	20	465	20	472	20	495	20	576	20	588	20	410	20	475	20	510
20	565	20	475	20	500	20	511	20	589	20	608	20	420	20	480	20	520
20	580	20	485	20	500	20	528	20	599	20	623	20	430	20	480	20	535
20	593	20	495	20	510	20	546	20	611	20	641	20	440	20	480	20	545
20	606	20	508	20	520	20	561	20	624	20	656	20	450			20	550
20	618	20	521	20	533	20	577	20	637	20	679	20	460			20	560
20	634	20	533	20	541	20	592	20	652	20	692	20	470			20	565
20	646	20	551	20	551	20	602	20	665	20	710	20	500			20	575
20	662	20	564	20	563	20	612	20	680	20	730	20	525			20	580
20	674	20	577	20	574	20	620	20	698	20	745	20	550			20	585
20	687	20	592	20	586	20	630	20	713	20	766	20	580			20	590
20	702	20	602	20	596	20	640	20	728	20	788	20	605			20	595
20	715	20	610	20	607	20	655	20	743	20	816	20	620			20	600
20	730	20	622	20	619	20	665	20	761	20	844	20	640			20	605
20	745	20	632	20	629	20	678	20	774	20	885	20	660			20	610
20	766	20	643	20	640	20	691	20	792	20	920	20	680				
20	789	20	653	20	650	20	701	20	807			20	690				
20	817	20	665	20	662	20	714	20	822			20	710				

Soil Type: GW-Quick

Thumper SN #1						Thumper SN #5						Manual DCP					
A6		C1		B3		B5		A1		C4		A5		B2		B4	
No. of Blows	Accum. Penetration (mm)	No. of Blows	Accum. Penetration (mm)	No. of Blows	Accum. Penetration (mm)	No. of Blows	Accum. Penetration (mm)	No. of Blows	Accum. Penetration (mm)	No. of Blows	Accum. Penetration (mm)	No. of Blows	Accum. Penetration (mm)	No. of Blows	Accum. Penetration (mm)	No. of Blows	Accum. Penetration (mm)
2	31	2	30	3	40	1	25	1	31	1	30	0	0	0	0	0	0
2	56	3	58	4	70	4	56	2	59	4	63	1	25	1	20	1	20
4	87	4	86	4	96	4	84	4	92	3	91	1	35	1	35	1	30
6	115	3	117	4	124	4	114	3	118	3	121	1	55	1	45	2	45
10	142	6	145	5	149	5	140	4	146	3	147	2	75	2	70	2	70
8	168	9	170	7	180	7	168	7	174	5	172	2	105	2	95	2	95
8	193	9	198	6	205	9	196	6	204	5	200	2	115	2	120	2	115
8	221	10	226	6	230	8	226	6	230	5	228	2	130	2	135	2	130
7	249	9	251	6	258	6	251	6	260	5	261	3	175	3	160	3	150
7	277	8	277	6	284	6	277	7	285	4	289	3	195	3	180	3	170
7	303	10	302	5	309	7	305	10	311	6	314	3	215	3	195	3	195
10	320	10	325	9	335	10	330	10	339	8	342	3	235	3	210	3	220
10	341	10	348	9	362	8	356	9	364	8	370	3	255	3	230	3	245
10	369	10	366	9	388	7	381	8	392	8	398	3	275	3	255	3	270
10	394	9	394	7	416	7	409	10	418	8	426	3	290	3	275	3	295
10	419	9	419	9	441	8	434	10	435	6	452	3	310	3	295	3	305
10	440	10	442	10	467	10	457	10	453	8	477	4	320	3	305	4	320
10	452	10	457	10	484	10	475	10	473	8	505	4	340	4	315	4	335
10	468	10	475	10	500	10	498	10	496	7	533	5	360	5	335	5	365
10	483	10	495	10	517	9	526	10	517	7	558	5	380	5	360	5	385
10	498	10	513	10	538	10	551	10	534	10	584	5	410	5	380	5	410
10	508	10	536	10	563	10	577	10	557	8	612	5	425	5	395	5	435
10	523	10	556	10	583	10	599	10	578	10	634	5	445	5	420	5	455
10	539	10	577	10	599	10	615	10	600	10	665	5	465	5	440	5	475
10	554	10	599	10	616	10	645	10	628	8	693	5	475	5	455	5	495
10	564	10	620	10	637	10	673	10	656	7	718	5	490	6	475	5	525
10	579	10	640	10	655	10	701	9	682	7	744	6	510	6	495	5	545
10	592	10	660	10	677	10	716	9	710	10	772	6	535	6	505	5	570
10	605	10	683	10	695	10	732	9	738	10	789	6	555	7	535	5	585
10	617	9	711	10	713	10	742	9	763	10	810	6	570	7	550	5	600
10	635	10	737	10	731	10	747	8	788	10	838	6	585	7	570	7	630
10	650	10	759	10	743	10	765	8	816	8	866	7	610	7	585	7	660
10	666	10	777	10	756	10	780	7	844	6	891	8	640	8	600	7	690
10	678	10	792	10	766	10	798	8	870	8	916	8	660	8	615	7	715
10	691	10	818	10	776	10	823	6	895	2	924	8	685	8	630	7	725
10	704	9	846	10	789	9	851	7	923			8	710	8	655	7	745
10	717	6	874	10	802	7	876					8	725	8	675		
10	729	10	894	10	817	7	907							8	705		
10	742	10	922	10	835	2	917							8	720		
10	755	2	930	10	855									8	735		
10	767			10	878												
10	785			9	903												
10	803			8	931												

Soil Type: ML-Opt

Thumper SN #1						Thumper SN #5						Manual DCP					
A6		C1		B3		B5		A1		C4		A5		B2		B4	
No. of Blows	Accum. Penetration (mm)	No. of Blows	Accum. Penetration (mm)	No. of Blows	Accum. Penetration (mm)	No. of Blows	Accum. Penetration (mm)	No. of Blows	Accum. Penetration (mm)	No. of Blows	Accum. Penetration (mm)	No. of Blows	Accum. Penetration (mm)	No. of Blows	Accum. Penetration (mm)	No. of Blows	Accum. Penetration (mm)
2	27	3	35	2	28	1	28	2	33	1	42	0	0	0	0	0	0
4	55	5	65	3	58	3	56	5	64	4	70	1	25	1	30	1	35
5	86	6	93	4	86	5	87	6	89	5	96	1	45	1	45	1	50
7	116	5	118	5	114	5	115	6	117	5	124	1	60	1	65	1	70
7	144	6	146	5	139	5	142	6	142	6	152	1	75	1	80	1	85
8	172	7	177	6	165	6	170	7	170	6	177	2	105	1	95	1	105
8	202	7	202	7	193	6	198	8	198	7	208	2	125	1	110	1	120
7	230	7	233	7	218	6	224	8	226	6	233	2	150	1	125	1	130
6	258	5	258	6	246	4	252	7	254	6	263	2	170	2	150	2	150
6	286	5	289	5	272	5	282	7	279	5	291	2	190	2	170	2	175
6	312	5	314	5	297	4	308	8	310	5	319	2	215	2	190	2	200
6	342	6	342	6	325	5	338	7	335	5	345	2	240	2	215	2	220
6	373	5	367	6	350	4	363	6	363	5	373	2	260	2	240	2	245
5	398	6	395	6	376	3	394	5	389	5	403	2	280	2	260	2	265
6	426	5	421	5	401	4	424	6	417	5	434	2	300	2	285	2	285
7	451	5	446	6	432	4	452	7	445	5	462	2	320	2	300	2	305
7	482	8	474	7	459	5	480	8	475	5	487	2	340	2	320	2	320
5	507	10	502	8	487	5	506	8	500	5	512	2	365	2	335	2	340
5	535	8	530	7	513	4	539	7	528	5	543	2	385	2	350	2	355
5	561	7	560	7	541	4	569	5	554	5	573	2	405	3	380	2	375
6	589	7	588	7	569	3	595	6	582	4	601	2	420	3	405	2	395
6	616	7	614	6	594	3	620	6	610	4	629	2	440	3	430	2	415
5	642	7	642	6	620	5	650	6	638	5	657	2	455	3	450	2	430
5	670	7	670	6	645	5	678	6	665	5	682	2	475	3	470	2	445
4	698	7	700	7	675	5	706	5	699	6	713	2	495	3	490	3	465
3	728	7	731	6	701	5	737	4	729	5	738	2	515	3	510	3	490
3	759	6	758	5	726	4	767	5	757	5	771	2	535	3	535	3	515
3	789	5	786	4	754	3	793	4	782	3	797	2	555	3	555	3	540
2	817	4	817	4	787	3	823	4	815	3	827	2	575	3	580	3	560
2	850	4	847	3	825	3	859	3	843	2	855	2	590	3	605	3	590
2	896	4	878	2	851	2	887	3	881	2	888	2	605	3	625	3	620
1	921	4	906	3	879	3	922	2	912	2	921	2	620	3	645	3	640
		4	921	4	907	1	935	1	930	2	942	2	635	3	670	3	660
		2	921	2	922							2	655	3	695	3	680
												2	675	3	730	3	705
												2	705			3	735
												2	735				

Soil Type: ML-Wet

Thumper SN #1						Thumper SN #5						Manual DCP					
A6		C1		B3		B5		A1		C4		A5		B2		B4	
No. of Blows	Accum. Penetration (mm)	No. of Blows	Accum. Penetration (mm)	No. of Blows	Accum. Penetration (mm)	No. of Blows	Accum. Penetration (mm)	No. of Blows	Accum. Penetration (mm)	No. of Blows	Accum. Penetration (mm)	No. of Blows	Accum. Penetration (mm)	No. of Blows	Accum. Penetration (mm)	No. of Blows	Accum. Penetration (mm)
2	40	2	49	2	35	1	46	1	44	1	33	0	0	0	0	0	0
1	68	1	97	1	88	1	89	1	92	1	84	1	70	1	85	1	75
1	116	1	146	1	136	1	140	1	141	1	137	1	140	1	165	1	160
1	193	1	196	1	187	1	185	1	184	1	173	1	235	1	245	1	245
1	248	1	237	1	230	1	239	1	227	1	226	1	325	1	325	1	320
1	276	1	293	1	284	1	284	1	270	1	282	1	390	1	390	1	385
1	335	1	339	1	329	1	318	1	316	1	318	1	460	1	460	1	450
1	373	1	367	1	360	1	348	1	354	1	345	1	540	1	525	1	520
1	444	1	422	1	408	1	414	1	405	1	389	1	620	1	595	1	580
1	492	1	473	1	454	1	475	1	448	1	445	1	685	1	665	1	650
1	548	1	519	1	502	1	531	1	476	1	533	1	735	1	730	1	720
1	596	1	562	1	550	1	561	1	512	1	566	1	790	1	780	1	780
1	645	1	610	1	604	1	622	1	560	1	627	1	830	1	825	1	825
1	685	1	638	1	634	1	671	1	603	1	686						
1	718	1	694	1	695	1	706	1	644	1	734						
1	746	1	737	1	738	1	742	1	682	1	775						
1	774	2	775	1	776	1	772	1	707	1	813						
2	820	2	801	1	809	1	800	1	745	1	853						
2	850	2	839	1	848	1	838	1	776	1	886						
3	881	3	869	1	876	1	864	1	804	2	919						
3	909	4	897	4	909	2	899	1	832	1	925						
2	924	6	933	2	924	1	917	2	860								
								2	887								
								2	918								
								1	931								

Soil Type: SP

Thumper SN #1						Thumper SN #5						Manual DCP					
A6		C1		B3		B5		A1		C4		A5		B2		B4	
No. of Blows	Accum. Penetration (mm)	No. of Blows	Accum. Penetration (mm)	No. of Blows	Accum. Penetration (mm)	No. of Blows	Accum. Penetration (mm)	No. of Blows	Accum. Penetration (mm)	No. of Blows	Accum. Penetration (mm)	No. of Blows	Accum. Penetration (mm)	No. of Blows	Accum. Penetration (mm)	No. of Blows	Accum. Penetration (mm)
1	65	1	54	1	36	1	20	1	58	1	82	0	0	0	0	0	0
1	103	1	92	1	74	1	53	1	111	1	115	1	95	1	95	1	115
1	141	1	120	1	113	1	84	1	162	1	141	1	140	1	140	1	165
2	184	2	156	2	156	2	117	2	187	2	176	1	170	1	170	1	195
2	214	2	181	2	186	2	147	1	220	2	202	1	205	1	200	1	220
3	245	3	214	3	217	3	180	2	264	3	235	1	230	1	225	1	245
2	273	3	245	1	245	3	211	2	294	3	263	1	250	1	250	1	265
3	303	3	275	3	275	3	241	2	320	3	291	1	270	1	275	1	285
3	331	3	301	3	303	3	269	3	355	3	316	2	300	1	295	1	305
3	357	4	331	3	328	3	295	3	383	3	341	2	330	1	315	1	325
4	390	4	359	4	361	3	323	3	414	3	367	2	365	2	350	2	355
4	423	4	387	4	394	4	356	3	441	3	392	2	390	2	380	2	390
3	451	4	415	3	422	3	381	3	469	3	420	2	420	2	415	2	420
4	481	4	440	4	453	3	406	3	500	3	446	2	445	2	445	2	450
4	512	4	468	4	483	4	439	3	530	3	473	2	475	2	480	2	480
4	539	4	499	4	511	4	470	3	558	3	501	2	500	2	510	2	510
4	570	4	527	4	542	4	498	4	589	4	534	2	520	2	540	2	530
5	600	5	557	5	572	4	523	4	619	4	562	2	545	2	565	2	555
5	628	5	585	5	600	5	551	4	647	4	588	2	565	2	585	2	575
6	656	6	613	6	628	5	582	4	678	5	613	2	585	2	605	2	595
5	684	6	641	5	656	5	610	4	706	4	644	3	615	3	635	2	625
5	712	6	672	5	684	5	638	4	734	5	674	3	645	3	665	3	655
5	738	5	700	5	709	5	665	4	764	5	705	3	675	3	690	3	680
5	766	5	727	5	737	5	696	4	795	5	735	3	700			3	710
5	793	5	758	5	765	5	724	3	822	5	766						
5	824	5	786	5	796	5	754	3	855	5	796						
5	857	4	811	5	829	4	780	3	891	4	824						
4	882	4	844	4	854	4	813	2	922	4	852						
4	915	4	875	4	887	3	843	2	952	4	882						
3	943	3	903	3	915	2	879			3	908						
3	976	3	931	3	948	2	907			3	938						
		1	941														

Soil Type: SM-5

Thumper SN #1						Thumper SN #5						Manual DCP					
A6		C1		B3		B5		A1		C4		A5		B2		B4	
No. of Blows	Accum. Penetration (mm)	No. of Blows	Accum. Penetration (mm)	No. of Blows	Accum. Penetration (mm)	No. of Blows	Accum. Penetration (mm)	No. of Blows	Accum. Penetration (mm)	No. of Blows	Accum. Penetration (mm)	No. of Blows	Accum. Penetration (mm)	No. of Blows	Accum. Penetration (mm)	No. of Blows	Accum. Penetration (mm)
2	39	2	36	2	46	1	38	1	40	1	55	0	0	0	0	0	0
2	80	2	72	2	77	2	76	2	70	2	90	1	35	1	45	1	40
2	110	2	100	2	102	2	117	2	111	2	123	1	65	1	70	1	65
3	146	3	133	3	133	2	150	2	139	2	154	1	90	1	95	1	95
3	174	3	158	4	166	2	175	3	167	2	179	1	110	1	120	1	120
3	202	3	186	4	191	2	201	2	195	3	212	1	130	1	140	1	140
4	230	5	214	4	217	2	234	3	220	3	245	1	155	1	160	1	155
4	263	5	242	4	242	2	259	3	246	3	276	1	170	1	175	1	170
3	288	4	273	4	275	3	292	3	274	3	311	1	185	1	190	1	185
3	316	4	300	4	306	3	320	3	299	3	342	1	200	1	200	1	200
5	346	5	331	4	336	3	345	4	335	3	375	1	220	2	230	1	215
4	372	6	359	4	361	3	371	4	368	2	400	1	235	2	255	1	230
4	397	5	387	4	394	3	404	4	398	2	428	1	250	2	285	1	245
4	425	5	420	3	430	3	442	3	423	2	461	2	285	2	310	1	265
4	456	3	445	2	455	3	478	3	451	2	494	2	310	2	330	1	280
4	484	3	471	2	483	4	508	3	477	3	530	2	335	2	350	1	300
6	514	3	499	3	511	4	538	4	507	3	563	2	360	2	375	1	315
6	542	6	527	4	544	4	572	4	535	3	588	2	385	2	395	1	330
5	570	5	552	3	570	4	602	4	566	2	621	2	410	2	425	1	350
4	600	6	580	3	600	4	635	3	591	3	649	2	440	2	455	1	365
3	633	5	608	3	628	3	660	4	627	2	687	2	465	2	485	1	380
5	661	5	633	3	654	3	688	3	652	2	718	2	490	2	505	1	405
3	692	6	664	4	694	3	714	3	677	2	748	2	510	2	525	1	430
5	720	6	694	4	712	4	747	4	708	2	776	2	530	2	545	1	455
5	750	6	722	4	740	3	775	4	738	2	807	2	545	2	565	1	485
4	778	5	748	4	768	3	805	3	771	2	840	2	565	2	600	1	500
4	809	5	778	4	796	3	833	3	802	2	878	2	590	2	615	1	515
3	839	4	806	3	821	2	869	3	835	2	908	2	610	2	635	1	530
3	865	4	836	4	849	2	897	3	873	2	934	2	630	2	655	1	545
3	898	3	862	3	875	2	925	2	903	1	946	2	650	2	675	1	560
3	931	3	890	3	913			2	939			1	670	2	700	1	575
		3	918	2	938							2	695	2	720	1	590
		1	928									2	715	2	735	1	610
												2	735			1	625
																1	640
																1	660
																1	680
																1	695
																1	715
																1	730

Soil Type: SM-Opt

Thumper SN #1						Thumper SN #5						Manual DCP					
A6		C1		B3		B5		A1		C4		A5		B2		B4	
No. of Blows	Accum. Penetration (mm)	No. of Blows	Accum. Penetration (mm)	No. of Blows	Accum. Penetration (mm)	No. of Blows	Accum. Penetration (mm)	No. of Blows	Accum. Penetration (mm)	No. of Blows	Accum. Penetration (mm)	No. of Blows	Accum. Penetration (mm)	No. of Blows	Accum. Penetration (mm)	No. of Blows	Accum. Penetration (mm)
2	47	2	36	2	31	1	30	1	51	1	60	0	0	0	0	0	0
2	72	1	69	1	64	1	66	1	84	1	90	1	60	1	45	1	115
2	116	1	97	3	107	2	114	2	114	1	138	1	110	1	85	1	165
2	146	2	143	1	143	2	142	2	150	2	187	1	140	1	125	1	195
2	171	2	171	1	173	1	170	2	183	2	220	1	175	1	160	1	220
2	199	1	199	5	207	3	201	2	221	3	258	1	205	1	190	1	245
3	227	1	224	3	234	3	229	2	249	3	293	1	230	1	210	1	265
3	260	3	257	3	262	3	254	3	279	3	331	1	250	1	230	1	285
3	288	3	288	3	290	3	282	3	312	3	370	1	265	1	250	1	305
3	316	3	321	3	321	3	310	3	343	3	398	1	290	1	270	1	325
3	347	3	354	3	351	3	340	3	371	3	431	1	305	2	305	2	355
3	372	3	379	3	379	3	373	3	396	3	458	1	330	2	340	2	390
4	405	4	407	4	410	3	401	3	427	3	484	1	350	2	375	2	420
4	433	4	432	3	435	3	429	4	457	3	514	1	370	2	400	2	450
5	461	5	463	4	466	4	460	4	488	3	542	1	390	2	430	2	480
5	489	5	496	4	494	3	485	4	518	4	575	1	405	2	455	2	510
5	514	4	521	4	521	4	518	4	549	4	608	1	420	2	485	2	530
5	542	4	547	5	549	4	549	4	577	4	636	2	450	2	510	2	555
5	573	5	577	5	575	4	577	5	607	3	664	2	480	2	535	2	575
5	598	6	605	6	603	4	602	5	632	3	690	2	510	2	555	2	595
6	626	6	633	6	628	4	630	5	665	3	718	2	530	2	570	2	625
6	652	6	661	6	654	3	660	5	693	3	745	2	550	2	605	3	655
6	679	6	689	6	681	4	688	4	724	3	776	2	580	3	630	3	680
6	705	5	714	5	709	4	716	4	749	3	801	2	605	3	660	3	710
6	733	6	742	5	740	4	747	5	780	4	834	2	620	3	695		
6	758	5	768	5	770	4	775	4	805	4	865	2	645	3	730		
7	786	5	793	5	796	4	800	4	836	3	893	2	660	3	760		
7	812	5	821	6	821	4	828	3	864	3	923	3	690				
7	842	4	849	6	847	4	856	2	897	1	933	3	720				
6	867	4	877	6	875	3	886	2	925			3	765				
5	893	3	897	5	902	2	909										
5	923			4	928												
1	928																

Soil Type: CH-Tensar

Thumper SN #1						Thumper SN #5						Manual DCP					
A6		C1		B3		B5		A1		C4		A5		B2		B4	
No. of Blows	Accum. Penetration (mm)	No. of Blows	Accum. Penetration (mm)	No. of Blows	Accum. Penetration (mm)	No. of Blows	Accum. Penetration (mm)	No. of Blows	Accum. Penetration (mm)	No. of Blows	Accum. Penetration (mm)	No. of Blows	Accum. Penetration (mm)	No. of Blows	Accum. Penetration (mm)	No. of Blows	Accum. Penetration (mm)
1	138	1	82	1	164	1	53	Blows	(mm)	Blows	(mm)	0	0	0	0	0	0
1	179	1	148	1	194	1	109	1	206	1	236	1	80	1	105	1	80
1	217	1	214	1	258	1	152	1	259	1	289	1	125	1	145	1	135
1	258	1	273	1	296	1	188	1	302	1	338	1	160	1	175	1	175
1	288	1	301	2	329	1	218	1	340	1	373	1	190	1	210	1	230
1	321	1	329	2	377	1	249	1	373	1	406	1	215	1	235	1	290
1	347	1	357	2	425	1	279	1	406	1	437	1	240	1	260	1	335
1	375	2	405	2	456	1	307	1	434	1	470	1	260	1	280	1	375
2	423	2	443	2	499	1	335	2	480	1	498	1	285	1	305	1	405
2	458	1	484	2	530	2	373	2	513	1	526	1	305	1	325	1	430
2	486	2	509	2	560	1	406	1	538	1	551	1	325	1	345	1	460
2	519	2	555	2	588	2	447	2	574	1	576	1	340	1	360	1	480
3	558	2	593	2	613	2	472	2	605	1	617	1	370	1	375	1	505
3	593	2	628	2	639	5	498	2	635	2	647	1	400	1	410	1	520
5	618	2	656	3	669	6	526	3	660	2	678	1	430	1	425	1	540
9	644	1	682	7	695	5	556	6	688	2	703	1	455	1	440	1	560
9	672	3	710	10	720	4	584	5	716	6	731	1	485	1	470	2	575
9	697	4	735	10	738	4	615	4	747	9	757	1	510	1	500	2	605
8	728	6	763	10	756	4	645	4	772	9	782	1	535	1	525	2	635
6	753	6	788	10	776	4	678	4	800	8	807	2	555	1	550	2	665
5	784	6	819	10	796	4	711	4	828	6	835	2	580	1	575	2	680
5	814	5	847	10	824	3	737	4	856	5	866	2	600	1	595	2	690
5	842	5	877	9	852	4	767	4	884	5	899	2	615	2	620	2	700
5	872	4	903	6	880	4	800	4	914	4	924	2	625	2	640	2	730
5	903	5	933	5	911	3	823	3	937	3	942	2	640	2	660	3	750
5	928			4	936							2	665	3	675	3	760
2	939			1	941							2	685	3	685	3	775
2	939											2	710	3	695	3	790
2	939											2	730	3	700	3	805
2	939											2	755	3	715	3	825
2	939											2	785	3	730	3	845
2	939											2	815	3	755		

Soil Type: CH-Mat

Thumper SN #1						Thumper SN #5						Manual DCP					
A6		C1		B3		B5		A1		C4		A5		B2		B4	
No. of Blows	Accum. Penetration (mm)	No. of Blows	Accum. Penetration (mm)	No. of Blows	Accum. Penetration (mm)	No. of Blows	Accum. Penetration (mm)	No. of Blows	Accum. Penetration (mm)	No. of Blows	Accum. Penetration (mm)	No. of Blows	Accum. Penetration (mm)	No. of Blows	Accum. Penetration (mm)	No. of Blows	Accum. Penetration (mm)
10	265	10	265	1	23	2	61	1	49	1	56	0	0	0	0	0	0
3	300	2	293	1	69	1	91	1	107	1	107	1	110	1	80	1	90
2	328	4	328	1	117	1	135	1	158	1	155	1	180	1	150	1	160
3	356	3	359	1	150	1	183	1	194	1	191	1	225	1	195	1	205
3	384	3	384	2	196	1	224	2	237	1	226	1	260	1	230	1	235
3	409	2	412	2	229	1	249	2	273	2	269	1	285	1	255	1	265
3	442	4	445	2	255	2	290	2	306	2	302	1	315	1	280	1	290
2	470	5	473	3	290	2	328	2	331	2	335	1	335	1	300	1	315
5	501	2	488	3	323	2	358	2	356	2	363	1	355	1	320	1	335
2	521			3	356	2	389	3	389	2	389	1	375	1	340	1	355
				3	384	2	417	3	415	3	424	1	390	1	355	1	370
				4	417	2	442	2	443	3	455	1	430	1	370	1	385
				4	448	3	475	3	468	3	483	1	460	1	390	1	410
				4	475	1	485	4	501	4	511	1	485	1	405	1	435
								4	532	3	536			1	415	1	455
								4	557	4	564			1	440		
								4	585	5	592			1	465		
								5	615	5	622						
								5	648	5	648						
								5	674	5	676						
								5	702	6	706						
								5	727	5	732						
								6	755	6	762						
								6	783	6	790						
								6	808	6	815						
								6	834	6	841						
								7	864	6	866						
								7	892	7	894						
								7	920	6	919						

Appendix C: Selected Data from Second Generation A-DCP Testing

Selected data from field testing, organized by soil type and depth of testing, follow.

Soil Type	Rationale	Depth (in.)	Avg. Truck CBR (%)	Avg. DCP CBR (%)
SP - Sand		0	3.8	1.7
		6	6.0	5.7
		12	10.9	11.3
		18	10.2	15.0
	Representative overburden weight	24	-	22.0
	could not be obtained at these depths.	30	-	8.7
ML - Optimum	Not enough overburden	0	15.0	6.3
		6	22.3	20.3
		12	20.3	25.0
	Rod friction	18	19.0	30.7
	Rod friction	24	12.7	33.7
	Rod friction	30	7.0	18.3
CH - Wet (1 CBR)		0	3.7	3.0
		6	4.0	6.3
	Rod friction	12	4.3	10.3
	Rod friction	18	5.0	15.0
	Rod friction	24	5.0	23.0
	Rod friction	30	5.7	26.3
CH - Tensar (2 CBR)		6	2.0	6.7
	Rod friction	12	1.9	22.3
	Rod friction	18	2.1	24.0
CH - Mat test (6 CBR)		0	4.1	3.0
		6	5.5	6.3
		12	6.4	9.3
	Rod friction	18	5.8	10.0
SM - Optimum	Not enough overburden	0	10.1	2.7
	Not enough overburden	6	14.6	5.7
		12	11.8	10.0
		18	12.1	14.0
		24	12.7	26.7
		30	10.7	22.0
SM - 5% moisture	Not enough overburden	0	11.7	4.7
		6	14.7	14.0
		12	13.6	17.7
		18	14.7	12.3
		24	14.6	19.3
		30	13.3	22.3

Soil Type	Rationale	Depth (in.)	Avg. Truck CBR (%)	Avg. DCP CBR (%)
Limestone		0	95.3	96.3
GW - Optimum		6	100.0	99.0
		12	89.0	99.0
		18	100.0	99.0
		24	93.3	99.0
	Rod provided irregular data at depth	30	65.7	33.0
Limestone	Not enough overburden	0	35.0	9.3
GW - Optimum		6	30.3	35.0
Quicklime		12	32.3	58.7
		18	61.7	74.3
		24	30.0	68.0
	Unable to get Truck CBR at depth	30	-	96.0
Clayey Sand		0	5.0	4.0
SC - Wet		6	6.1	13.0
		12	5.2	11.3
		18	11.5	12.7
		24	14.4	22.7
		30	9.8	10.7
Clayey Sand	Not enough overburden	0	44.7	10.7
SC - Optimum		6	46.3	39.3
		12	48.0	44.3
		18	34.3	31.7
		24	26.7	32.0
		30	24.0	14.3
CL - Optimum		0	10.0	10.0
		6	13.0	11.3
		12	10.3	11.3
		18	12.7	11.3
		24	6.7	12.0
		30	13.3	12.7
CL - Dry		0	30.8	23.7
		6	24.5	18.7
		12	18.2	23.7
		18	18.2	25.3
		24	17.3	14.7
		30	8.2	12.3
ML - Wet	Assumed that DCP correlation was uniformly off with depth	0	0.6	2.3
		6	0.6	2.0
		12	0.6	3.0
		18	0.6	2.7
		24	0.7	3.0
		30	1.2	4.3

Appendix D: Second Generation A-DCP Correlation Data

The following is a collection of all data points used in the generation of the A-DCP correlation.

Section Label	Soil Type	Depth	Truck CBR	SN1 Pen/Blow	SN5 Pen/Blow	DCP Pen/Blow
ML Wet	ML	0	0.5	28	43	70
	ML	0	0.6	48	48	85
	ML	0	0.6	53	51	75
	ML	6	0.6	56	46	95
	ML	6	0.6	43	36	85
	ML	6	0.6	41	43	56
	ML	12	0.6	38	30	65
	ML	12	0.5	30	28	65
	ML	12	0.7	28	38	38
	ML	18	0.6	56	56	80
	ML	18	0.7	48	89	70
	ML	18	0.6	46	36	56
	ML	24	0.7	48	48	65
	ML	24	0.7	30	58	70
	ML	24	0.7	28	41	48
	ML	30	1	28	28	40
	ML	30	1.4	43	28	45
	ML	30	1.1	43	38	28
SM Opt	SM	12	11.6	10.16	10.16	25
	SM	12	12.7	10.16	12.7	18
	SM	12	11.1	11.01	10.16	20
	SM	18	12.4	5.59	8.47	15
	SM	18	11.5	6.99	8.47	14
	SM	18	12.5	6.6	7.62	14
	SM	24	13.1	4.66	6.99	8
	SM	24	12.4	4.23	6.98	8
	SM	24	12.7	4.66	5.08	10
	SM	30	10.8	3.99	6.35	10
	SM	30	10.3	5.08	6.1	10
	SM	30	10.9	5.08	8.47	10
CH Wet	CH	0	3	28	28	100
	CH	0	4	33	41	100
	CH	0	4	61	25	100
	CH	6	4	28		55
	CH	6	4	28	43	55
	CH	6	4	33	48	28

Section Label	Soil Type	Depth	Truck CBR	SN1 Pen/Blow	SN5 Pen/Blow	DCP Pen/Blow
ML Opt	ML	6	24	3.81	4.66	10
	ML	6	23	3.99	4.35	13
	ML	6	20	4.35	3.49	10
	ML	12	18	5.08	6.1	10
	ML	12	22	4.23	5.08	8
	ML	12	21	4.66	3.63	10
SP	SP	0	3.6	38.1	33.02	95
	SP	0	3.7	38.1	53.34	95
	SP	0	4	38.1	33.02	115
	SP	6	6	21.59	11.01	35
	SP	6	6.1	15.24	12.7	30
	SP	6	6	12.7	12.7	30
	SP	12	10.6	9.31	9.31	15
	SP	12	11	8.47	8.47	20
	SP	12	11.1	7.62	12.7	20
	SP	18	8.8	7.62	6.99	13
	SP	18	11	7.62	9.31	15
	SP	18	10.7	7.62	10.16	15
GW Opt	GW	0	100	2.82	2.82	10
	GW	0	86	1.52	3.63	10
	GW	0	100	1.78	2.54	10
	GW	6	100	1.4	1.78	2
	GW	6	100	0.76	1.78	3
	GW	6	100	1.27	1.91	3
	GW	12	100	0.89	0.89	1
	GW	12	100	0.76	1.52	1
	GW	12	67	0.76	1.02	2
	GW	18	100	0.76	0.63	1
	GW	18	100	0.64	0.89	1
	GW	18	100	0.51	0.89	1
	GW	24	100	0.64	0.51	1
	GW	24	80	0.64	0.76	0
	GW	24	100	0.64	0.64	0.3
CH Tensar	CH	6	2	41	36	30
2 CBR	CH	6	2	30	53	35
	CH	6	1.9	66	53	55

Section Label	Soil Type	Depth	Truck CBR	SN1 Pen/Blow	SN5 Pen/Blow	DCP Pen/Blow
SM - 5%	SM	6	12.3	20.32	19.05	35
	SM	6	10.3	17.78	15.24	45
	SM	6	12.5	15.24	17.78	40
	SM	12	17.3	9.31	12.7	15
	SM	12	13.5	6.35	12.7	15
	SM	12	13.3	9.31	13.97	15
	SM	18	14.9	6.1	9.31	13
	SM	18	13.3	7.62	10.16	10
	SM	18	12.5	6.1	8.89	15
	SM	24	17	6.99	7.62	13
	SM	24	13.5	13.97	16.51	15
	SM	24	13.5	9.31	7.62	30
	SM	30	13.9	11.01	8.47	10
	SM	30	16.8	9.31	9.31	10
	SM	30	13.1	5.08	8.47	15
GW Opt	GW	6	33	3.18	3.1	7
Quick	GW	6	28	4.23	5.59	7
	GW	6	30	3.1	5.08	7
	GW	12	29	2.03	2.54	5
	GW	12	43	2.82	3.49	4
	GW	12	25	2.29	2.79	4
	GW	18	59	1.52	1.78	3
	GW	18	73	1.78	3.18	3
	GW	18	53	1.78	2.03	4
	GW	24	36	1.78	3.05	4
	GW	24	28	2.03	2.29	3
	GW	24	26	2.03	2.79	4
SC Opt	GC	6	49	5.08	6.1	7
	GC	6	46	4.23	5.59	5
	GC	6	44	4.23	5.08	7
	GC	12	45	2.54	4.66	5
	GC	12	49	2.54	5.08	6
	GC	12	50	2.03	6.99	5
	GC	18	37	2.82	5.08	8
	GC	18	36	3.1	5.08	6
	GC	18	30	3.49	6.35	8
	GC	24	22	3.99	5.08	6
	GC	24	27	3.63	5.08	7
	GC	24	31	5.08	5.59	10
	GC	30	23	5.5	9.31	20
	GC	30	28	4.23	11.01	13
	GC	30	21	5.08	8.26	13
CH Mat	CH	0	4.5		43	70
6 CBR	CH	0	4.5		51	70
	CH	0	3.4	48	48	70
	CH	6	5.8		48	45
	CH	6	5.2	23	36	35
	CH	6	5.4		36	30
	CH	12	6.9	14	19	30
	CH	12	6.6	11	17	20
	CH	12	5.6	9	13	25

Section Label	Soil Type	Depth	Truck CBR	SN1 Pen/Blow	SN5 Pen/Blow	DCP Pen/Blow
CL Opt	CL	0	6	13.97	16.51	15
	CL	0	14	11.01	15.24	25
	CL	0	10	15.24	15.2	25
	CL	6	14	10.16	15.24	15
	CL	6	13	17.78	13.97	20
	CL	6	12	8.26	20.32	20
	CL	12	13	9.31	11.85	15
	CL	12	8	13.97	15.24	20
	CL	12	10	11.01	15.24	20
	CL	18	14	12.7	11.85	15
	CL	18	13	13.97	12.7	20
	CL	18	11	11.01	13.97	15
	CL	24	10	12.7	30.48	10
	CL	24	6	16.51	17.78	30
	CL	24	4	19.05	13.97	25
	CL	30	12	17.78	13.97	10
	CL	30	13	12.7	19.05	25
	CL	30	15	10.16	13.97	25
CL Dry	CL	0	27.7	3.99	6.1	10
	CL	0	31.9	5.59	8.26	10
	CL	0	32.9	3.99	7.62	8
	CL	6	23.6	6.99	10.16	10
	CL	6	23.9	6.35	10.16	13
	CL	6	26	11.01	11.01	13
	CL	12	24.7	5.08	6.35	10
	CL	12	14.8	6.35	8.47	8
	CL	12	15	6.1	8.47	10
	CL	18	16.8	7.62	8.26	8
	CL	18	19.8	5.59	10.16	8
	CL	18	18.1	6.35	7.62	10
	CL	24	18.9	10.16	13.97	15
	CL	24	19.8	9.31	25.4	10
	CL	24	13.3	6.35	6.98	25
	CL	30	8.7	6.99	11.85	30
	CL	30	8	13.97	8.47	12
	CL	30	7.9	8.26	19.05	18
SC Wet	GC	0	5.2	22.9	20.3	45
	GC	0	5.1	16.5	30.5	45
	GC	0	4.7	10.2	35.6	45
	GC	6	5.9	15.2	13.6	15
	GC	6	7.3	14	17.8	25
	GC	6	5.2	16.5	22.9	13
	GC	12	5.9	14	15.2	20
	GC	12	5.5	14	11	18
	GC	12	4.3	14	25.4	18
	GC	18	10.1	11	9.3	15
	GC	18	14.4	9.3	11	15
	GC	18	10	5.1	8.5	20
	GC	24	14.4	7	13.6	8
	GC	24	14.8	11	11	8
	GC	24	14	6.1	8.9	15
	GC	30	10.3	9.3	17.78	25
	GC	30	10.7	11	16.5	15
	GC	30	8.5	15.2	12.7	20

Appendix E: Second Generation A-DCP Correlation Results

The following represents the improved response of the A-DCP to capture the in situ CBR based on the introduction of the new calibration curve. For each soil tested, a comparison is shown of the CBR response with depth using the original manual DCP correlation (Legacy Cal) and the response using the new correlation equation developed during this research (New Cal).

SM – 5%
SN1

Legacy Cal

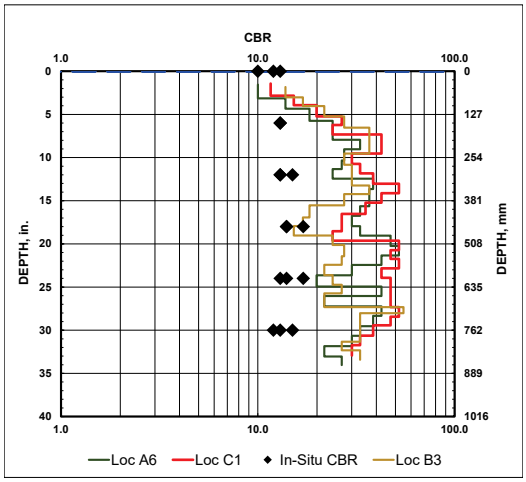

New Cal

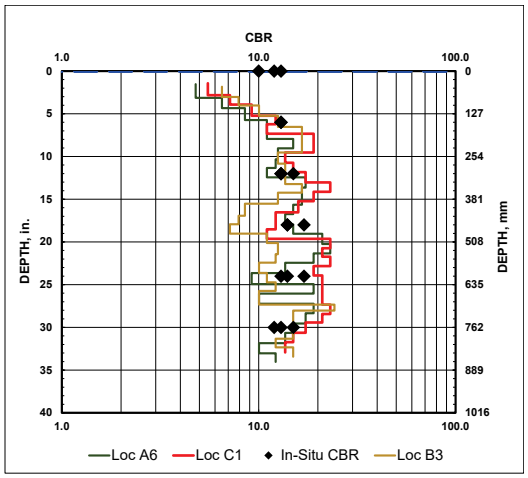

SM – 5%
SN5

Legacy Cal

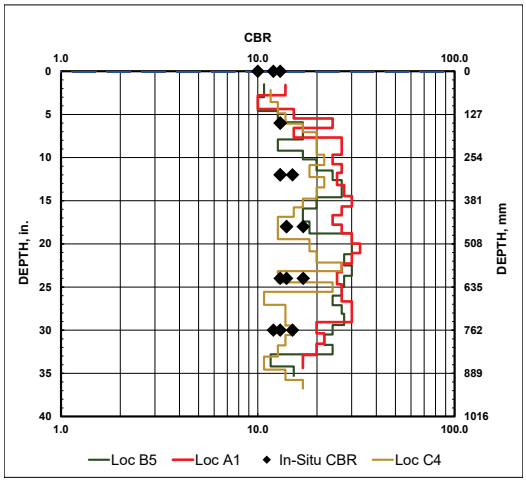

New Cal

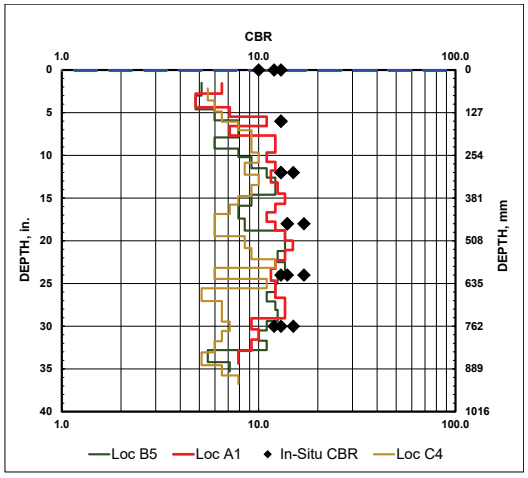

SM – Opt
SN1

Legacy Cal

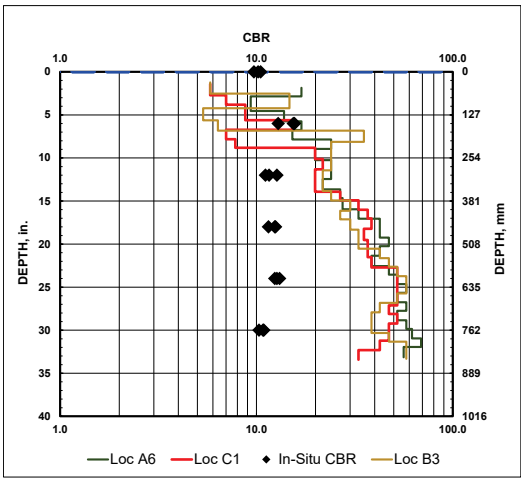

New Cal

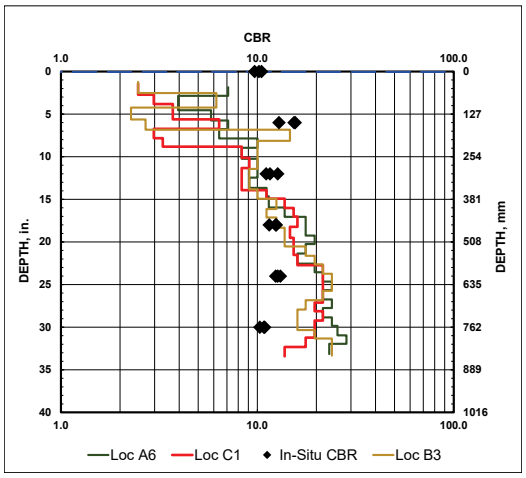

SM – Opt
SN5

Legacy Cal

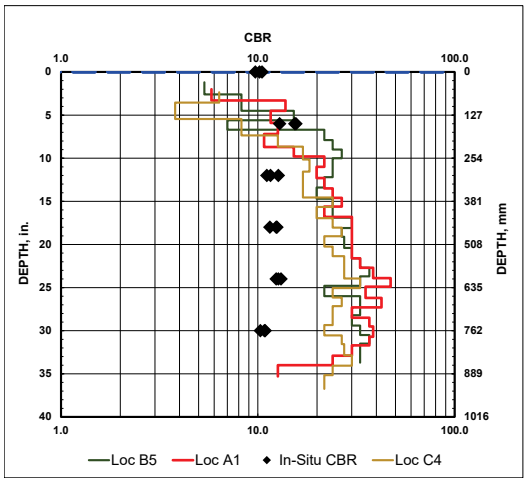

New Cal

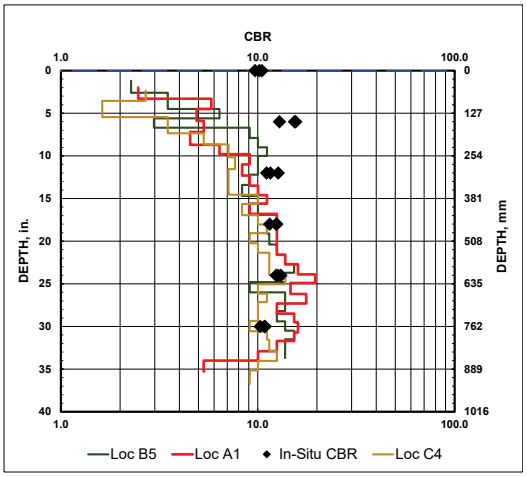

CH
SN1

Legacy Cal

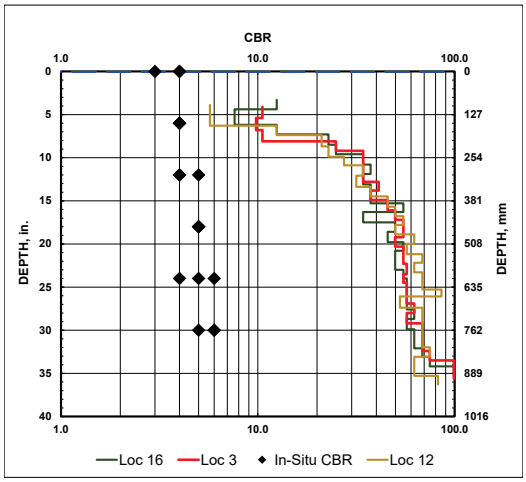

New Cal

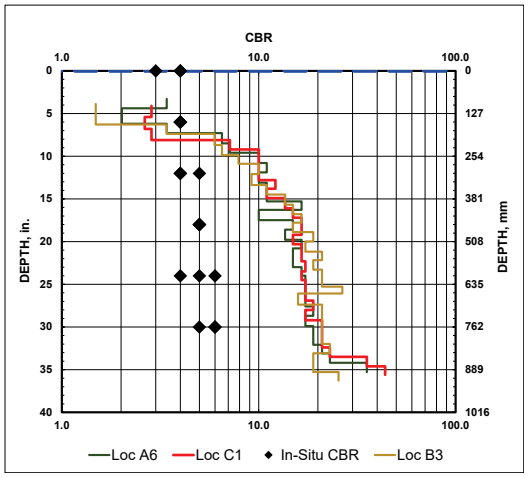

CH
SN5

Legacy Cal

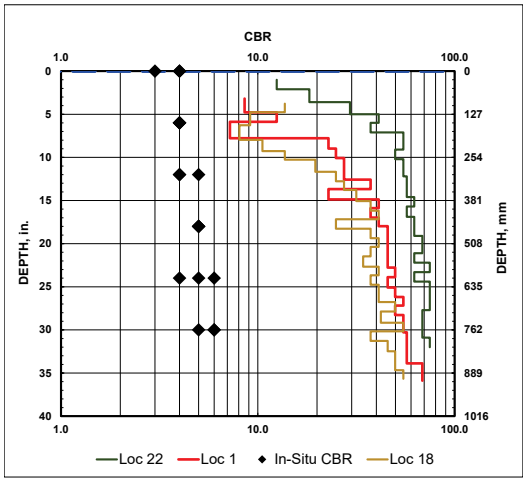

New Cal

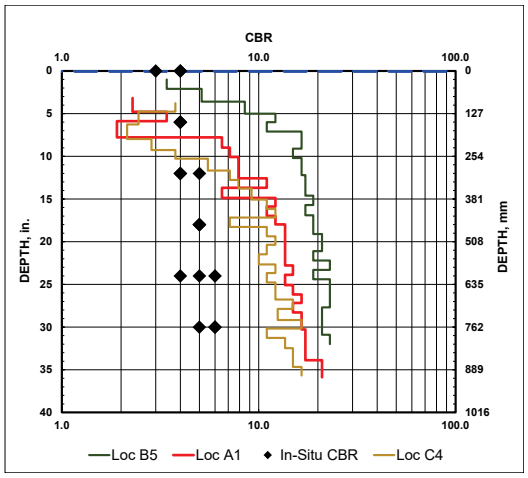

SC-Opt
SN1

Legacy Cal

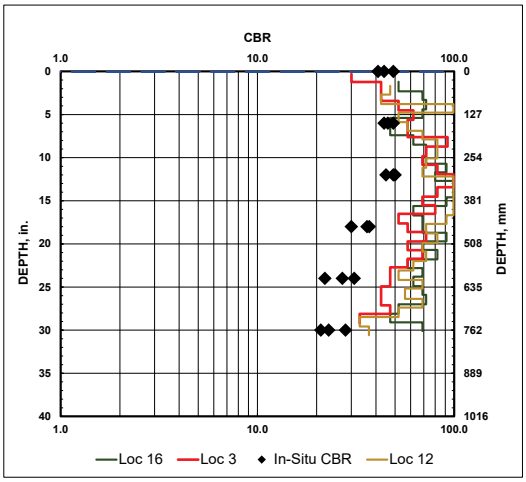

New Cal

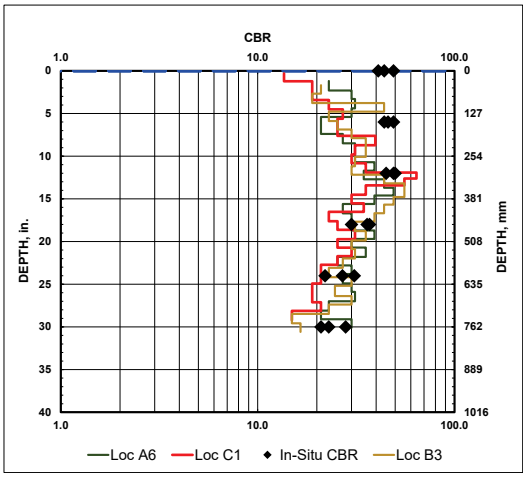

SC-Opt
SN5

Legacy Cal

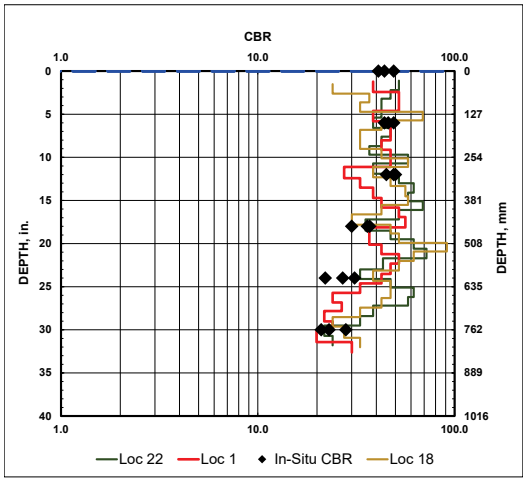

New Cal

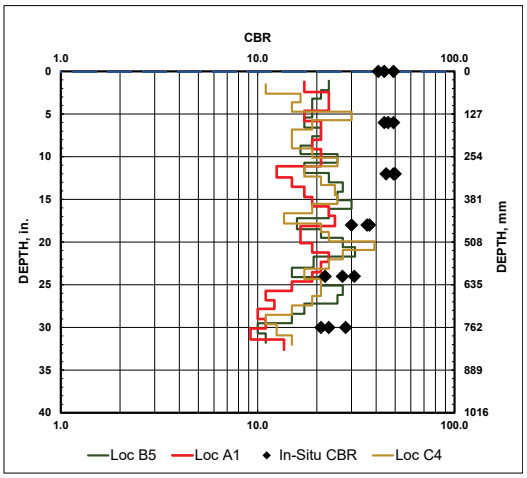

SC-Wet
SN1

Legacy Cal

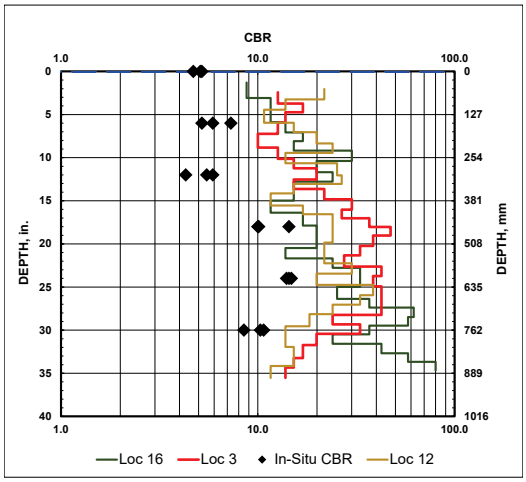

New Cal

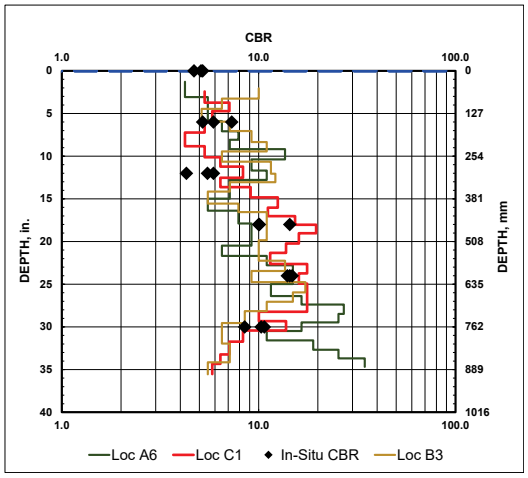

SC-Wet
SN5

Legacy Cal

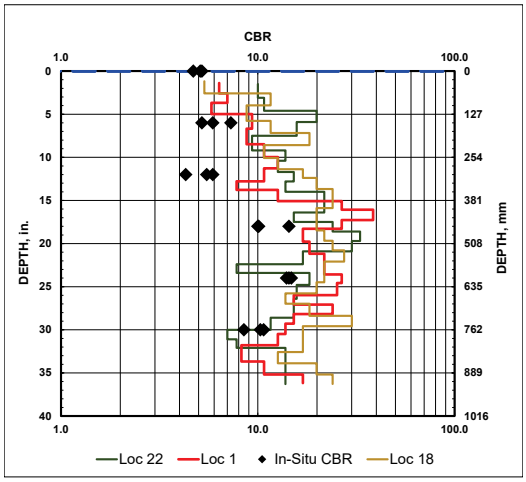

New Cal

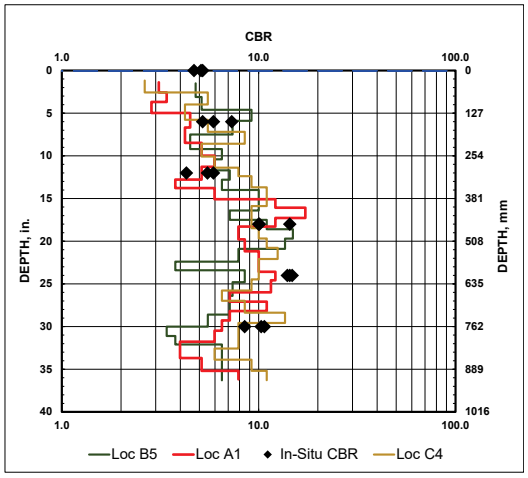

CL-Dry
SN1

Legacy Cal

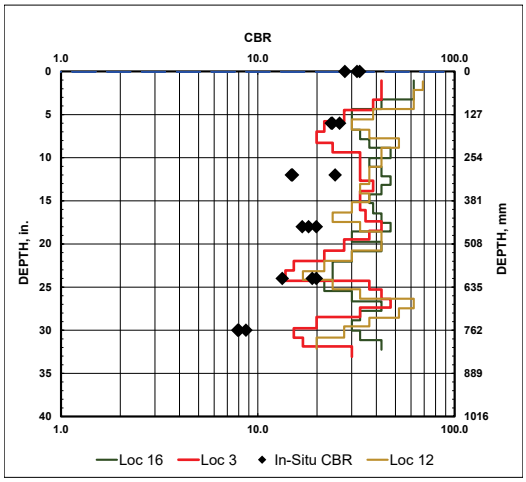

New Cal

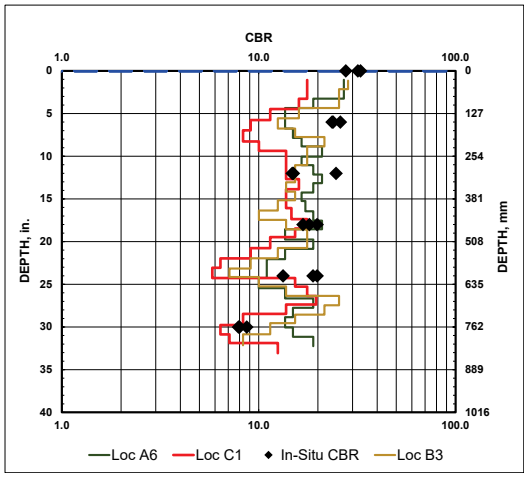

CL-Dry
SN5

Legacy Cal

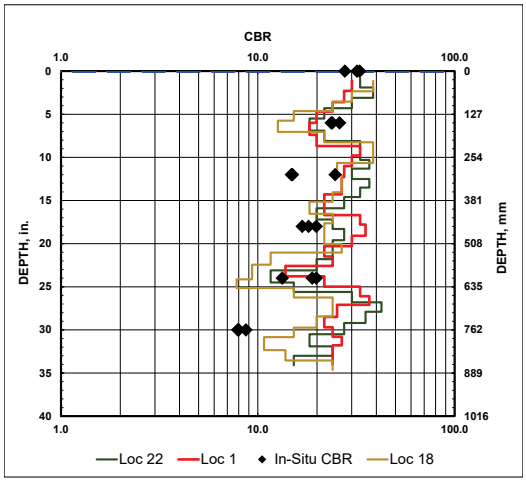

New Cal

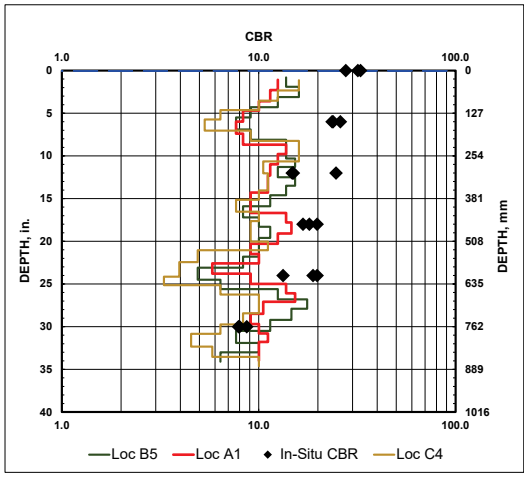

CL-Opt
SN1

Legacy Cal

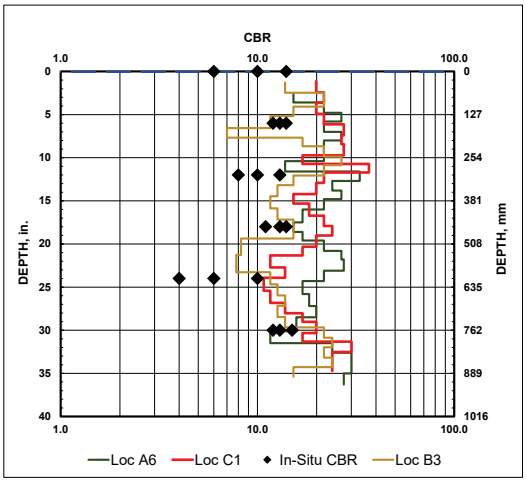

New Cal

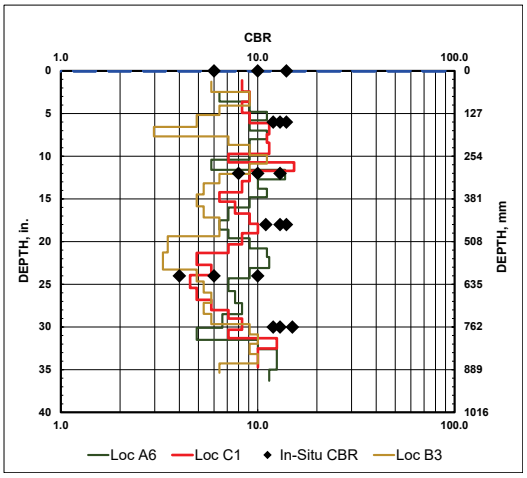

CL-Opt
SN5

Legacy Cal

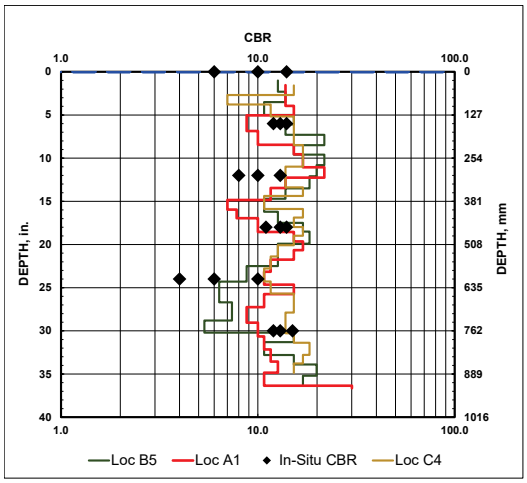

New Cal

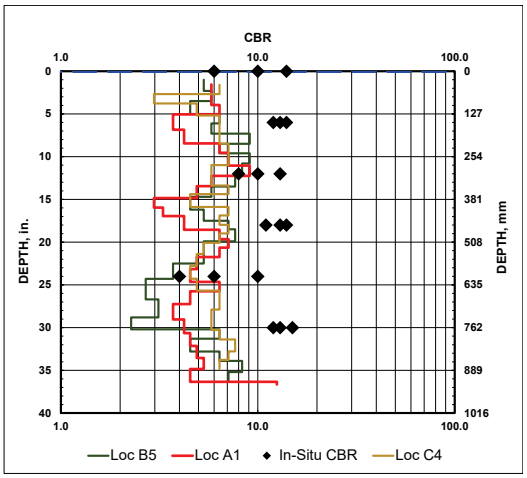

GW-Opt
SN1

Legacy Cal

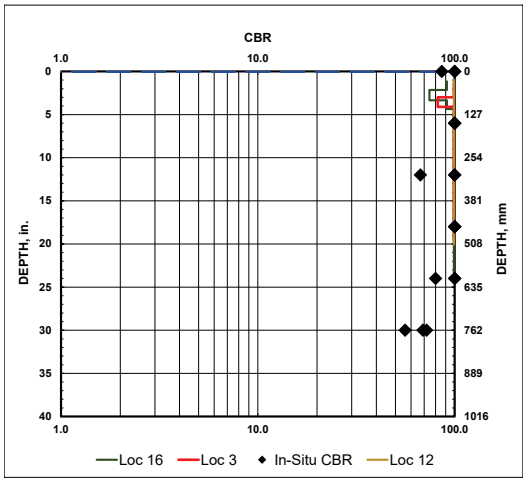

New Cal

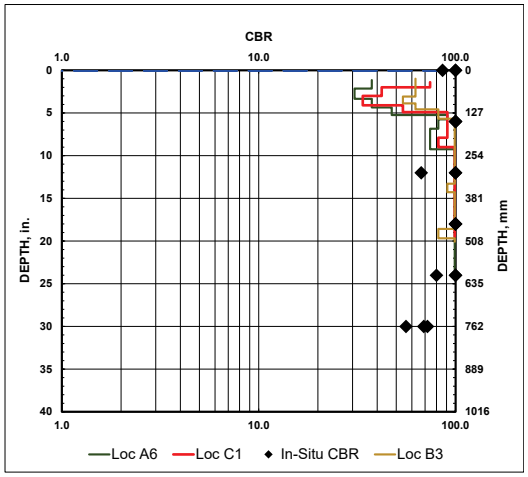

GW-Opt
SN5

Legacy Cal

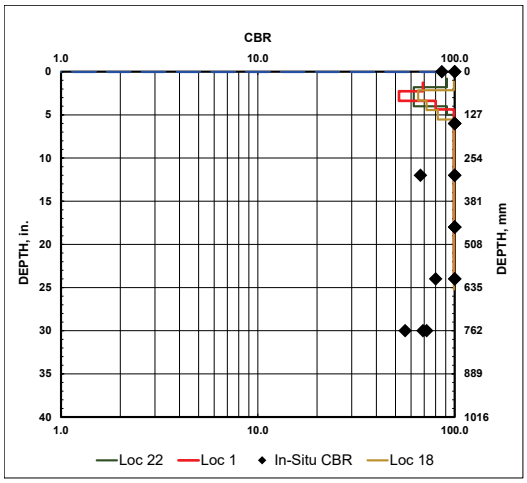

New Cal

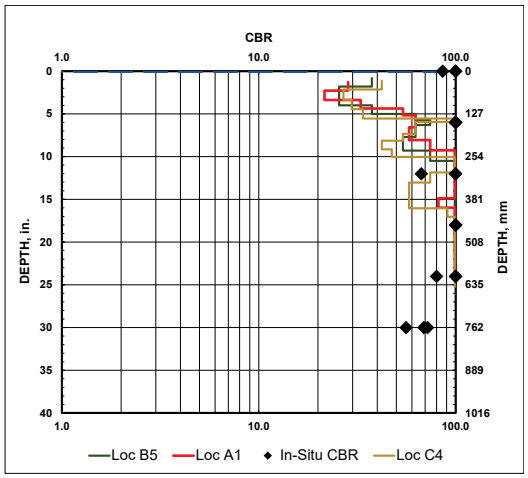

GW-Quick
SN1

Legacy Cal

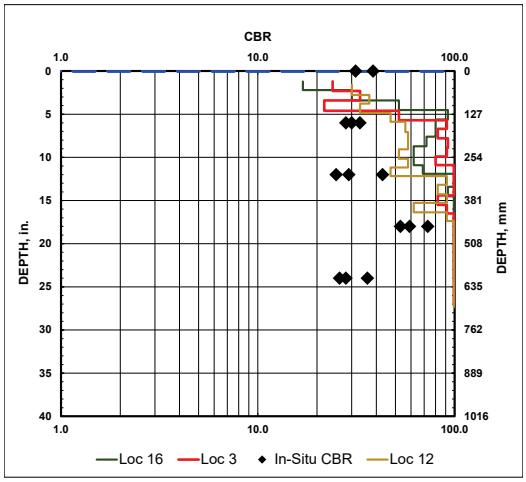

New Cal

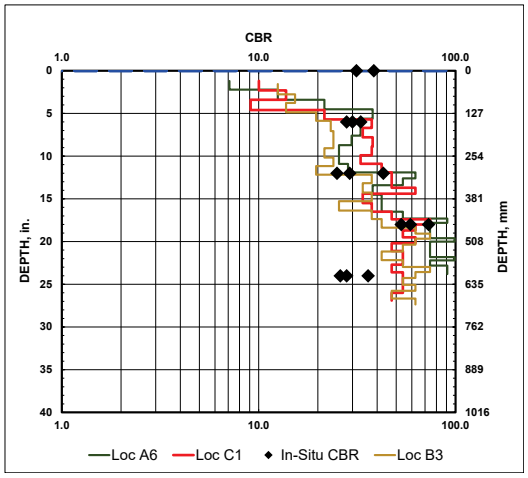

GW-Quick
SN5

Legacy Cal

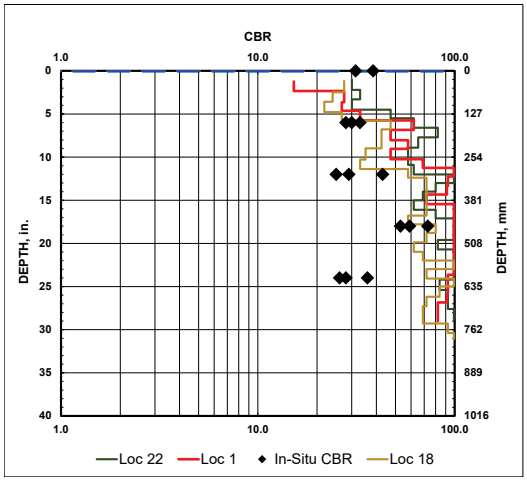

New Cal

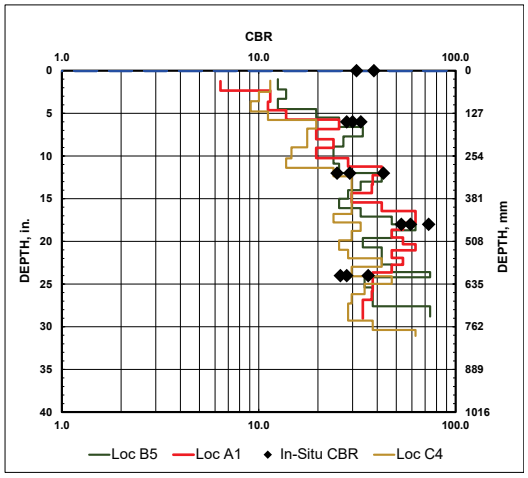

ML-Opt
SN1

Legacy Cal

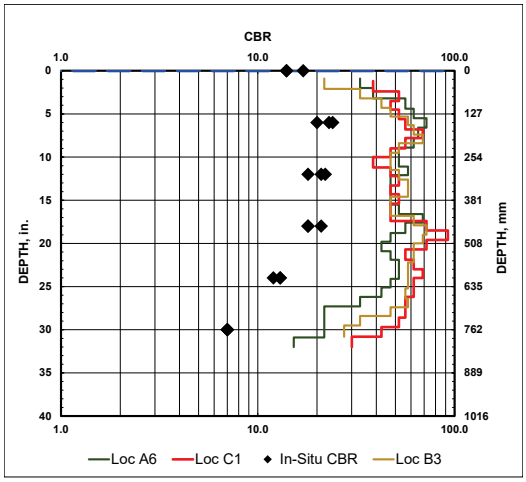

New Cal

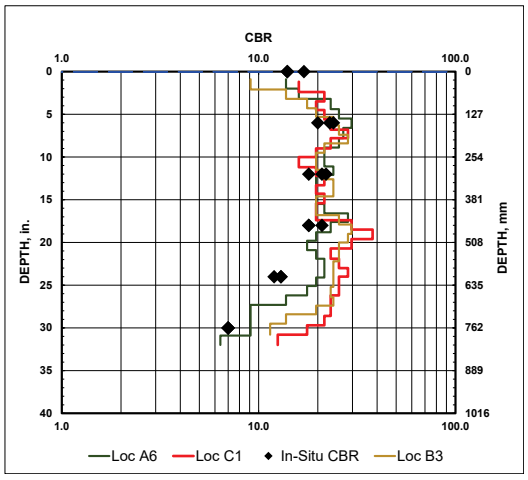

ML-Opt
SN5

Legacy Cal

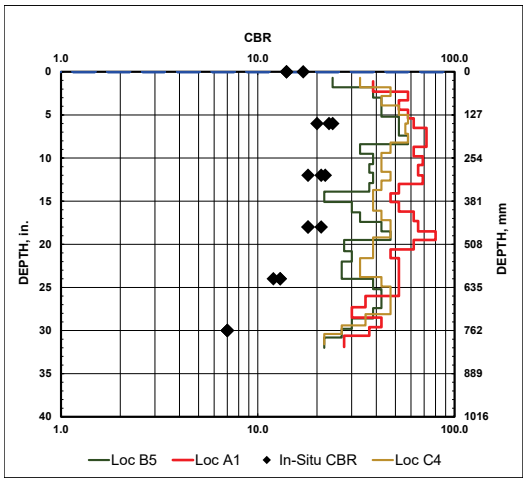

New Cal

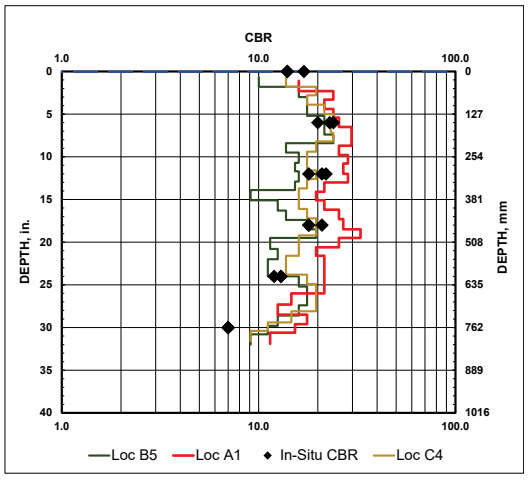

ML-Wet
SN1

Legacy Cal

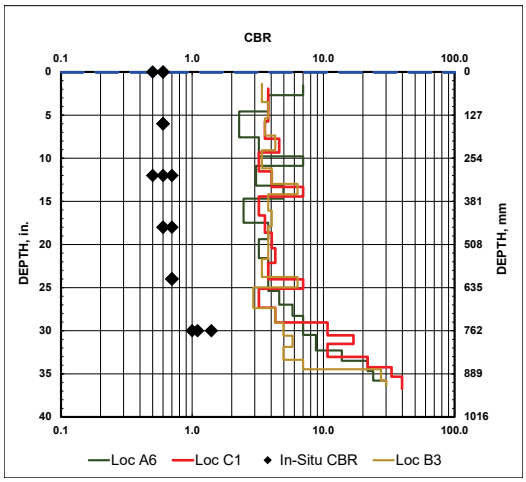

New Cal

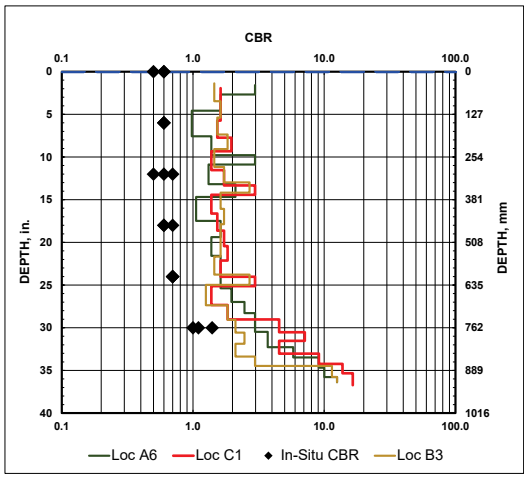

ML-Wet
SN5

Legacy Cal

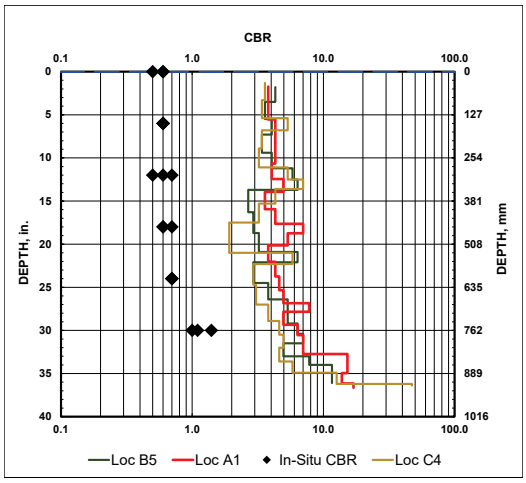

New Cal

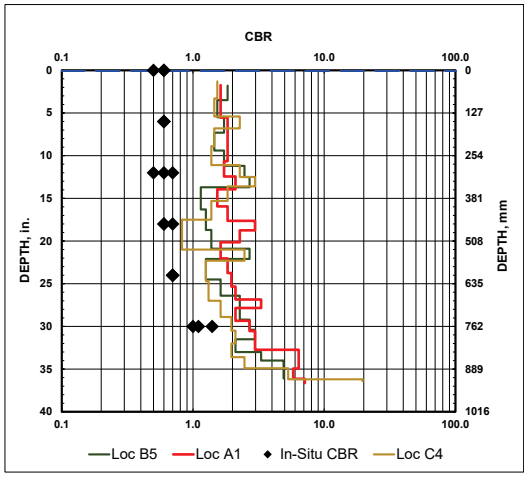

SP-Sand
SN1

Legacy Cal

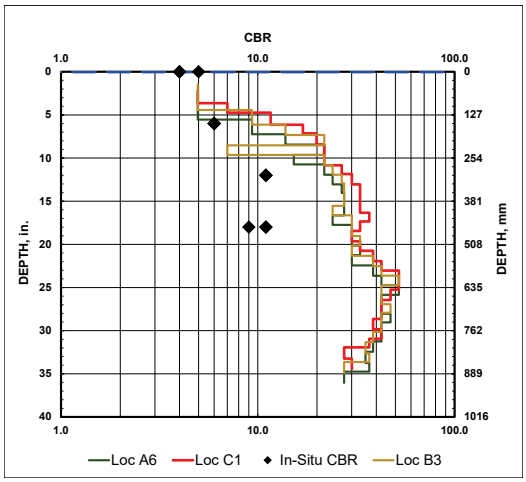

New Cal

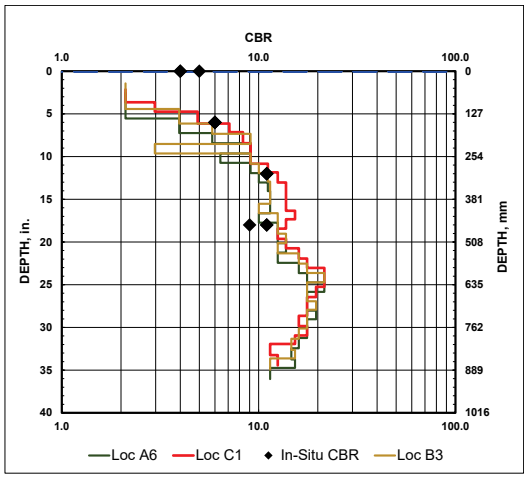

SP-Sand
SN5

Legacy Cal

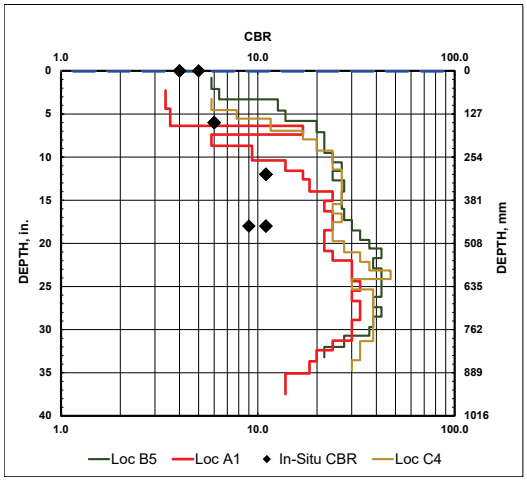

New Cal

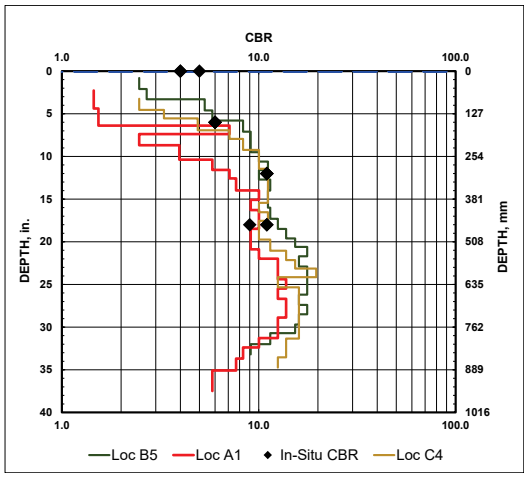

Unit Conversion Factors

Multiply	By	To Obtain
cubic feet	0.02831685	cubic meters
cubic inches	1.6387064 E-05	cubic meters
cubic yards	0.7645549	cubic meters
degrees (angle)	0.01745329	radians
feet	0.3048	meters
inches	0.0254	meters
pounds (force)	4.448222	newtons
pounds (force) per foot	14.59390	newtons per meter
pounds (force) per square foot	47.88026	pascals
pounds (force) per square inch	6.894757	kilopascals
pounds (mass)	0.45359237	kilograms
pounds (mass) per cubic foot	16.01846	kilograms per cubic meter
pounds (mass) per cubic inch	2.757990 E+04	kilograms per cubic meter
pounds (mass) per square foot	4.882428	kilograms per square meter
pounds (mass) per square yard	0.542492	kilograms per square meter
square feet	0.09290304	square meters
square inches	6.4516 E-04	square meters
square yards	0.8361274	square meters
tons (force)	8,896.443	newtons
yards	0.9144	meters

REPORT DOCUMENTATION PAGE

Form Approved
OMB No. 0704-0188

Public reporting burden for this collection of information is estimated to average 1 hour per response, including the time for reviewing instructions, searching existing data sources, gathering and maintaining the data needed, and completing and reviewing this collection of information. Send comments regarding this burden estimate or any other aspect of this collection of information, including suggestions for reducing this burden to Department of Defense, Washington Headquarters Services, Directorate for Information Operations and Reports (0704-0188), 1215 Jefferson Davis Highway, Suite 1204, Arlington, VA 22202-4302. Respondents should be aware that notwithstanding any other provision of law, no person shall be subject to any penalty for failing to comply with a collection of information if it does not display a currently valid OMB control number. **PLEASE DO NOT RETURN YOUR FORM TO THE ABOVE ADDRESS.**

1. REPORT DATE *(DD-MM-YYYY)*	2. REPORT TYPE	3. DATES COVERED *(From - To)*
July 2022	Final	

4. TITLE AND SUBTITLE

Validation of the Automatic Dynamic Cone Penetrometer

5a. CONTRACT NUMBER

5b. GRANT NUMBER

5c. PROGRAM ELEMENT NUMBER

6. AUTHOR(S)

Ernest S. Berney IV, Jami Lynn Daugherty, and Lulu Edwards

5d. PROJECT NUMBER

5e. TASK NUMBER

5f. WORK UNIT NUMBER

7. PERFORMING ORGANIZATION NAME(S) AND ADDRESS(ES)

Geotechnical and Structures Laboratory
U.S. Army Engineer Research and Development Center
3909 Halls Ferry Road
Vicksburg, MS 39180-6199

8. PERFORMING ORGANIZATION REPORT NUMBER

ERDC/GSL TR-22-16

9. SPONSORING / MONITORING AGENCY NAME(S) AND ADDRESS(ES)

U.S. Army Research Laboratory
Adelphi, MD 20783-1197

10. SPONSOR/MONITOR'S ACRONYM(S)

11. SPONSOR/MONITOR'S REPORT NUMBER(S)

12. DISTRIBUTION / AVAILABILITY STATEMENT

Approved for public release; distribution is unlimited.

13. SUPPLEMENTARY NOTES

MIPR 011460210, "Validation of the Automatic Dynamic Cone Penetrometer"

14. ABSTRACT

The U.S. military requires a rapid means of measuring subsurface soil strength for construction and repair of expeditionary pavement surfaces. Traditionally, a dynamic cone penetrometer (DCP) has served this purpose, providing strength with depth profiles in natural and prepared pavement surfaces. To improve upon this device, the Engineer Research and Development Center (ERDC) validated a new battery-powered automatic dynamic cone penetrometer (A-DCP) apparatus that automates the driving process by using a motor-driven hammering cap placed on top of a traditional DCP rod. The device improves upon a traditional DCP by applying three to four blows per second while digitally recording depth, blow count, and California Bearing Ratio (CBR). An integrated Global Positioning Sensor (GPS) and Bluetooth® connection allow for real-time data capture and stationing. Similarities were illustrated between the DCP and the A-DCP by generation of a new A-DCP calibration curve. This curve relates penetration rate to field CBR that nearly follows the DCP calibration with the exception of a slight offset. Field testing of the A-DCP showed less variability and more consistent strength measurement with depth at a speed five times greater than that of the DCP with minimal physical exertion by the operator.

15. SUBJECT TERMS

Soil
Strength
Soil penetration test
Soils–Testing
Compaction
Dynamic Cone Penetrometer
Automated
Soil mechanics
Bearing capacity
California Bearing Ratio
Fast
Shear strength of soils
Penetrometers–Evaluation

16. SECURITY CLASSIFICATION OF:			17. LIMITATION OF ABSTRACT	18. NUMBER OF PAGES	19a. NAME OF RESPONSIBLE PERSON
a. REPORT	b. ABSTRACT	c. THIS PAGE			19b. TELEPHONE NUMBER *(include area code)*
Unclassified	Unclassified	Unclassified	SAR	151	